9   WESTINGHOUSE DOWNFLOW BARREL/BAFFLE DESIGNS

In this section, results from the Westinghouse downflow plant category are presented and discussed. The range of conditions and case matrix are provided in Section 9.1. Results from the analysis are presented in Section 9.2. This section is broken into several subsections and the material contained in each subsection is summarized as follows:

- In Section 9.2.1, results from a case that did not model debris build-up at the core inlet are used to describe the RCS state at the time of transfer to sump recirculation and the arrival of debris. Since all simulations are identical prior to reaching that point in time, the discussion in this section is applicable to all cases. In the simulations, transfer to sump recirculation occurs 20 minutes after the postulated LOCA.

- In Section 9.2.2, results from the case used to determine t_{block} are presented. This case did not apply partial blockage to the core inlet prior to the application of complete core inlet blockage. Complete core inlet blockage was applied instantaneously at time t_{block} and was applied uniformly across all core channels.

- In Section 9.2.3, results from the case used to determine a value for K_{max} are presented. This case applied partial blockage to the core inlet prior to the application of complete core inlet blockage. The partial blockage was applied instantaneously at the point of transfer to sump recirculation and was applied uniformly across all core channels. Complete core inlet blockage was also applied instantaneously at time t_{block} and was applied uniformly across all core channels.

- In Section 9.2.4, results from additional cases used to determine K_{split} and m_{split} are presented. For these cases, a linear ramp in resistance was applied uniformly across the core inlet and complete core inlet blockage was not simulated. Since these cases were used to assess the timing of the activation of the UHSN AFP, the build-up of core inlet resistance was applied more slowly compared to the cases used to determine K_{max}. As a result, the RCS response to core inlet blockage was much slower in that the downcomer fill rate and the activation of the UHSNs occurred over a longer period of time. It is noted that these simulations are more realistic with regard to the timing at which debris is expected to arrive at the core inlet.

Section 9.3 summarizes and discusses the key analysis results.

9.1   RANGE OF CONDITIONS AND CASE MATRIX

The simulation matrix used to determine t_{block} and K_{max} is shown in Table 9-1. For these cases, the plant model with maximum UHSN flow resistance was used. In the table, the loss coefficient column identifies the core inlet losses applied at the designated initiation times. All cases that modeled core inlet blockage applied a step change to the loss coefficient at the core inlet. Cases 0A and 0B did not model core inlet blockage and Cases 1A, 2A, and 2B applied step changes. The core inlet resistances applied for these cases are presented graphically in Figure 9-1 and Figure 9-2.

Step changes in loss coefficients are applied over a 60 second interval. For example, in Case 2A, a step change from 0 to 9.5×10^5 is applied from 1200 to 1260 seconds and an additional step change from

9.5×10^5 to 1×10^9 is applied from 15,600 to 15,660 seconds. For all simulations, the sump recirculation flow rate is applied 1200 seconds after the initiation of the event.

The simulation matrix used to determine K_{split} and m_{split} is shown in Table 9-2. For these cases, the plant model with minimum UHSN flow resistance was used. In the table, the loss coefficient column identifies the core inlet losses applied starting at the designated initiation time and ending at the designated end time. For example, in Case 1, a timewise-linear ramp of the loss coefficient at a rate of 6000 /hr is applied starting at 1200 seconds and ending at 19,200 seconds. The ending value of the loss coefficient is 30,000. Complete core inlet blockage is not applied to these cases. For all simulations, the sump recirculation flow rate is applied 1200 seconds after the initiation of the event.

Table 9-1   Simulation Matrix for t_{block} and K_{max} – Westinghouse Downflow Plant Design

Case	Sump Recirculation Flow Rate (gpm/FA)	Debris Bed Model	
		Loss Coefficient	Initiation Time (sec)
0A	40	NONE	N/A
0B	18	NONE	N/A
1A	40	1×10^9	15,600
2A	40	$9.5 \times 10^5 / 1 \times 10^9$	1200/15,600
2B	18	$6 \times 10^5 / 1 \times 10^9$	1200/12,000

Table 9-2   Simulation Matrix for K_{split} and m_{split} – Westinghouse Downflow Plant Design

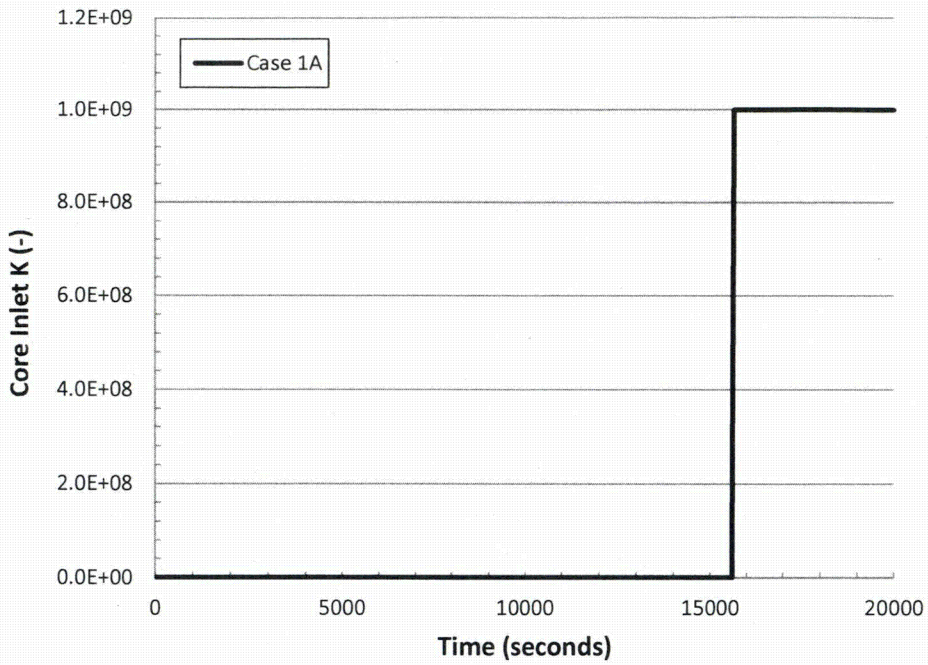| Case	Sump Recirculation Flow Rate (gpm/FA)	Debris Bed Model (Linear Ramp)		
		Loss Coefficient	Initiation Time (sec)	End Time (sec)
1	40	6000/hr	1200	19,200
2	30	6000/hr	1200	19,200
3	18	6000/hr	1200	19,200
4	12	12,000/hr	1200	26,400
5	8	12,000/hr	1200	37,200

Figure 9-1 Core Inlet Resistance Transient Applied to Case 1 Simulation from Westinghouse Downflow Analysis
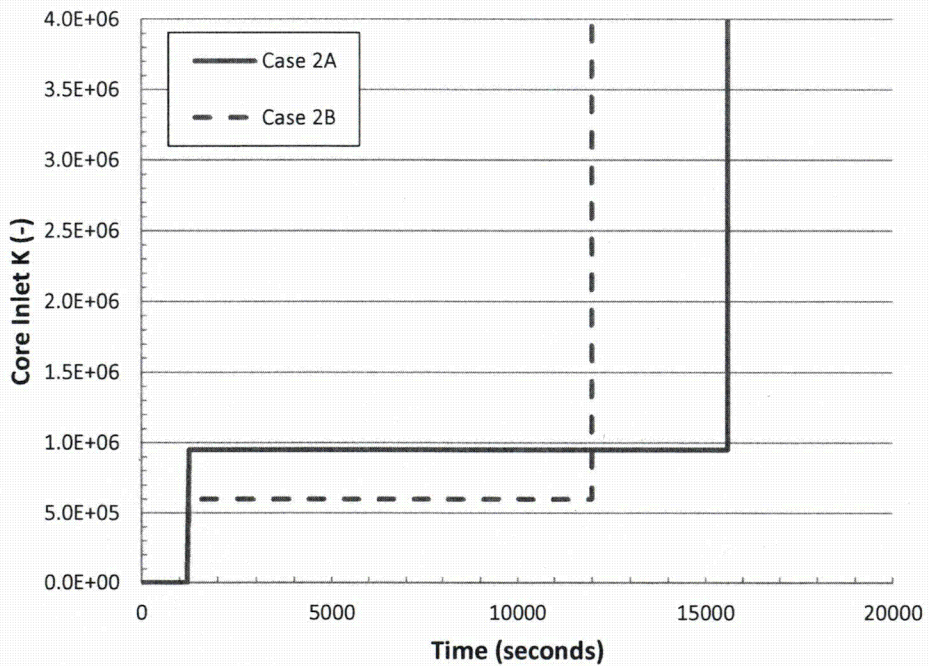

Figure 9-2 Core Inlet Resistance Transient Applied to Case 2 Simulations from Westinghouse Downflow Analysis

9.2   RESULTS OF ANALYSIS

Key results from the t_{block} and K_{max} simulations are summarized in Table 9-3. Cases 0A and 0B have no core inlet blockage applied. Case 1A applies complete core inlet blockage and determines the minimum time that complete blockage can be tolerated. Cases 2A and 2B apply resistances to the core inlet prior to reaching complete core inlet blockage and are used to determine the maximum resistance that can be tolerated prior to reaching complete blockage.

Based on the results presented in Table 9-3, it is concluded that LTCC can be maintained if complete core inlet blockage occurs 260 minutes (15,600 sec), or later, after the initiation of the LOCA event. This time is taken from the maximum ECCS recirculation flow case (Case 1A). Prior to reaching complete core inlet blockage, a maximum supportable K_{max} value of 6×10^5, corresponding to a pressure drop of 14.8 psid across the core inlet, is determined to be the limiting value when a uniform resistance is applied instantaneously upon entering sump recirculation. These values are taken from the minimum ECCS recirculation flow case (Case 2B) and bound the range of recirculation flows investigated.

With regard to BAPC, all cases demonstrate that, after core inlet blockage, the break exit quality remains sufficiently low such that boron is flushed from the core and concentrations are expected to remain well below the solubility limit. Further, all cases demonstrate that the core mixing patterns are such that the core can be considered well-mixed and no localized regions containing higher boron concentration are expected to form.

Key results from the K_{split} and m_{split} simulations are summarized in Table 9-4. The K_{split} values shown in the table are used in conjunction with the ECCS sump recirculation flow rates to generate the curve shown in Figure 9-3. This curve will be used in subsequent downstream calculations presented in Volume 1 to track the location of fibrous debris within the RV during the LTCC phase of the transient. The time that K_{split} occurs is determined by examination of the UHSN exit flow rate. The first timestep in which the UHSN exit flow rate becomes positive is defined as the K_{split} time. If flow oscillations (positive UHSN exit flow followed by a reversal to negative flow) occur, the time of K_{split} is selected after the flow oscillations stop and the UHSN exit flow remains positive. The fraction of ECCS flow through the core inlet and UHSN shown in Table 9-4 are taken at the end of the core inlet form-loss ramp. The transient flow split between the core inlet and UHSN is shown in Figure 9-4 for the five ECCS recirculation flow rates investigated. The flow split is represented as the fraction of total ECCS recirculation flow through the UHSN and is plotted as a function of the core inlet resistance following K_{split}. These curves will be used, in conjunction with K_{split}, in downstream calculations to track the location of fibrous debris within the RV during the LTCC phase of the transient as described in Volume 1.

Table 9-3   Summary of Results for t_{block} and K_{max} – Westinghouse Downflow Plant Design

Case	Time Core Inlet Resistance Applied	Core Inlet Loss Coefficient (K)	Core Inlet Average Mass Flow Rate per FA	Core Inlet Average Velocity	Pressure Drop across Debris Bed	Break Exit Quality	PCT
---	seconds	---	lbm/sec	ft/s	psid	---	°F
0A	N/A	N/A	5.3	0.54	N/A	0.05	<250
0B	N/A	N/A	1.6	0.16	N/A	0.25	<300
1A	15,600	1×10^9	5.3	0.54	-	0.6	<800
2A	1200/15,600	$9.5\times10^5/1\times10^9$	0.58	0.058	20.6	0.6	<650
2B	1200/12,000	$6\times10^5/1\times10^9$	0.62	0.062	14.8	0.5	<750

Table 9-4   Summary of Results for K_{split} and m_{split} – Westinghouse Downflow Plant Design

Case	Time of K_{split}	K_{split}	Fraction of ECCS Flow through Core Inlet	Fraction of ECCS Flow through UHSNs	Final Pressure Drop across Debris Bed
---	seconds	---	---	---	psid
1	2420.5	2034	0.33	0.67	6.1
2	3702	4170	0.50	0.50	7.6
3	11,250	16,750	0.81	0.19	7.0
4	13,928	42,427	0.74	0.26	7.8
5	27,888	88,960	0.89	0.11	6.8
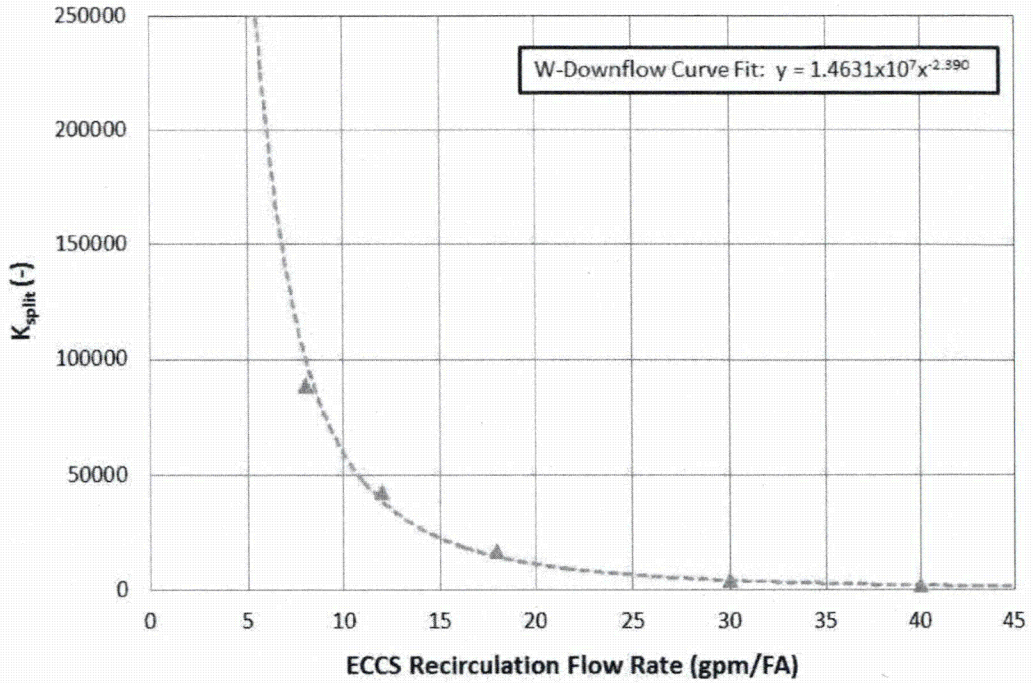
Figure 9-3 K_{split} as a Function of ECCS Recirculation Flow Rate from Westinghouse Downflow Analysis
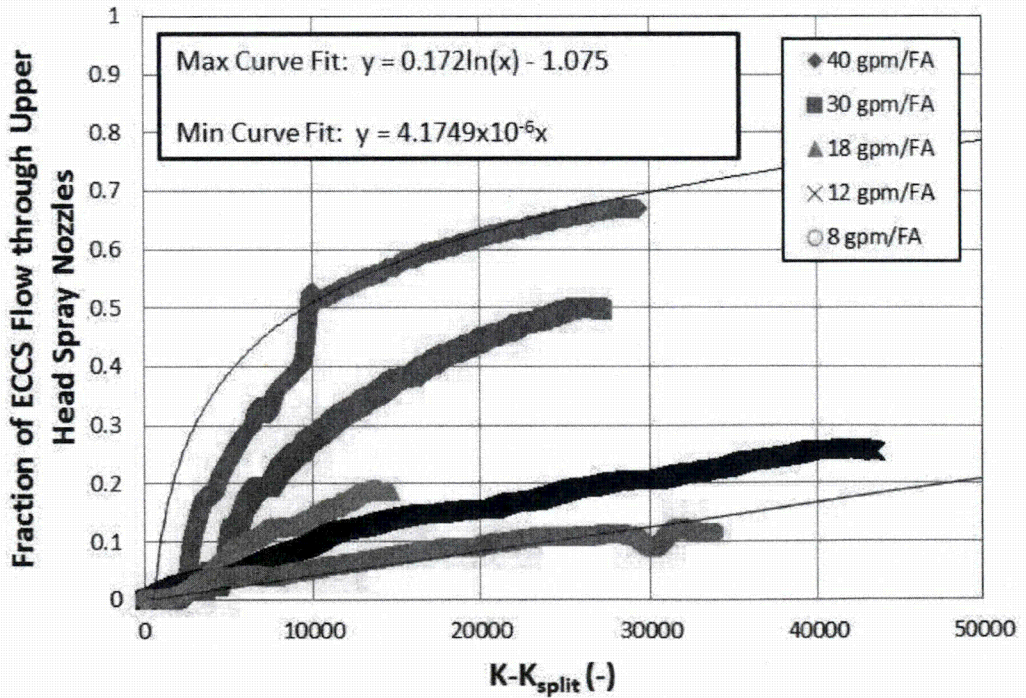
Figure 9-4 Fraction of ECCS Recirculation Flow through the BB following K_{split} from Westinghouse Downflow Analysis

9.2.1 All Cases – Before Debris Introduction

The results from Case 0A are used to describe the RCS state at the point of transfer to sump recirculation and the arrival of debris. Since all simulations are identical prior to that point in the transient, the discussion in this section is applicable to all cases. In the simulations, transfer to sump recirculation occurs 20 minutes after the postulated LOCA.

Just before transfer to sump recirculation, the RCS loop piping and SGs are mostly voided. The entire core has quenched and the cladding temperatures are just above saturation temperature as shown in Figure 9-5. The core region is covered with a two-phase mixture and the core collapsed liquid level is roughly 11feet into the active fuel region. Figure 9-6 shows the hot assembly collapsed liquid level, which indicates a sharp drop in the collapsed liquid level upon entry to sump recirculation. This is due to the removal of ECCS subcooling. During the RWST draindown phase, the ECCS coolant temperature is below 100°F. During the transfer to sump recirculation, the ECCS coolant temperature is changed to 212°F. This removal of subcooling results in increased core boiling and a reduction in the core collapsed liquid level.

Figure 9-7 shows the downcomer and upper head collapsed liquid levels. The figure indicates that the downcomer collapsed liquid level is just below the cold leg elevation at the time of transfer to sump recirculation, while the upper head has virtually no liquid in its volume.

As the pumped ECCS enters the cold legs, coolant can either travel toward the RV or go through the RCP and spill into the crossover legs of the RCS loop piping. For times prior to sump recirculation, and the arrival of debris, the ECCS flow split behavior is similar in the broken and intact loops. Figure 9-8 shows the integrated ECCS flow split on the broken loop. As shown in the figure, the slope of the integrated flow going in the direction of the RV is similar to the slope of the integrated total pumped ECCS flow, while the slope of the integrated flow going toward the RCP remains fairly flat. This behavior indicates that the majority of the total pumped ECCS flow is traveling to the RV. This behavior is expected given that the resistance to flow from the injection point to the downcomer is less than the resistance through the RCPs to the crossover legs.

Figure 9-9 and Figure 9-10 show the integrated mass flow rates at the core inlet for each of the four core channels. A positive slope indicates positive flow into the core. Just prior to sump recirculation, all of the slopes are positive, indicating flow from the LP into the four core channels (i.e., upflow). Figure 9-11 shows the integrated mass flow rate near the core outlet. The integrated outlet flow from the core is the summation of the hot assembly and two average core channels, all of which have positive flow out of the core, while the integrated outlet flow in the peripheral channel has downward flow from the UP to the peripheral channel. Figure 9-12 shows the integrated liquid mass flow through the intact SGs, UHSNs, and upper guide tubes. The figure indicates that, without core inlet blockage there is no liquid flow through the UHSNs and upper guide tubes. The figure also indicates that there is liquid flow out of the RV into the intact hot legs.

The integrated break mass flow is shown in Figure 9-13. The figure shows that all of the break flow is from the RV side, which indicates no liquid carryover through the broken loop SG to the break. The break exit quality is shown in Figure 9-14. The figure shows that the nominal break exit quality is less than 10% upon transfer to sump recirculation, which indicates a substantial amount of liquid carryover

out the break. Due to the large amount of liquid carryover prior to sump recirculation, BAP is controlled and boron concentration levels in the RV upon entry to sump recirculation are expected to be comparable to the ECCS source concentration.
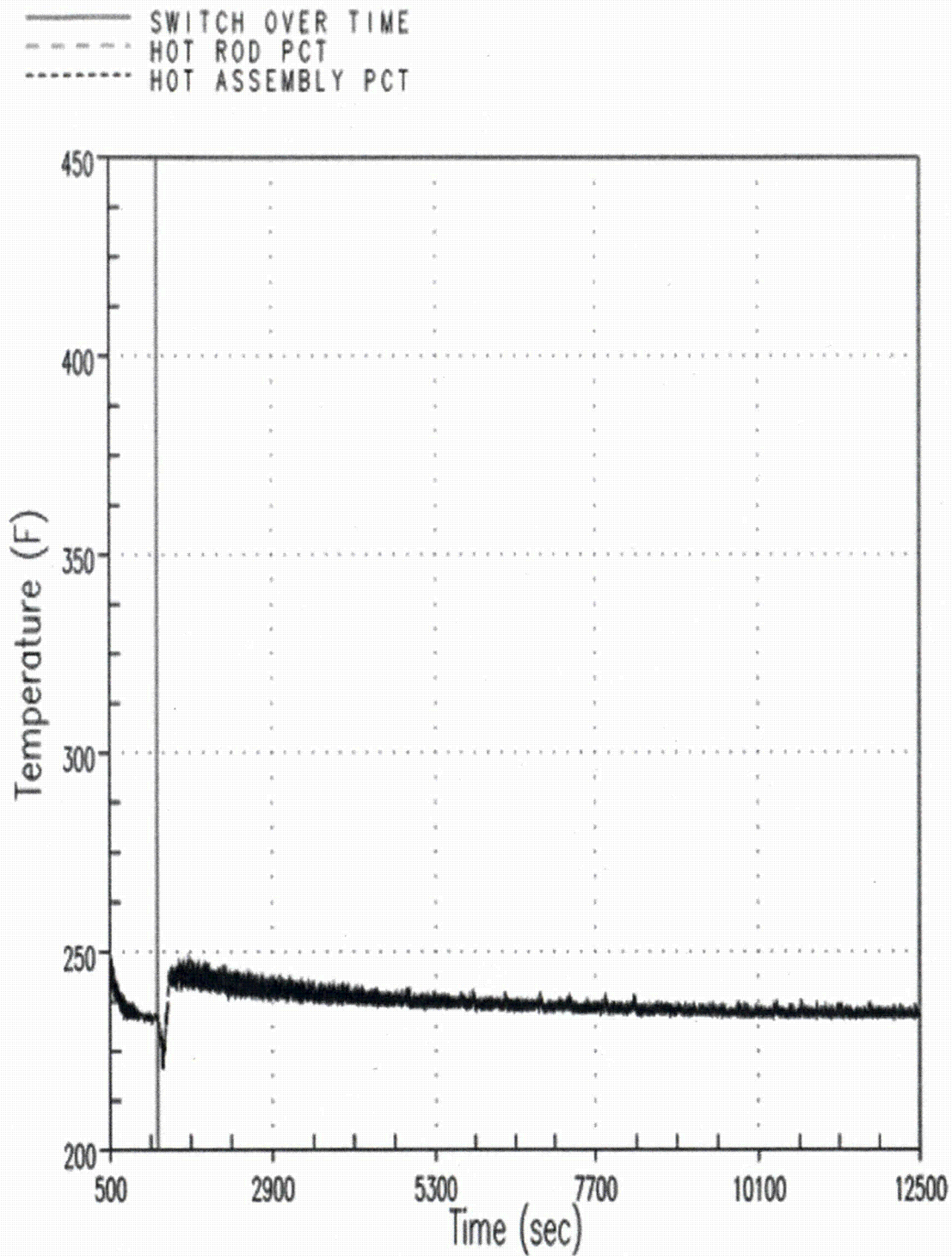
SWITCH OVER TIME
HOT ROD PCT
HOT ASSEMBLY PCT

Figure 9-5 Case 0A – Hot Rod and Hot Assembly Peak Cladding Temperatures
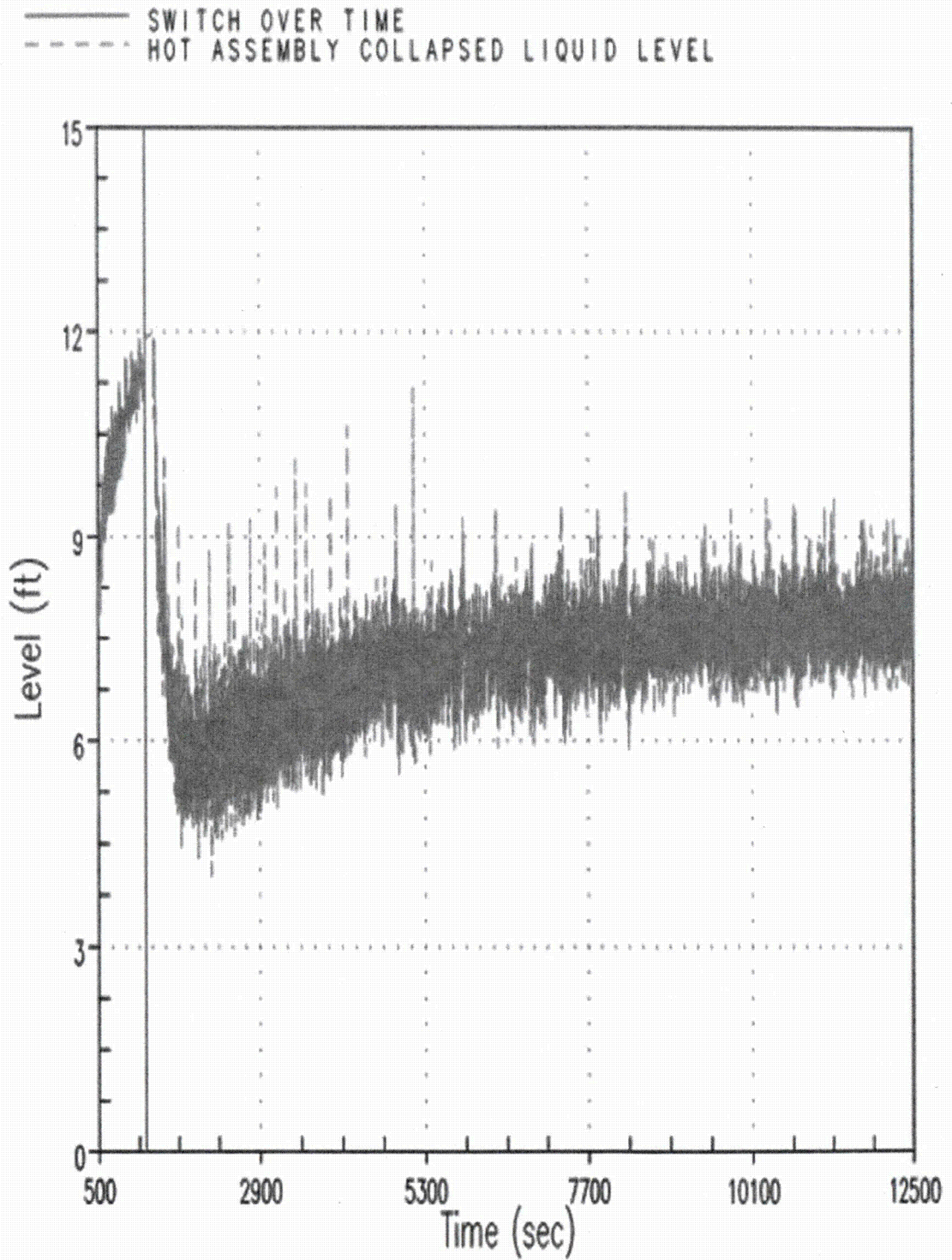
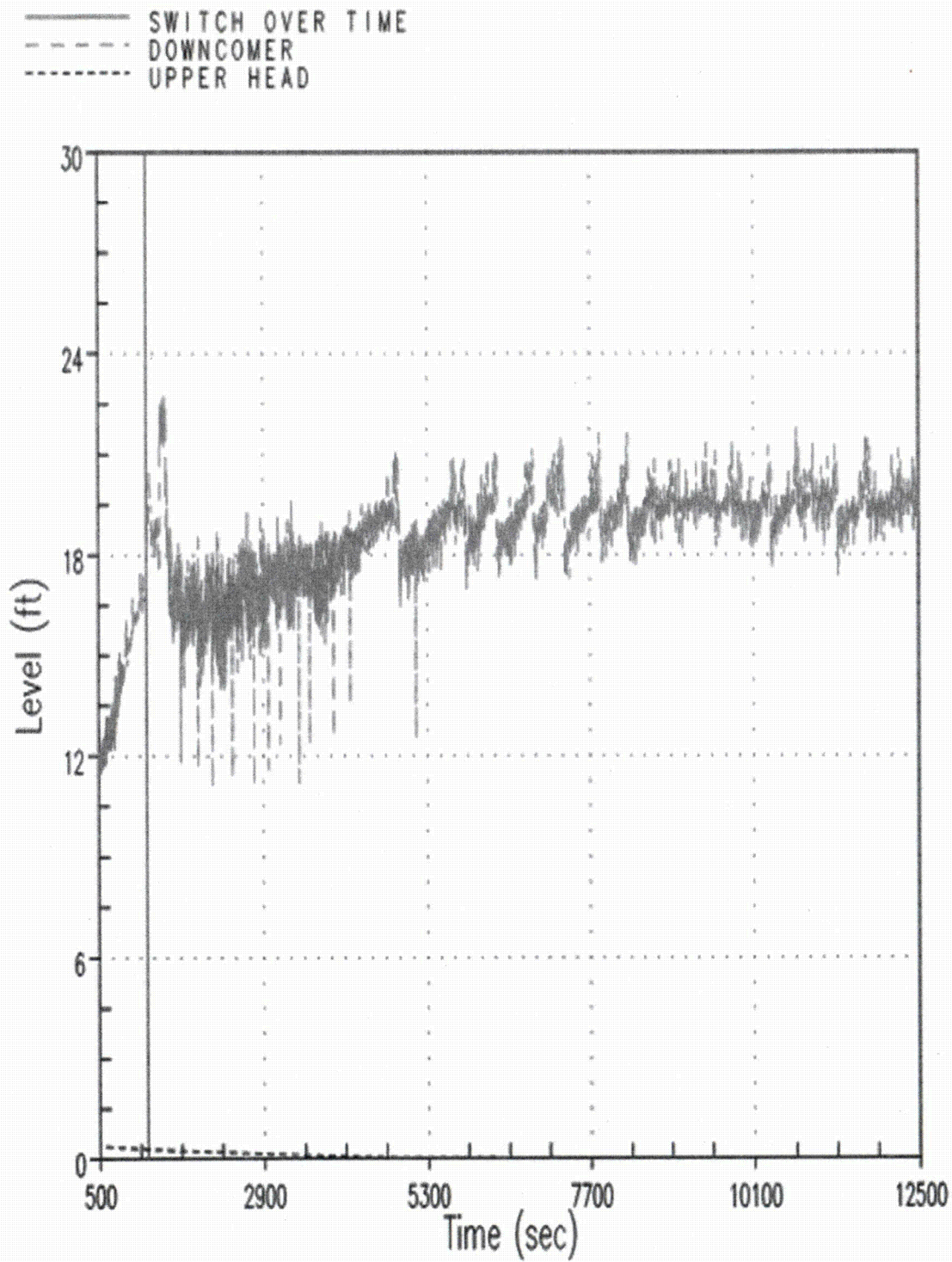**Figure 9-6 Case 0A – Hot Assembly Collapsed Liquid Level**
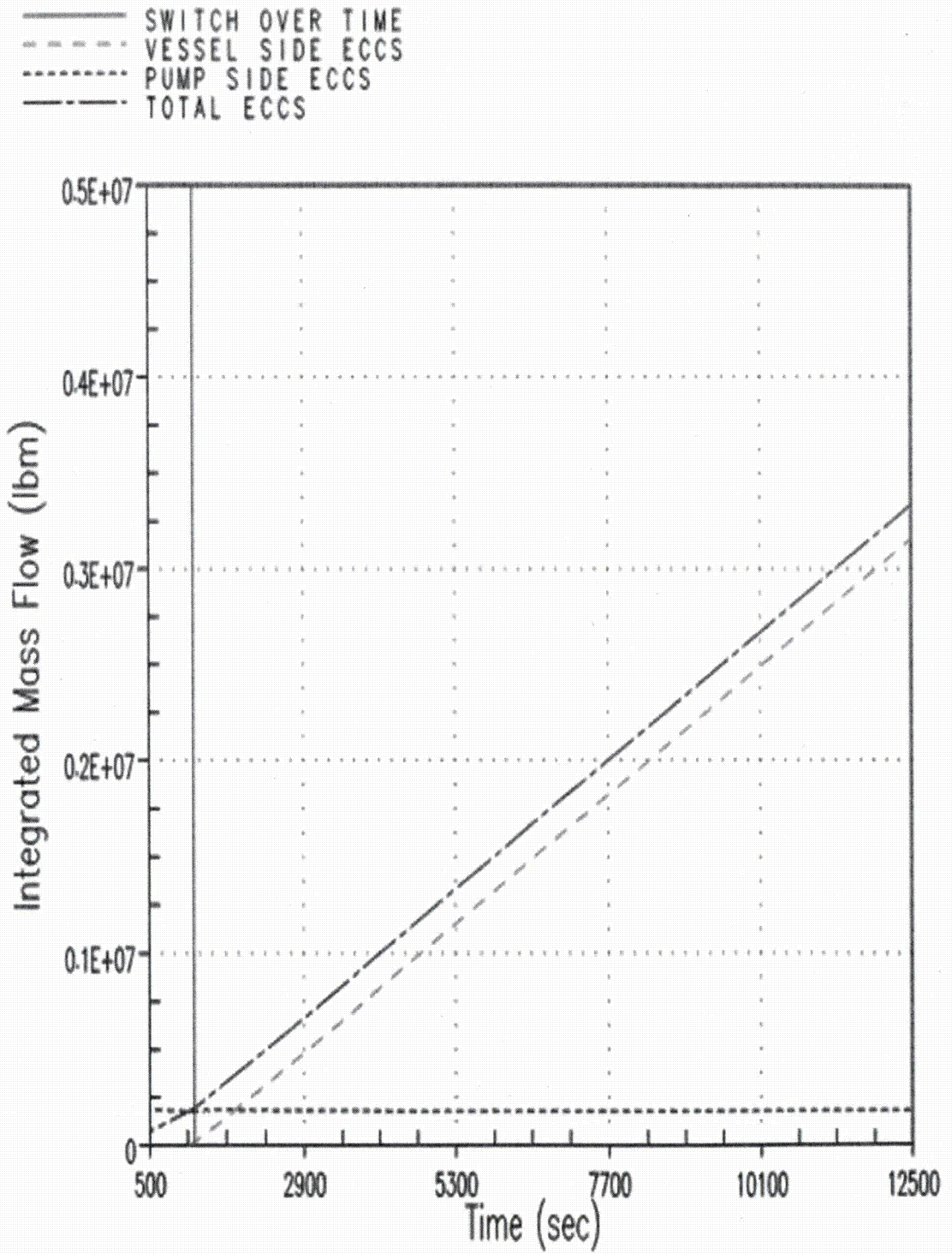
Figure 9-7 Case 0A – Downcomer and Upper Head Collapsed Liquid Levels

Figure 9-8 Case 0A – Integrated ECCS Flow Split in Broken Loop

Figure 9-9 Case 0A – Integrated Core Inlet Mass Flow from Average and Peripheral Channels
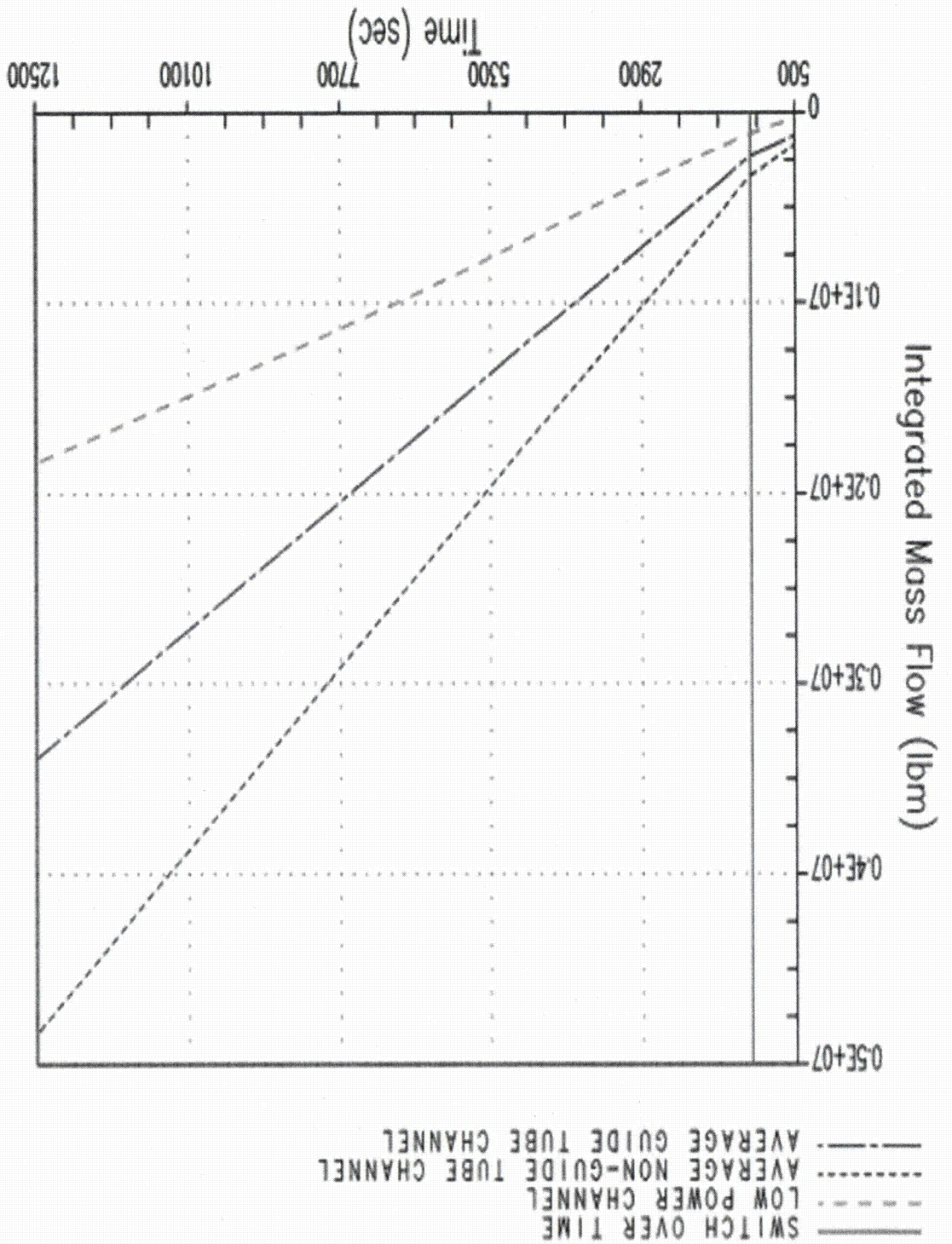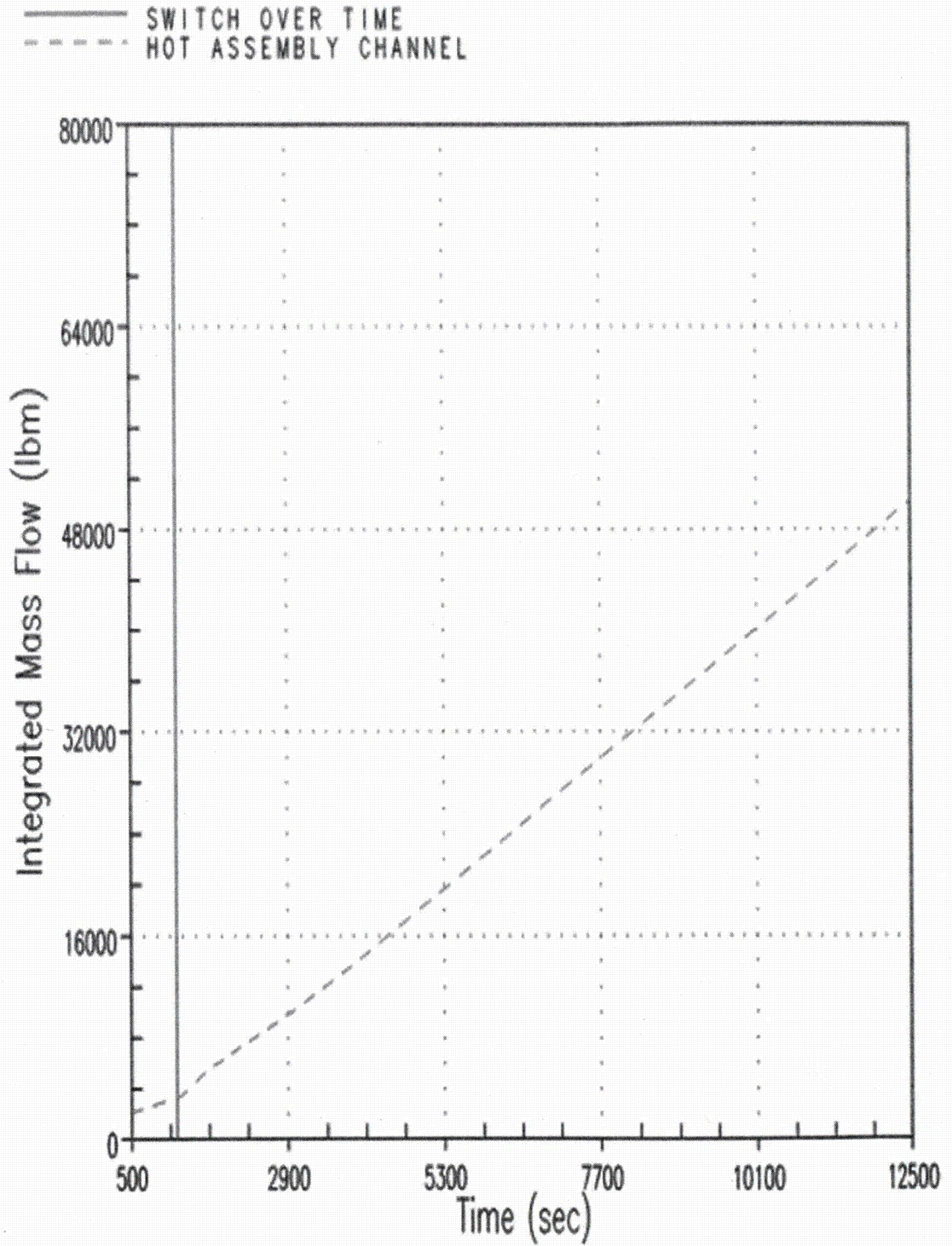
Figure 9-10 Case 0A – Integrated Core Inlet Mass Flow from Hot Assembly Channel
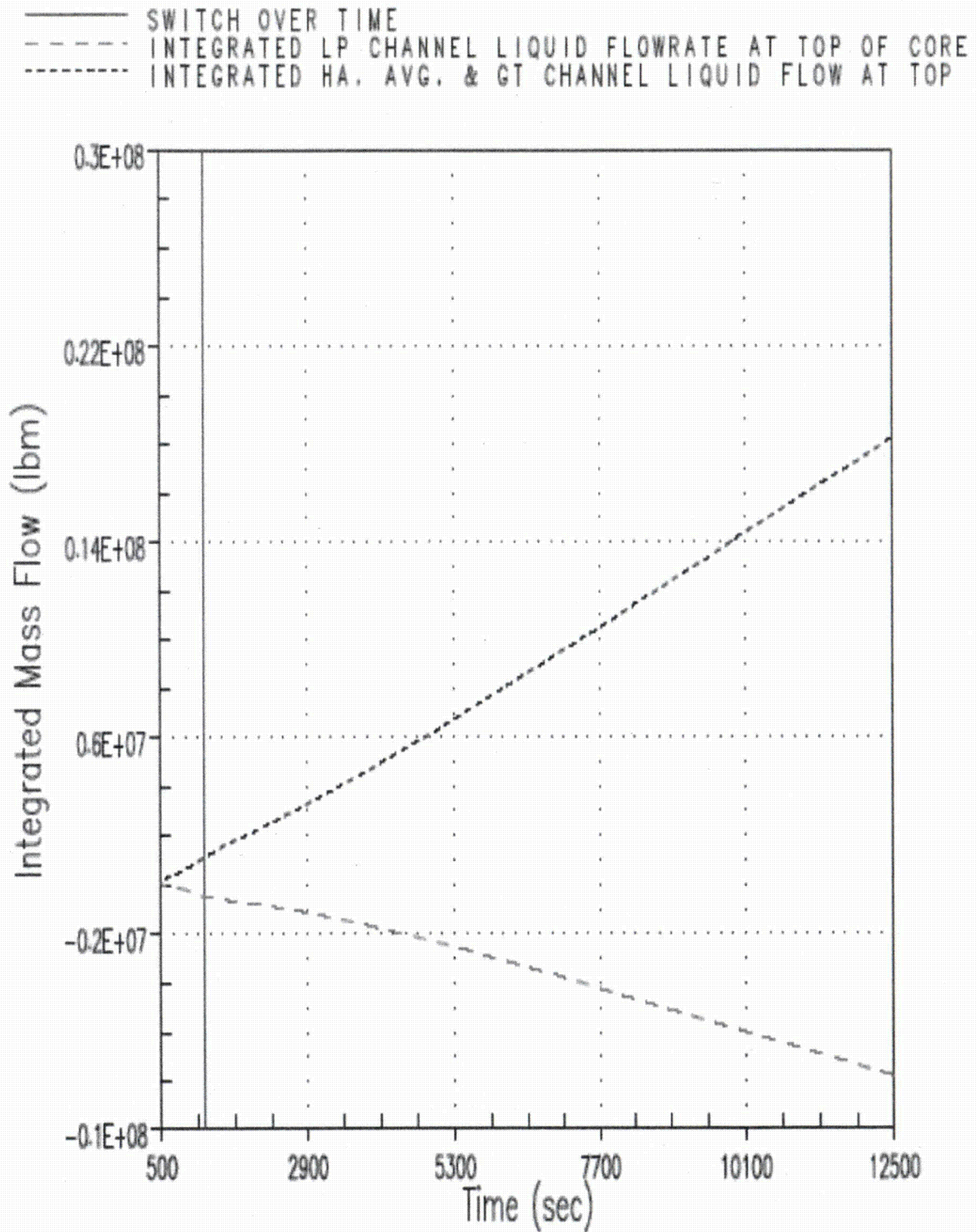
Figure 9-11 Case 0A – Integrated Core Exit Mass Flow
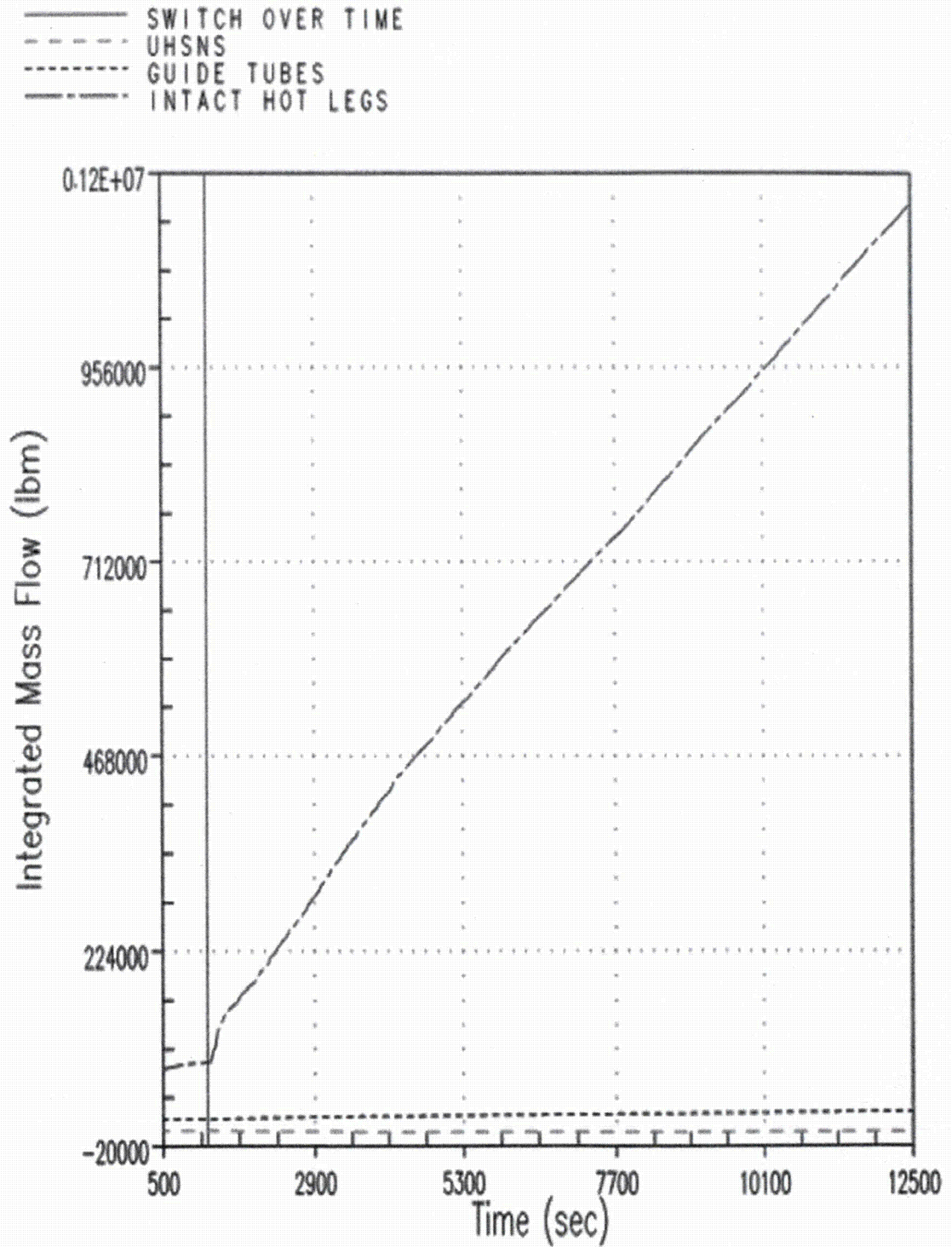
Figure 9-12 Case 0A – Integrated Liquid Flow through Intact Hot legs, Upper Head Spray Nozzles, and Upper Guide Tubes
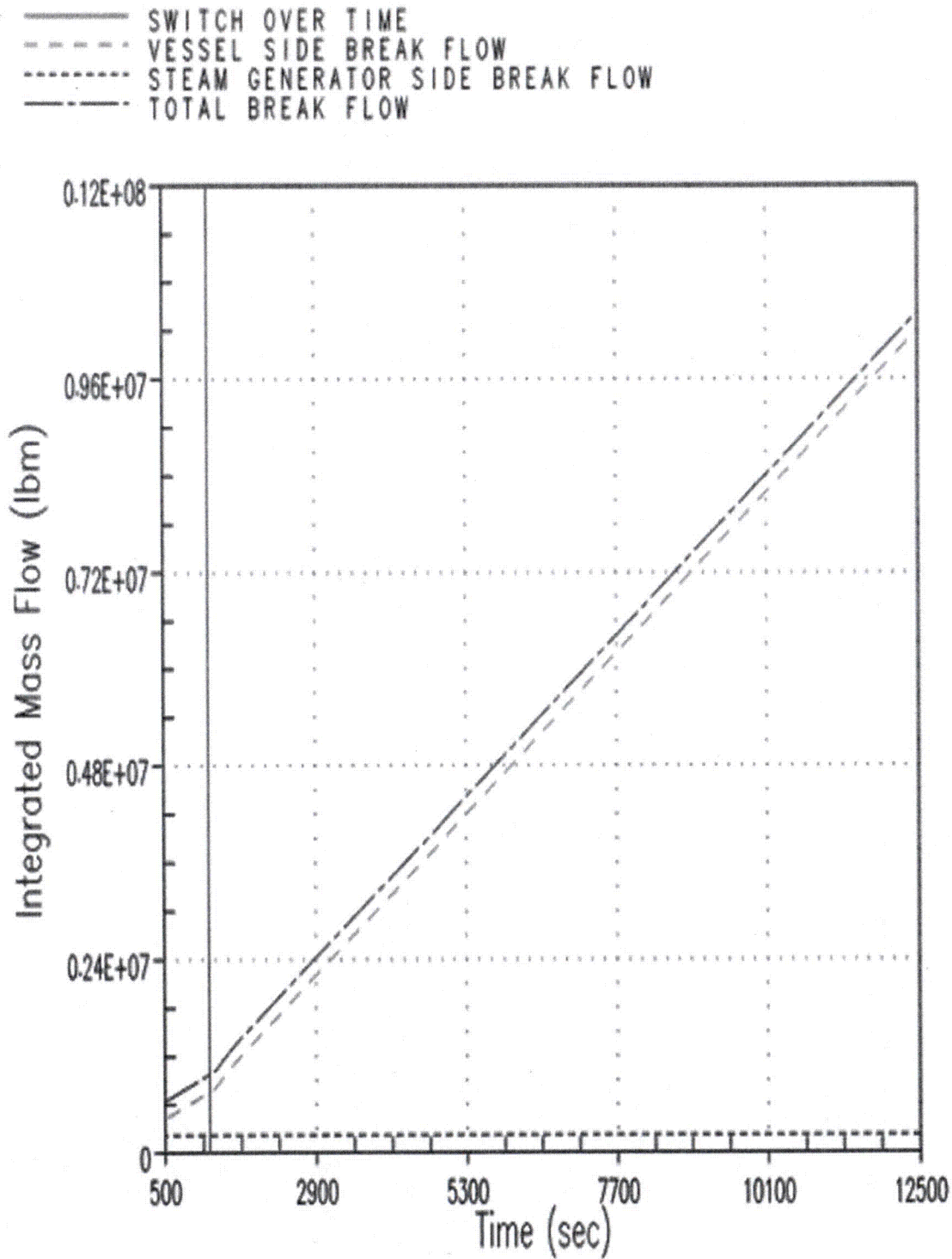
Figure 9-13 Case 0A – Integrated Mass Flow from the Break
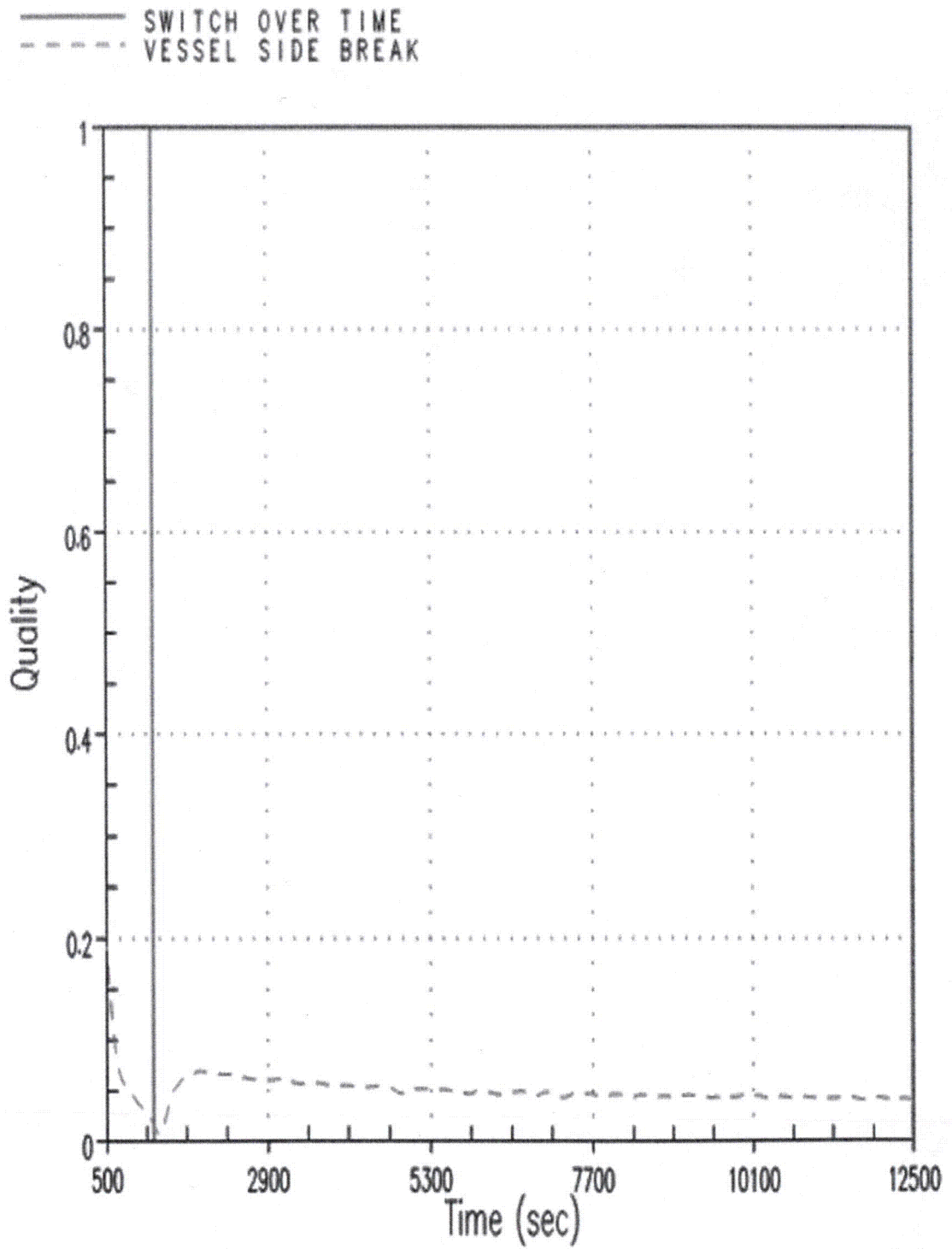
Figure 9-14 Case 0A – Break Exit Quality

9.2.2   After Debris Introduction – Calculation of t_{block}

Case 1A is used to determine t_{block}. This case does not apply any partial blockage to the core inlet prior to the application of complete core inlet blockage.

Throughout the duration of the transient, more-than-adequate core cooling flow is provided through the ECCS to the cold legs. Complete core inlet blockage is applied at 260 min (15,600 seconds). After the application of complete blockage, the ECCS flow backs up and fills the downcomer to the UHSN elevation. The ECCS continues to fill the RCS until the liquid level in the upper head reaches the upper guide tube elevation. At this point, coolant drains through the upper guide tubes into the UP where it is available to provide core cooling. Figure 9-15 shows that the core experiences a short-duration temperature excursion after the application of complete core inlet blockage; however, the PCT remains below 800°F. The temperature excursion occurs at the top of the core and is due to the delay time associated with filling the downcomer beyond the UHSN elevation. No coolant is being provided to the core while the downcomer is filling, which leads to dryout and core uncovery. Once the downcomer fills such that the UHSNs and upper guide tubes are active in providing coolant to the top of the core, the two-phase mixture level in the core is recovered as is the cladding temperature.

The RV fluid mass is shown in Figure 9-16. Prior to the application of complete core inlet blockage, the behavior is similar to that seen in the no blockage case. When complete core inlet blockage is applied, the simulation shows an initial reduction in RV fluid inventory, but the inventory quickly recovers and settles to a value that is greater than the RV fluid mass prior to complete blockage and remains fairly stable for the remainder of the transient. The increase in RV fluid volume after complete core inlet blockage can be attributed to the filling of the downcomer and resulting liquid inventory in the upper head. This trend is consistent with the behavior of the core collapsed liquid level as shown in Figure 9-17, which shows the hot assembly collapsed liquid level. The collapsed liquid levels in the other core channels show similar trends. The downcomer and upper head collapsed liquid levels are shown in Figure 9-18. When the blockage is applied, the downcomer collapsed liquid level quickly increases to the UHSN elevation due to the increased resistance at the core inlet. As a result, the upper head begins to flood with fluid from the downcomer and the total RV fluid mass increases due to the additional fluid in the upper downcomer and upper head.

The core inlet, guide tube and intact hot leg mass flow rates are compared to boil-off in Figure 9-19. The figure indicates that flow into the core is well in excess of boil-off prior to complete core inlet blockage. Flow from the RV to the intact hot legs exists prior to complete blockage and there is no liquid flow from the upper head to the UP through the guide tubes. After complete blockage, the core inlet flow is shown to decrease to zero. The intact hot leg flow is also shown to decrease, which is associated with the reduction in the core collapsed liquid level. The upper guide tube flow, which enters the top of the core, is shown to be in excess of boil-off and provides DHR.

The break exit quality is shown in Figure 9-20. The figure shows that the break exit quality remains below 60% after the application of complete core inlet blockage, which indicates a substantial amount of liquid carryover out the break. Due to the large amount of liquid carryover out the break, BAP is controlled and boron concentration levels in the RV will remain well below the solubility limit for the duration of the transient.

After complete blockage, core cooling is maintained due to flow from the upper downcomer into the upper head which drains through the upper guide tubes into the UP, where it is available to the top of the core. A review of the RV mixing patterns after complete core inlet blockage indicate that flow from the UP flows downward along the core periphery and feeds the average and hot assembly via cross flow. This trend is comparable to the core mixing patterns observed after complete core inlet blockage for the Westinghouse upflow plant category (discussed in Section 8).

SWITCH OVER TIME
COMPLETE BLOCKAGE
HOT ROD PCT
HOT ASSEMBLY PCT
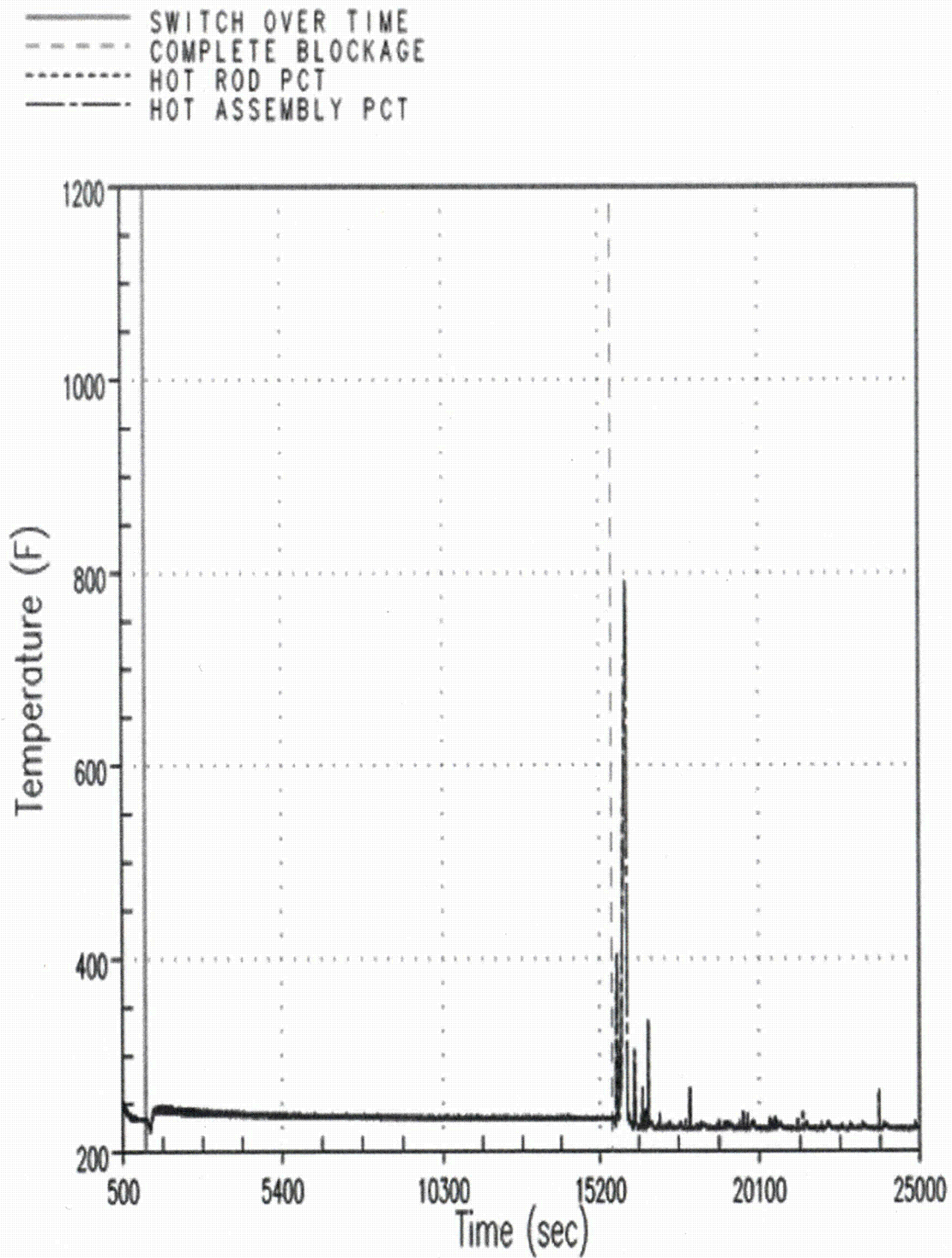
Figure 9-15 Case 1A – Hot Rod and Hot Assembly Peak Cladding Temperatures
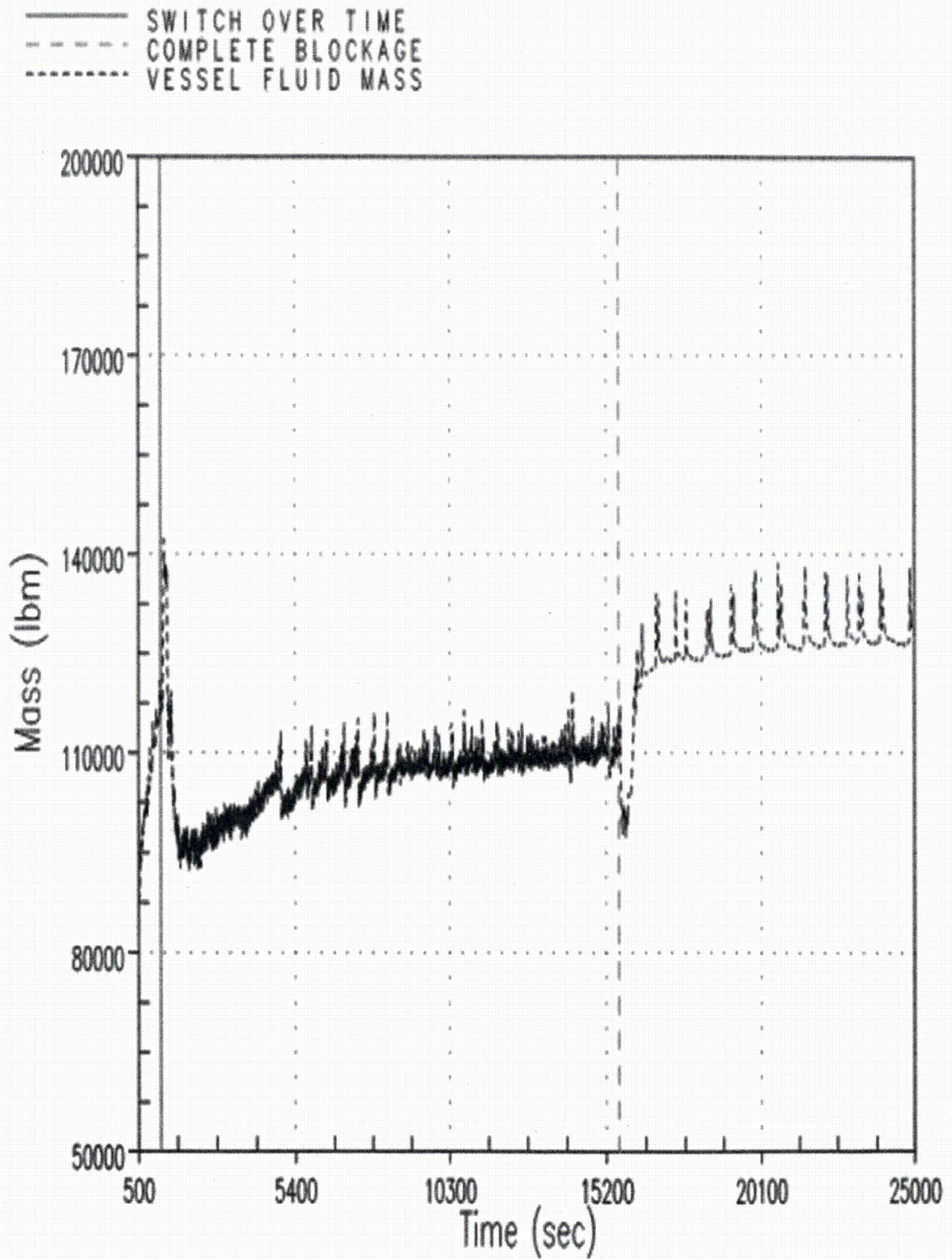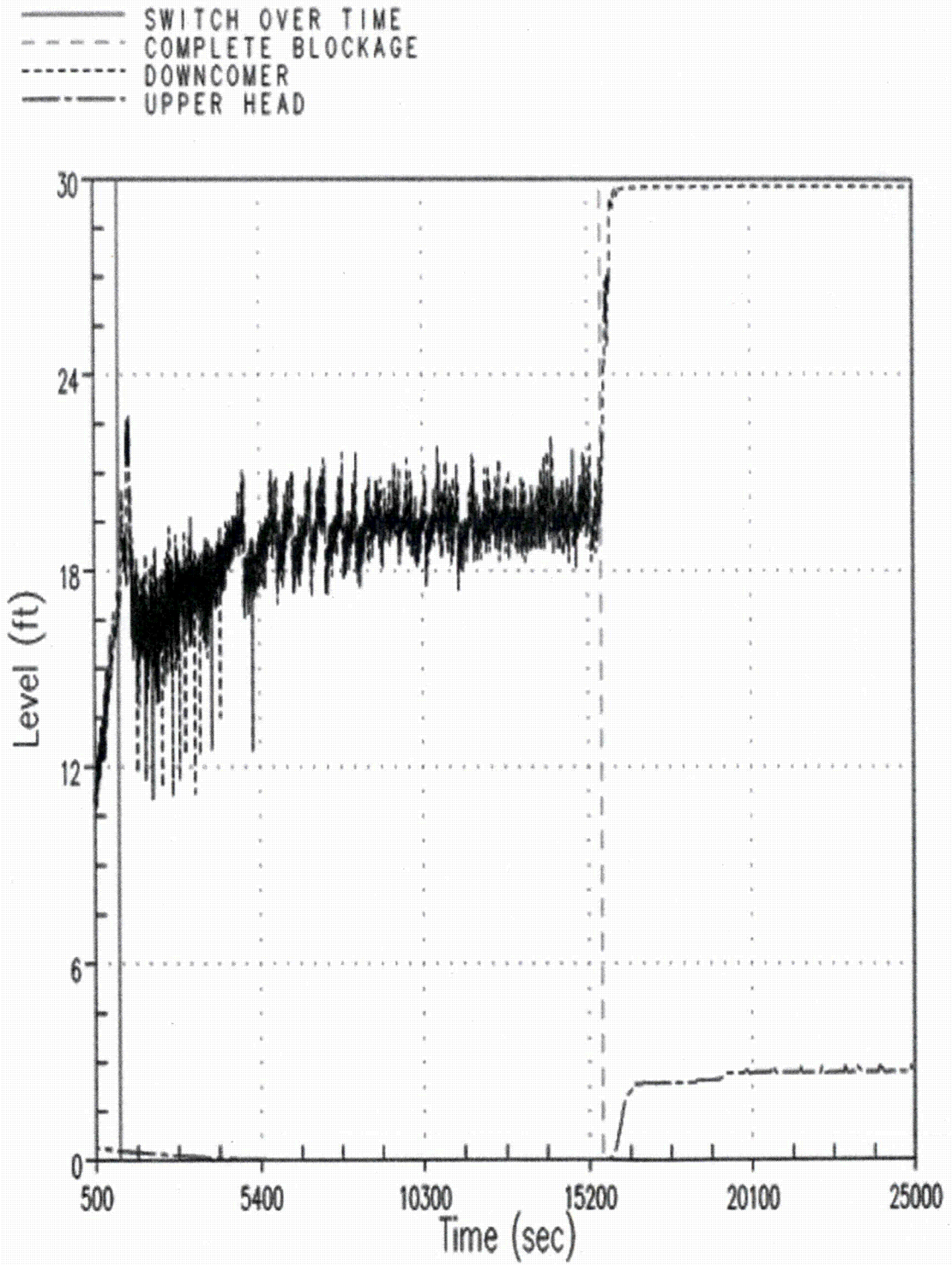
Figure 9-16 Case 1A – Reactor Vessel Fluid Mass

Figure 9-17 Case 1A – Hot Assembly Collapsed Liquid Level

Figure 9-18 Case 1A – Downcomer and Upper Head Collapsed Liquid Levels

```
——————  SWITCH OVER TIME
— · — · —  COMPLETE BLOCKAGE
· · · · · · ·  BOILOFF RATE
— · · —  CORE INLET FLOW RATE
— — —  GUIDE TUBE EXIT FLOW RATE
— —  INTACT HOT LEG FLOW RATE
```
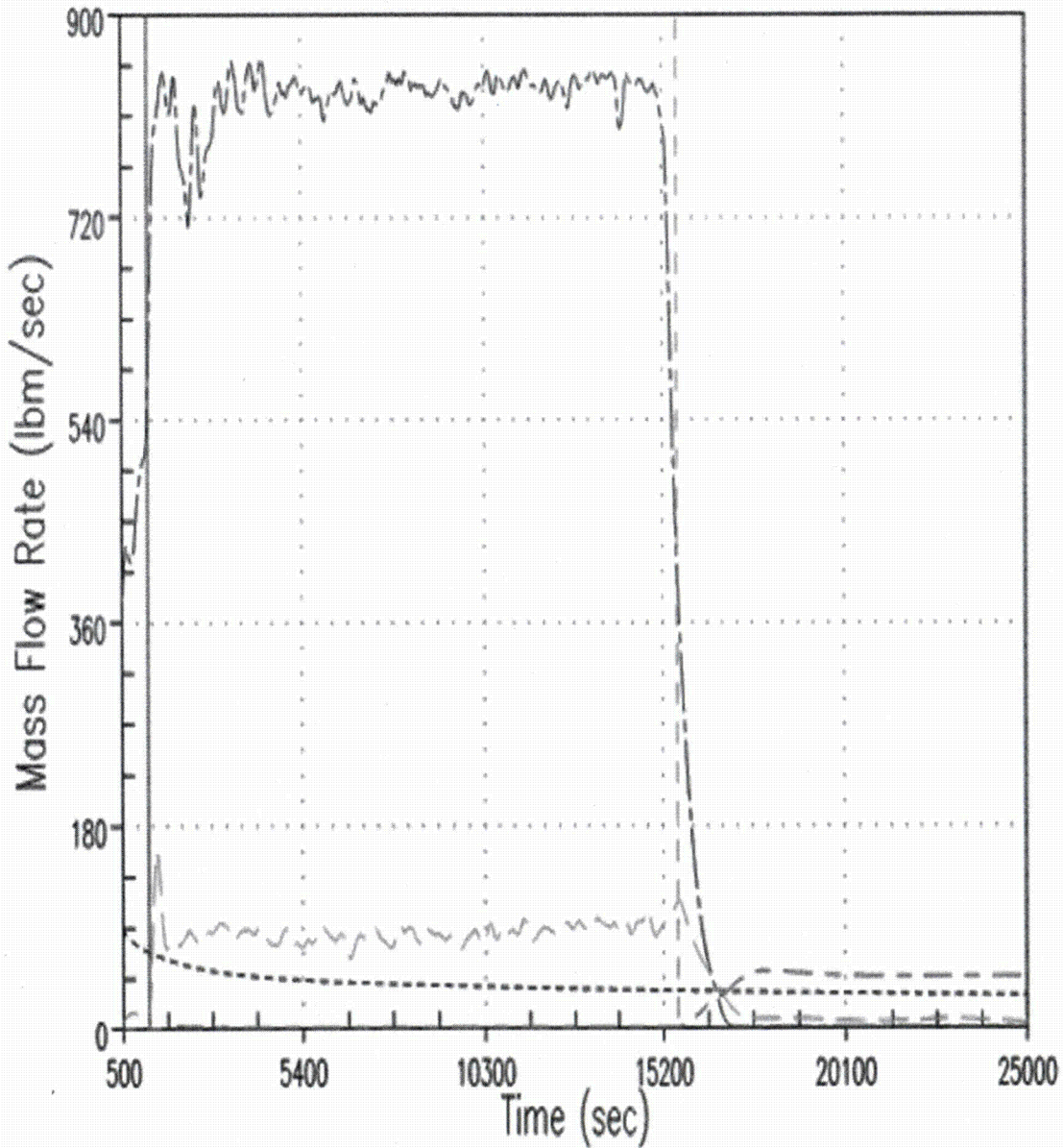
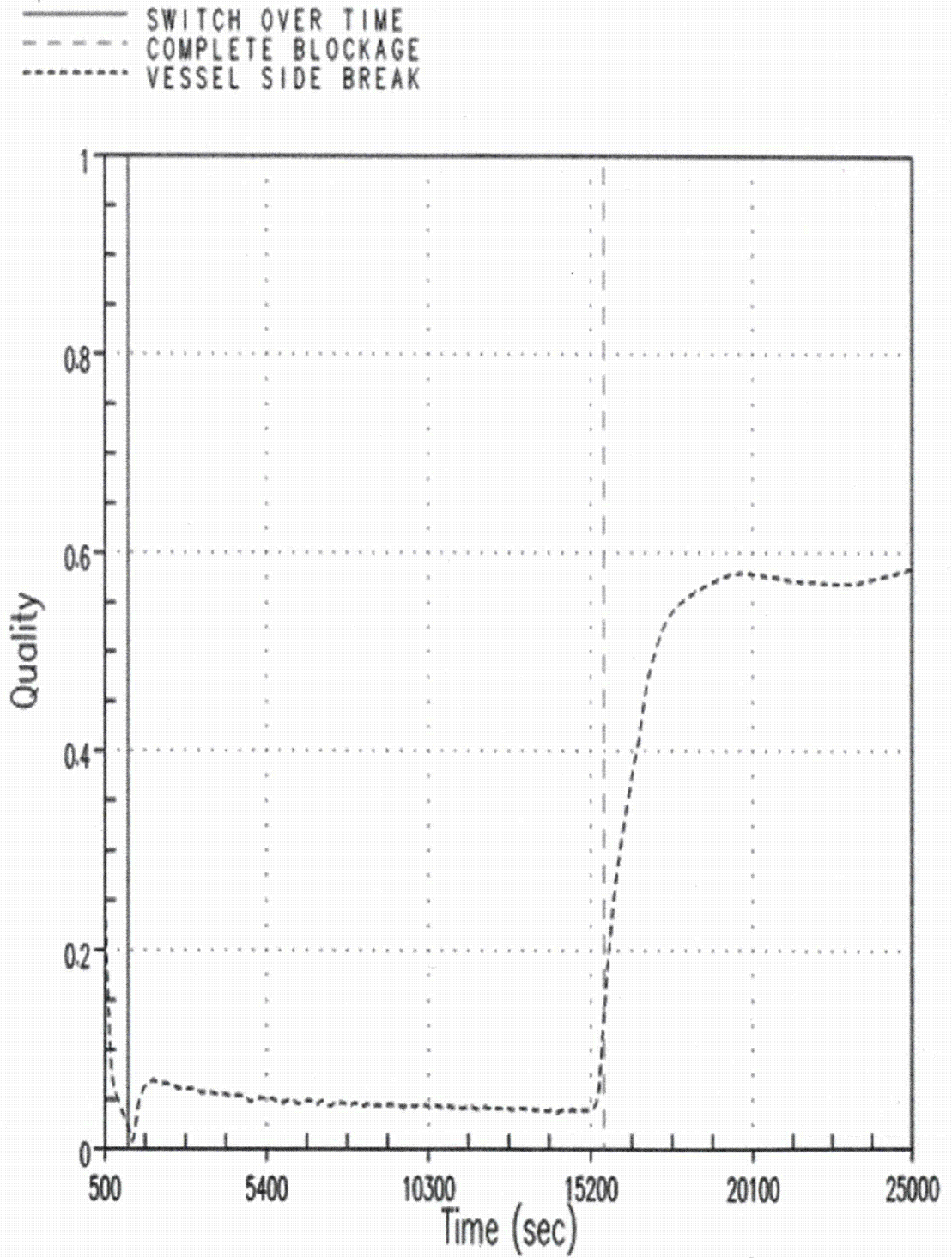Figure 9-19 Case 1A – Core Inlet, Guide Tube Exit, and Intact Hot legs Flow Rate Compared to Boil-off

Figure 9-20 Case 1A – Break Exit Quality

9.2.3   After Debris Introduction – Calculation of K_{max}

Cases 2A and 2B are used to determine a value for K_{max}. These cases apply partial blockage to the core inlet prior to the application of complete core inlet blockage. The partial blockages are applied instantaneously at the time of transfer to sump recirculation and are applied uniformly across all core channels. Case 2B produces the lowest K_{max} value and will be discussed in this section.

Throughout the duration of the transient, more-than-adequate core cooling flow is provided through the ECCS to the cold legs. The partial blockage is applied at 20 min (1200 seconds) and complete core inlet blockage is applied at 143 min (8580 seconds). After the partial blockage is applied, the RCS response is very similar to the response seen after complete core inlet blockage, as described in Section 9.2.2, except that flow continues through the core inlet at a reduced rate. Coolant from the ECCS backs-up and fills the downcomer to the UHSN elevation. From this point forward, the total flow entering the RV is split between the core inlet and the UHSNs. Figure 9-21 shows that the core experiences a short-duration temperature excursion after the application of partial core inlet blockage; however, PCT remains below 800°F. DHR is maintained via a combination of flow through the core inlet and flow through the UHSNs to the top of the core.

The RV fluid mass is shown in Figure 9-22. When partial core inlet blockage is applied, the response in RV fluid inventory is different compared to the no blockage and complete core inlet blockage cases (Case 0A and Case 1A). The no blockage and complete blockage cases showed a sharp decrease in RV inventory upon entry to sump recirculation due to the loss of ECCS subcooling. In this case, the initial decrease is not as sharp since the application of partial blockage results in an increase in the downcomer collapsed liquid level, which offsets the reduction in RV inventory due to the loss of ECCS subcooling. The application of complete core inlet blockage later in the transient has only minimal impact on the RV fluid inventory.   These trends are consistent with the behavior of the core collapsed liquid level as shown in Figure 9-23, which show the hot assembly collapsed liquid. The collapsed liquid levels in the other core channels show similar trends. The downcomer and upper head collapsed liquid levels are shown in Figure 9-24. When the blockage is applied, the downcomer collapsed liquid level quickly increases to the UHSN elevation due to the increased resistance at the core inlet. As a result, the upper head begins to flood with fluid from the downcomer and the total RV fluid mass increases due to the additional fluid in the upper downcomer and upper head.

The core inlet mass flow rate and guide tube exit flow rate are compared to boil-off in Figure 9-25. The figure indicates that flow in excess of boil-off is maintained through the core inlet even after the application of the partial blockage. It is not until complete core inlet blockage is applied that the core inlet flow decreases to zero. In terms of guide tube flow, it is seen that after partial blockage, there is a delay associated with filling the downcomer and upper head to the upper guide tube elevation, after which liquid flow through the guide tubes begins. After complete core inlet blockage is applied, the amount of flow through the guide tubes is equivalent to boil-off.

Figure 9-26 shows the pressure drop across the debris bed and the core inlet liquid velocities. The figure confirms that flow through the core inlet continues after the application of partial blockage and ceases after the application of complete core inlet blockage.

The break exit quality is shown in Figure 9-27. This figure shows that the quality prior to the application of partial core inlet blockage remains below 10%. After the application of partial blockage, the case shows a spike in the break quality (consistent with the core uncovery), which recovers and stabilizes at approximately 40% prior to the application of complete core inlet blockage. When complete core inlet blockage is applied, the break exit quality increases sharply and then recovers to a value of roughly 50%. Due to the large amount of liquid carryover out the break during the transient, BAP is controlled and boron concentrations in the RV will remain well below the solubility limit.

A review of the RV mixing patterns after complete core inlet blockage indicates that flow from the UP flows downward along the core periphery and feeds the average and hot assembly via cross flow. This trend is comparable to the core mixing patterns observed after complete core inlet blockage for the Westinghouse upflow plant category (discussed in Section 8).
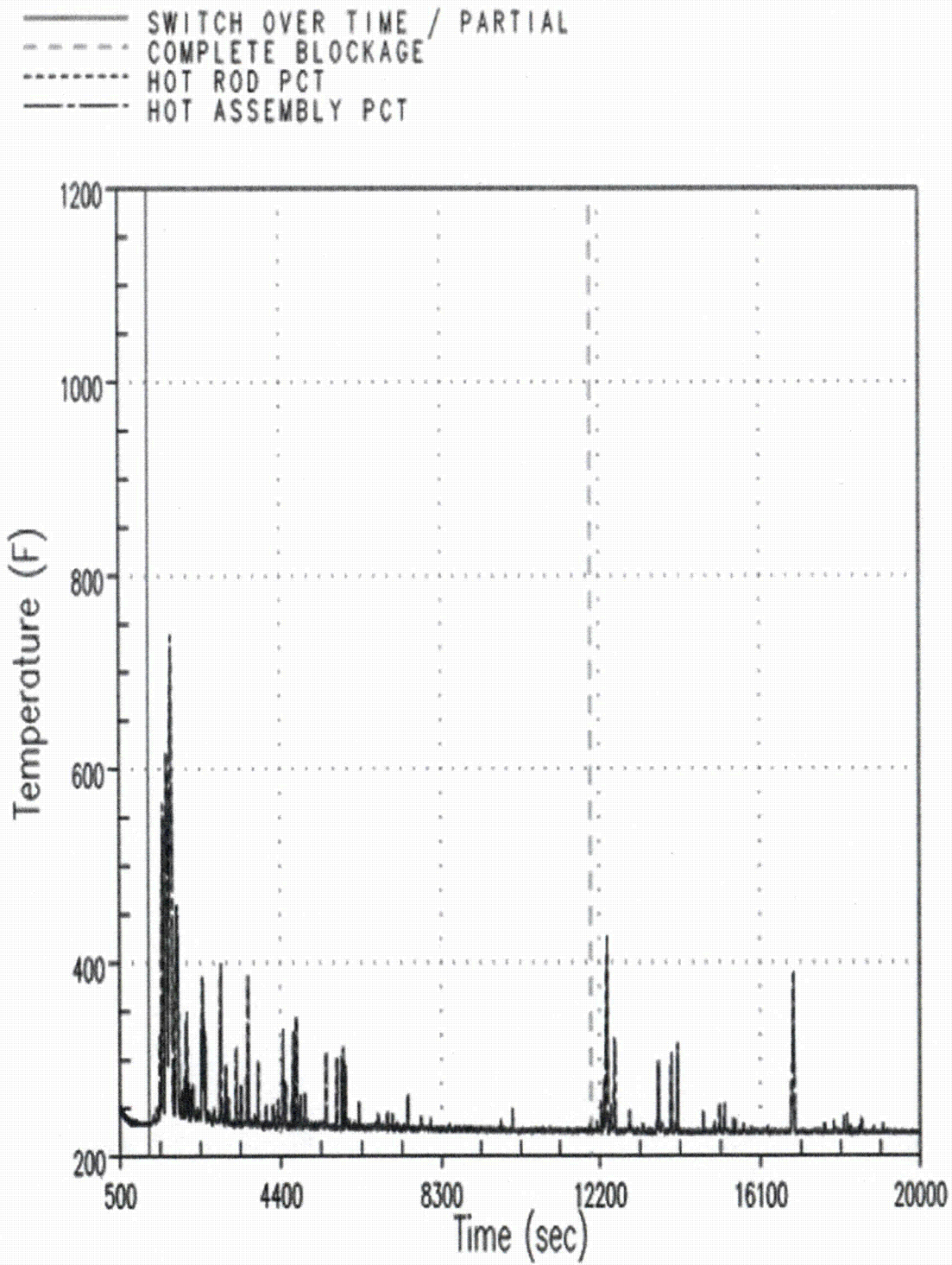
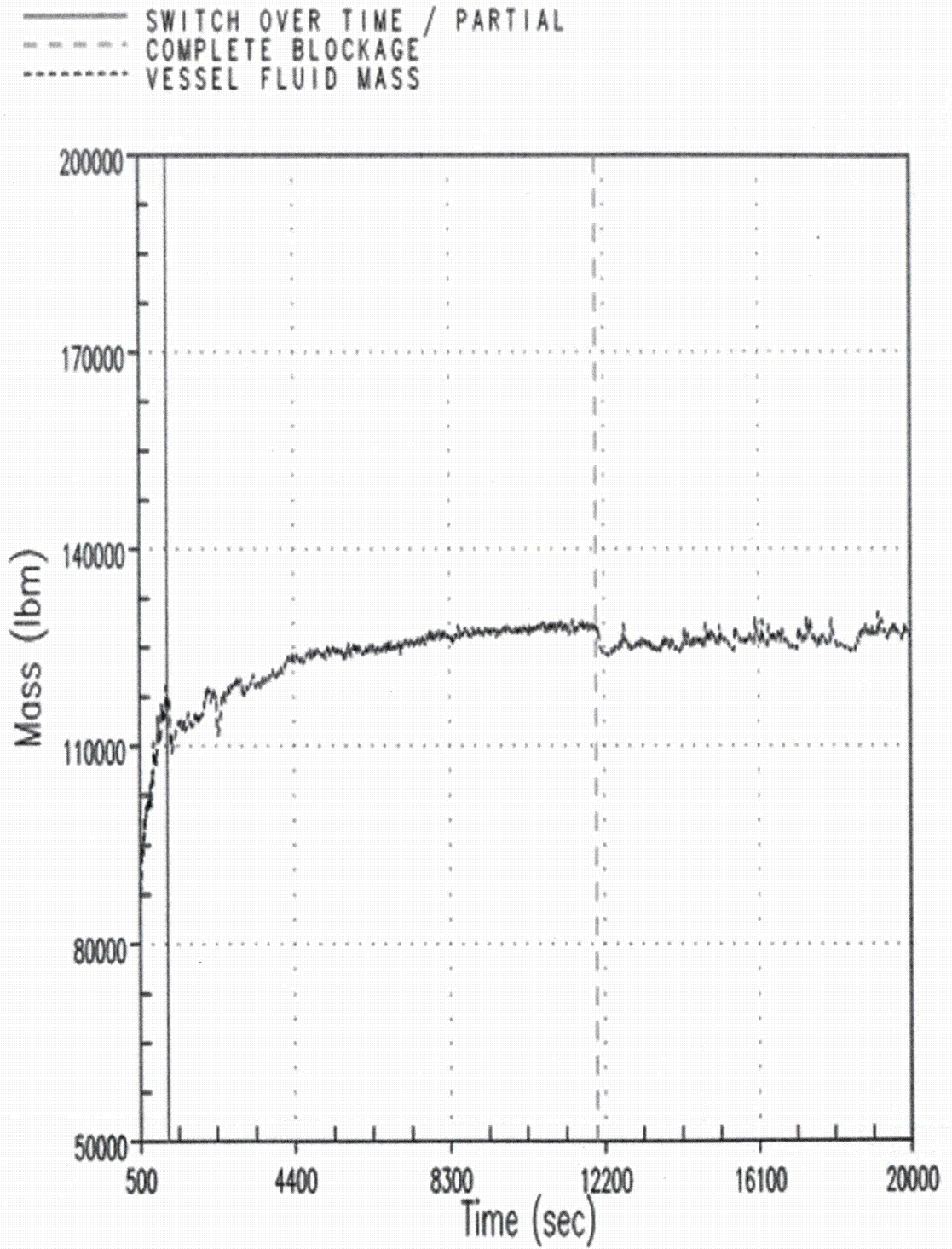**Figure 9-21 Case 2B – Hot Rod and Hot Assembly Peak Cladding Temperatures**
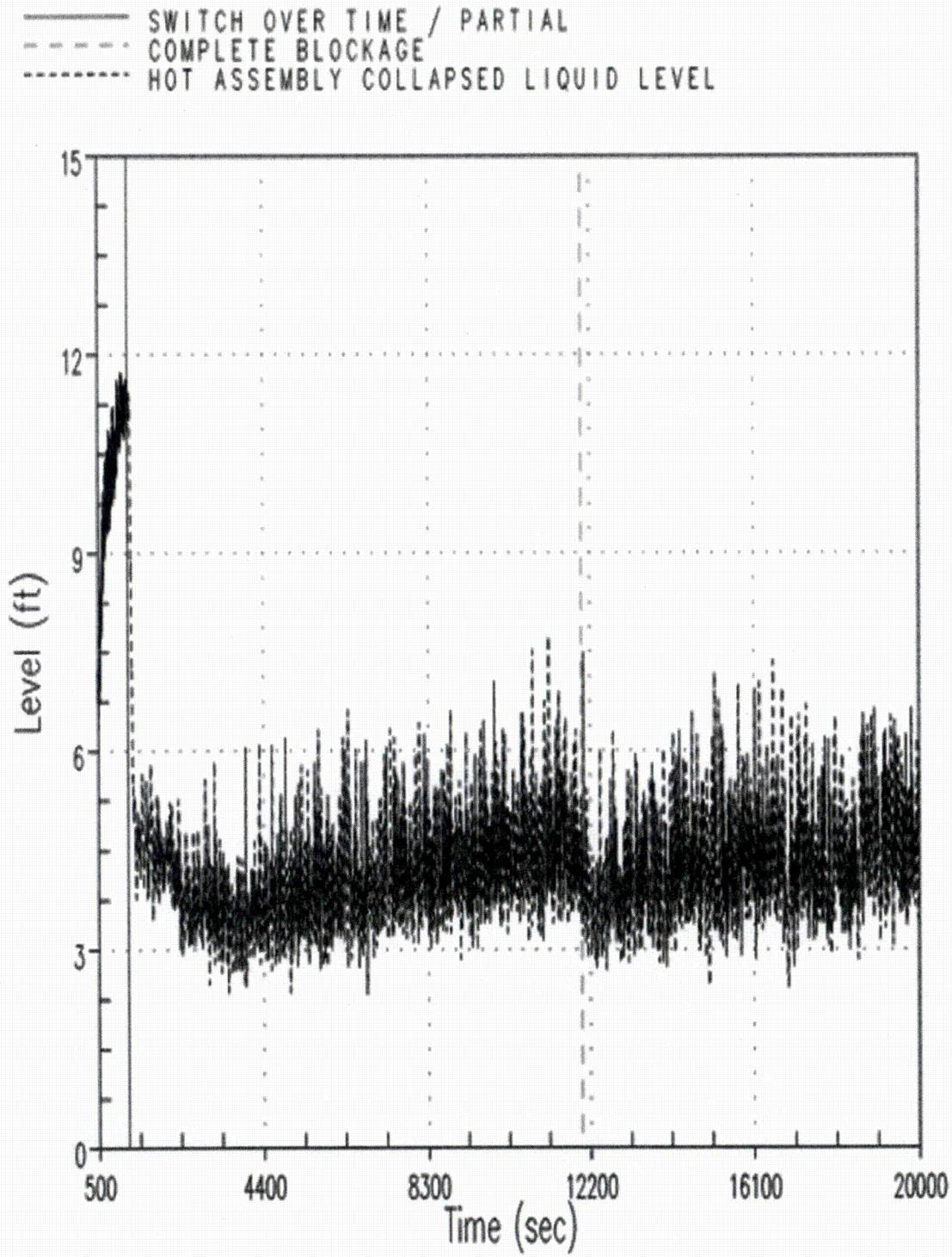
Figure 9-22 Case 2B – Reactor Vessel Fluid Mass

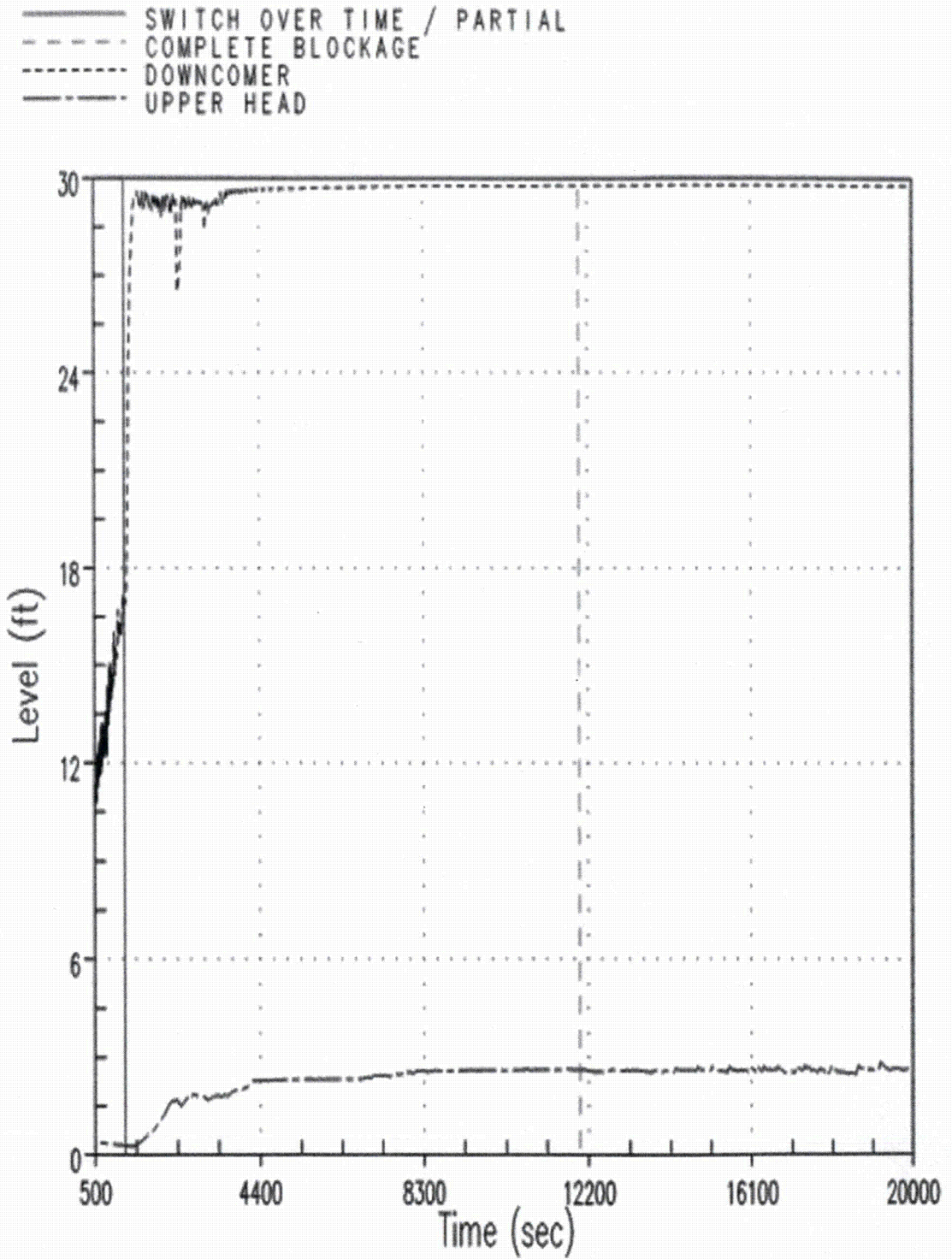Figure 9-23 Case 2B – Hot Assembly Collapsed Liquid Level
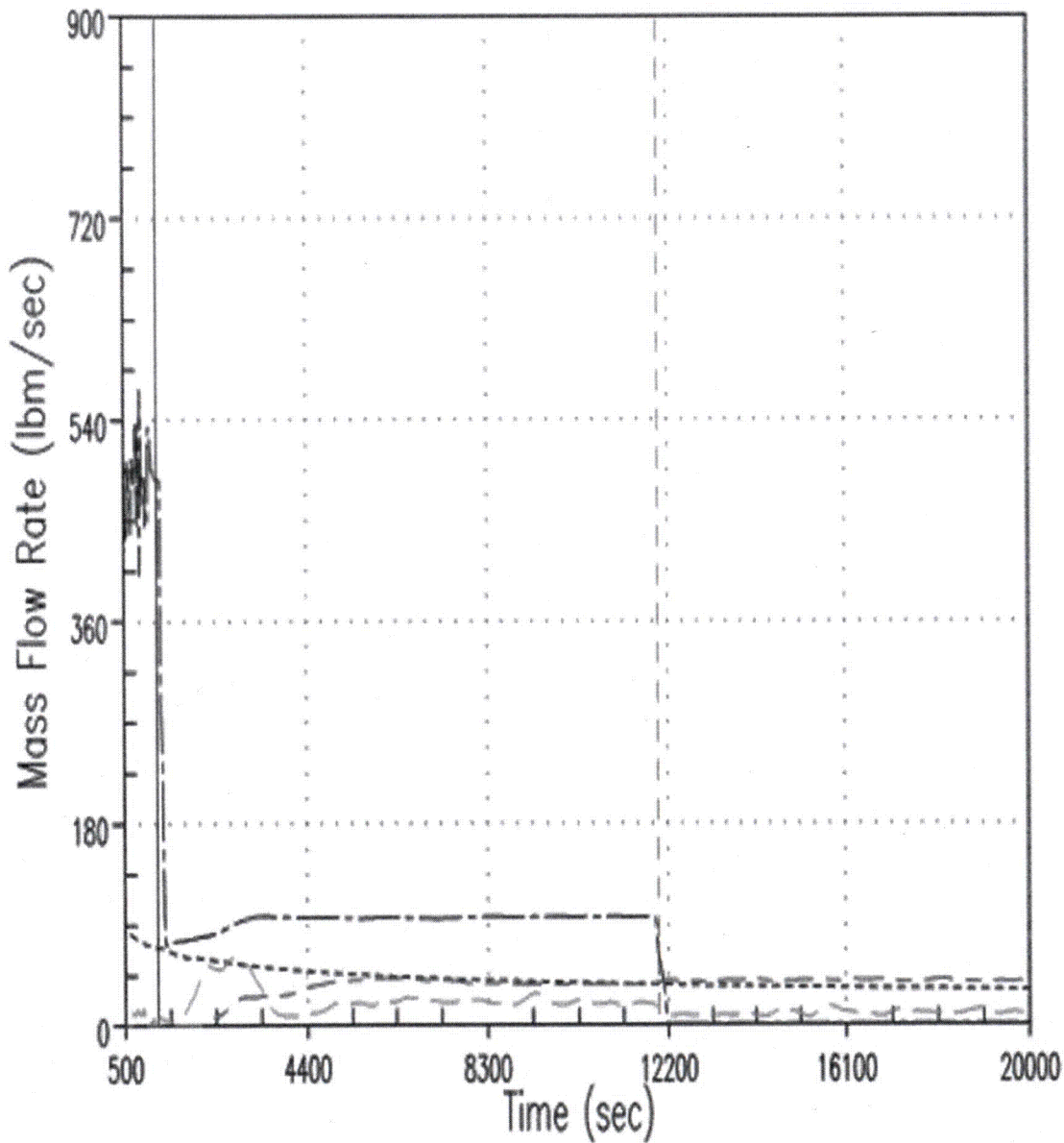
Figure 9-24 Case 2B – Downcomer and Upper Head Collapsed Liquid Levels

Figure 9-25 Case 2B – Core Inlet, Guide Tube Exit, and Intact Hot legs Flow Rate Compared to Boil-off

Pressure (psi)
⎯⎯⎯⎯ SWITCH OVER TIME / PARTIAL
— — — — COMPLETE BLOCKAGE
-------- DEBRIS BED PRESSURE DROP
Velocity (ft/sec)
⎯·⎯·⎯· LOW POWER INLET LIQUID VELOCITY
— —— — AVERAGE NON-GUIDE TUBE INLET LIQUID VELOCITY
⎯ ⎯ ⎯ AVERAGE GUIDE TUBE INLET LIQUID VELOCITY
⎯··⎯··⎯ HOT ASSEMBLY INLET LIQUID VELOCITY
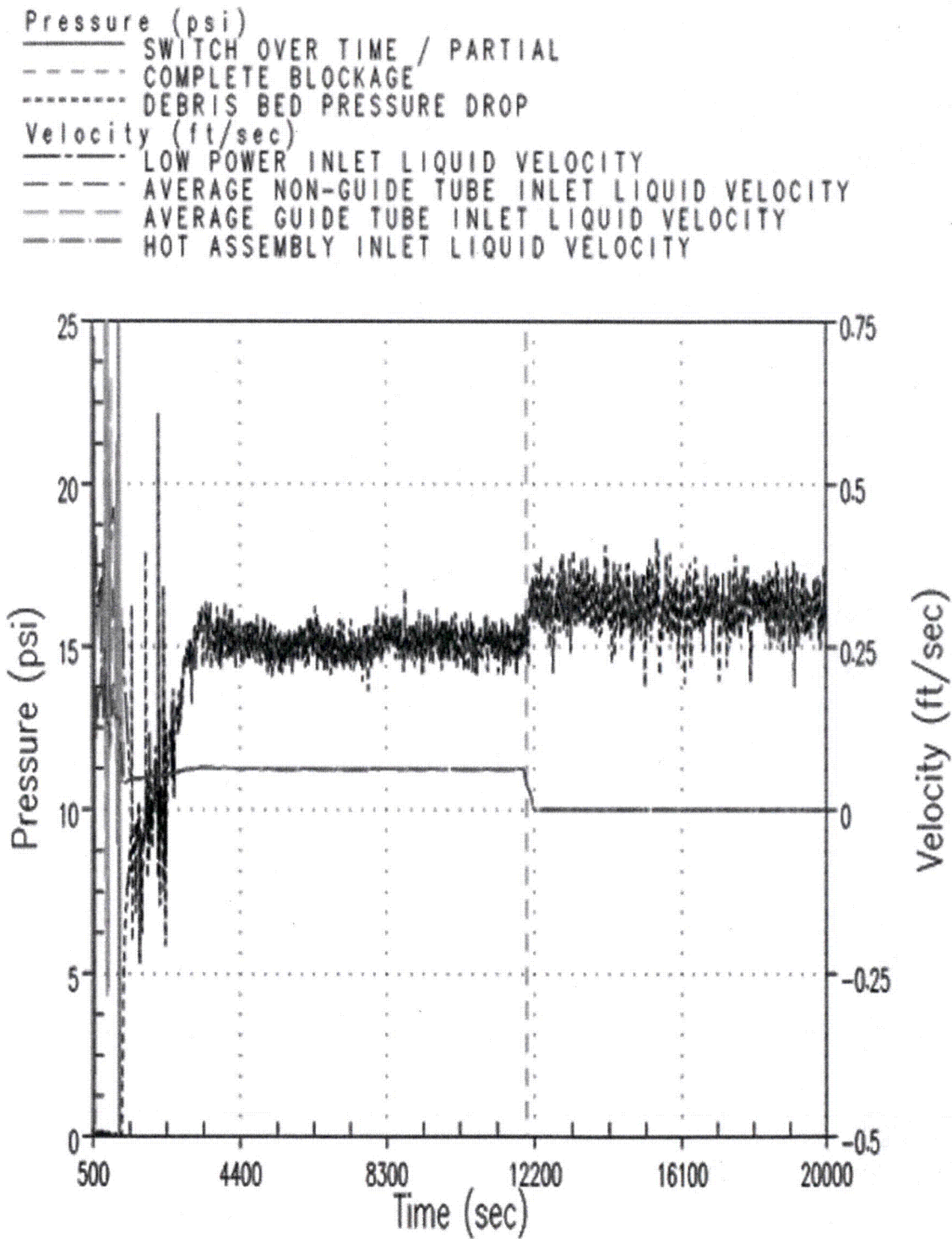
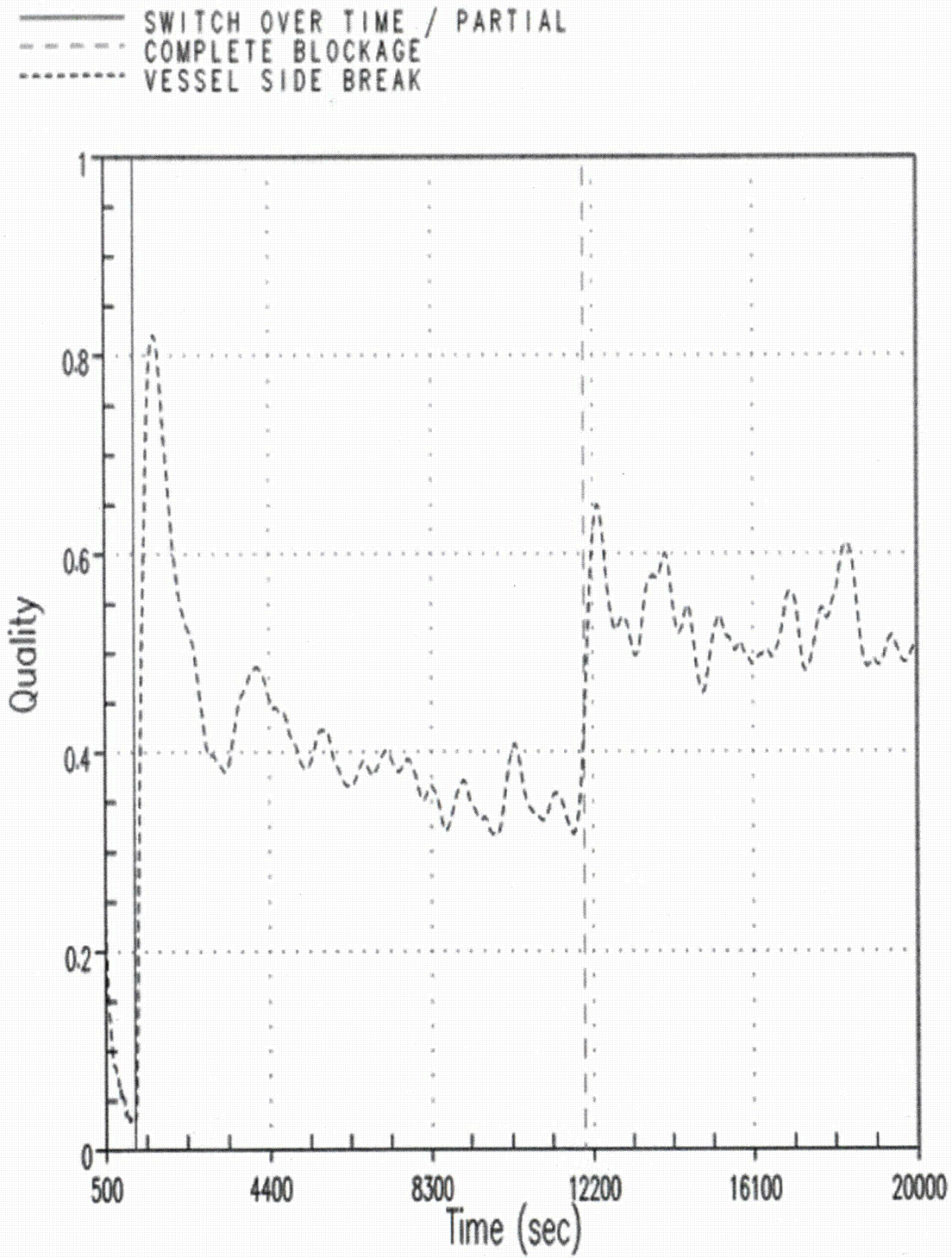**Figure 9-26 Case 2B – Pressure Drop across Debris Bed and Core Inlet Liquid Velocities**

Figure 9-27 Case 2B – Break Exit Quality

9.2.4   After Debris Introduction – Calculation of K_{split} and m_{split}

Five additional cases were run to determine K_{split} and m_{split}. For these cases, a linear ramp in resistance was applied at the core inlet and complete core inlet blockage was not simulated. Since these cases were used to assess the timing of the activation of the UHSN AFP, the build-up of core inlet resistance was applied more slowly compared to the cases used to determine K_{max}. As a result, the RCS response to core inlet blockage was much slower in that the downcomer fill rate and the activation of the UHSNs occurred over a longer period of time. It is noted that these simulations are more realistic with regard to the timing at which debris is expected to arrive at the core inlet.

Even though five simulations were completed to cover the full range of ECCS flows expected during sump recirculation, only the high-, mid-, and low-flow cases are selected for discussion in this section. Similar trends were observed in the two cases not discussed.

9.2.4.1   Case 1 – 40 gpm/FA

Select transient plots from Case 1 are shown in Figures 9-28 through 9-31. The RCS response to core inlet blockage was expected and is generally consistent with the transient response described in Section 9.2.3. Figure 9-28 shows the core inlet, UHSN, and guide tube flow rates compared to boil-off. The figure demonstrates that flow to the core is well above boil-off during the entire transient. The flow response to core inlet blockage is also shown by the figure. As core inlet blockage is applied, the pressure drop across the core inlet increases. Once K_{split} is reached, the UHSN and guide tube flow rate becomes positive and increases as the magnitude of core inlet blockage increases. As a result, the core inlet flow rate decreases consistent with the rate that the UHSN flow rate increases.

Figure 9-29 shows the transient downcomer and upper head collapsed liquid levels. As core inlet blockage is applied, the downcomer collapsed liquid level increases as expected. When K_{split} is reached, the downcomer collapsed liquid level has reached the UHSN elevation, and the upper head begins to flood. After a short delay, the upper head fills to the guide tube elevation, and coolant begins to enter the guide tubes and flows downward into the UP region of the RV.

The PCT transient is shown in Figure 9-30. The figure indicates that the PCT remains well below 800°F, and the lack of any significant heatups indicates that the core never uncovers after application of core inlet resistance.

Figure 9-31 shows the calculated pressure drop across the core inlet and the core inlet liquid velocity. As expected, the core inlet velocity decreases after K_{split} and the pressure drop across the simulated debris bed continues to increase.
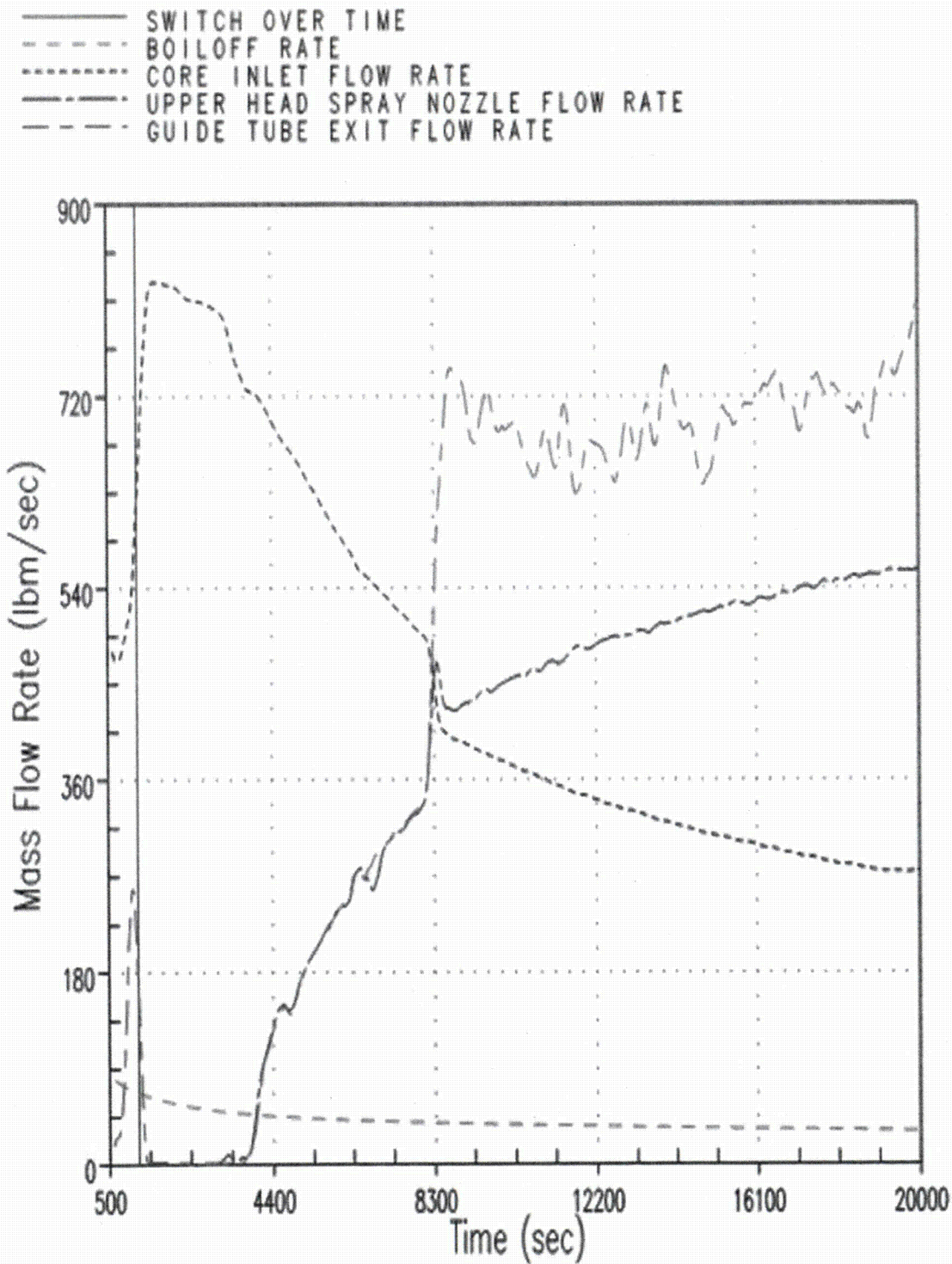
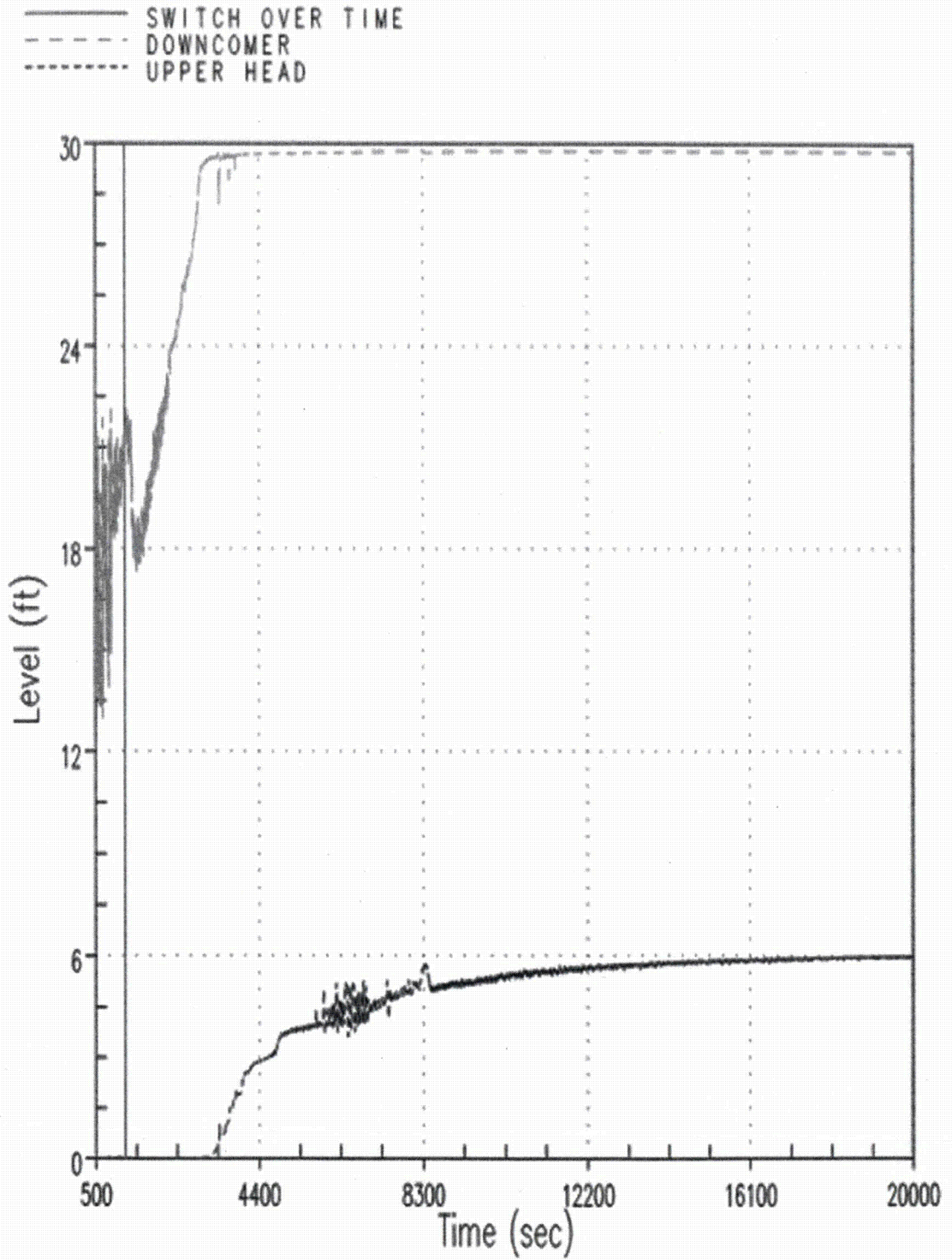**Figure 9-28 K_split Case 1 – Core Inlet and Upper Head Spray Nozzle Flow Rates Compared to Boil-off**

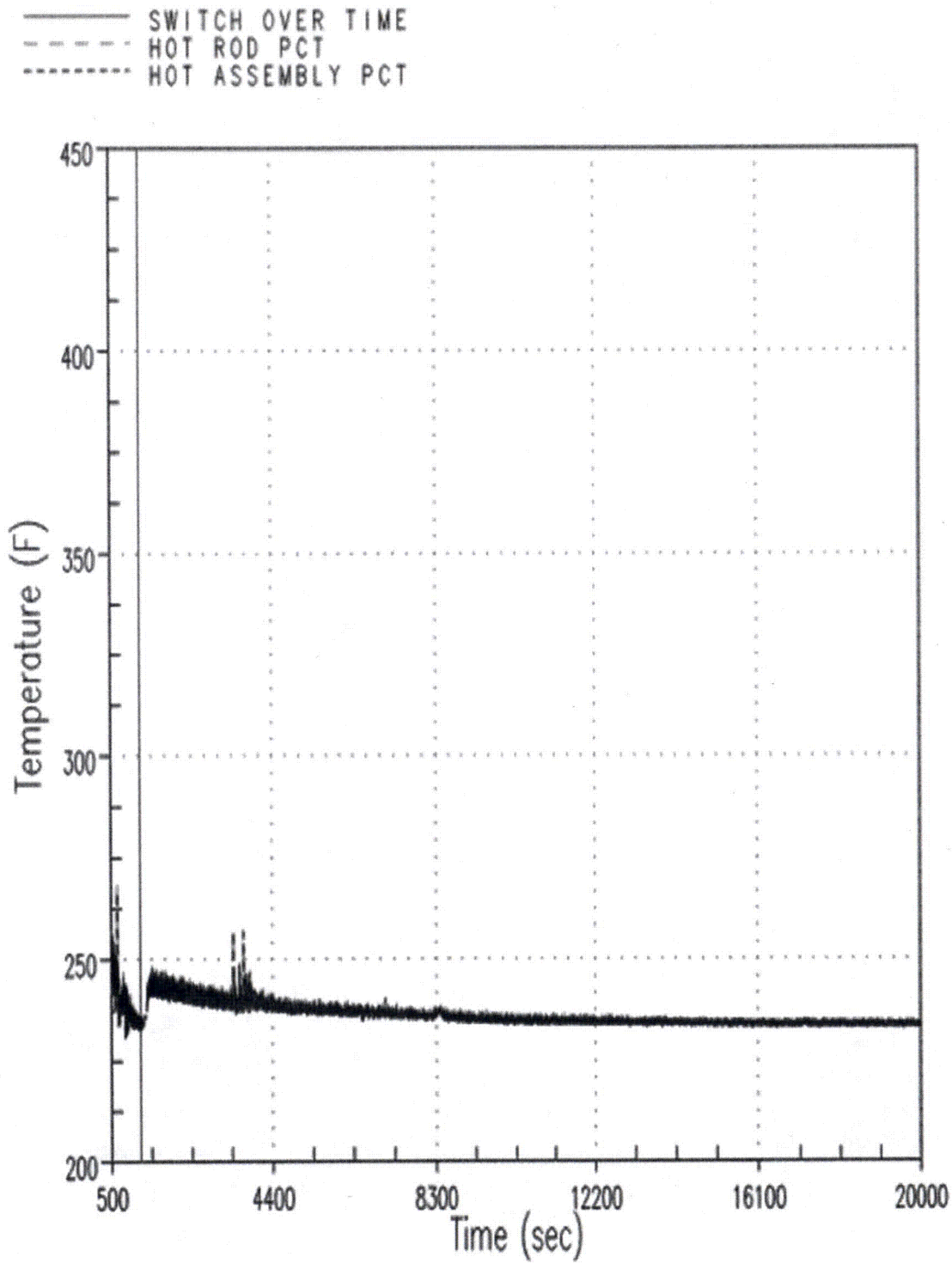**Figure 9-29 K_{split} Case 1 – Downcomer and Upper Head Collapsed Liquid Levels**

Figure 9-30 K$_{split}$ Case 1 – Hot Rod and Hot Assembly Peak Cladding Temperatures
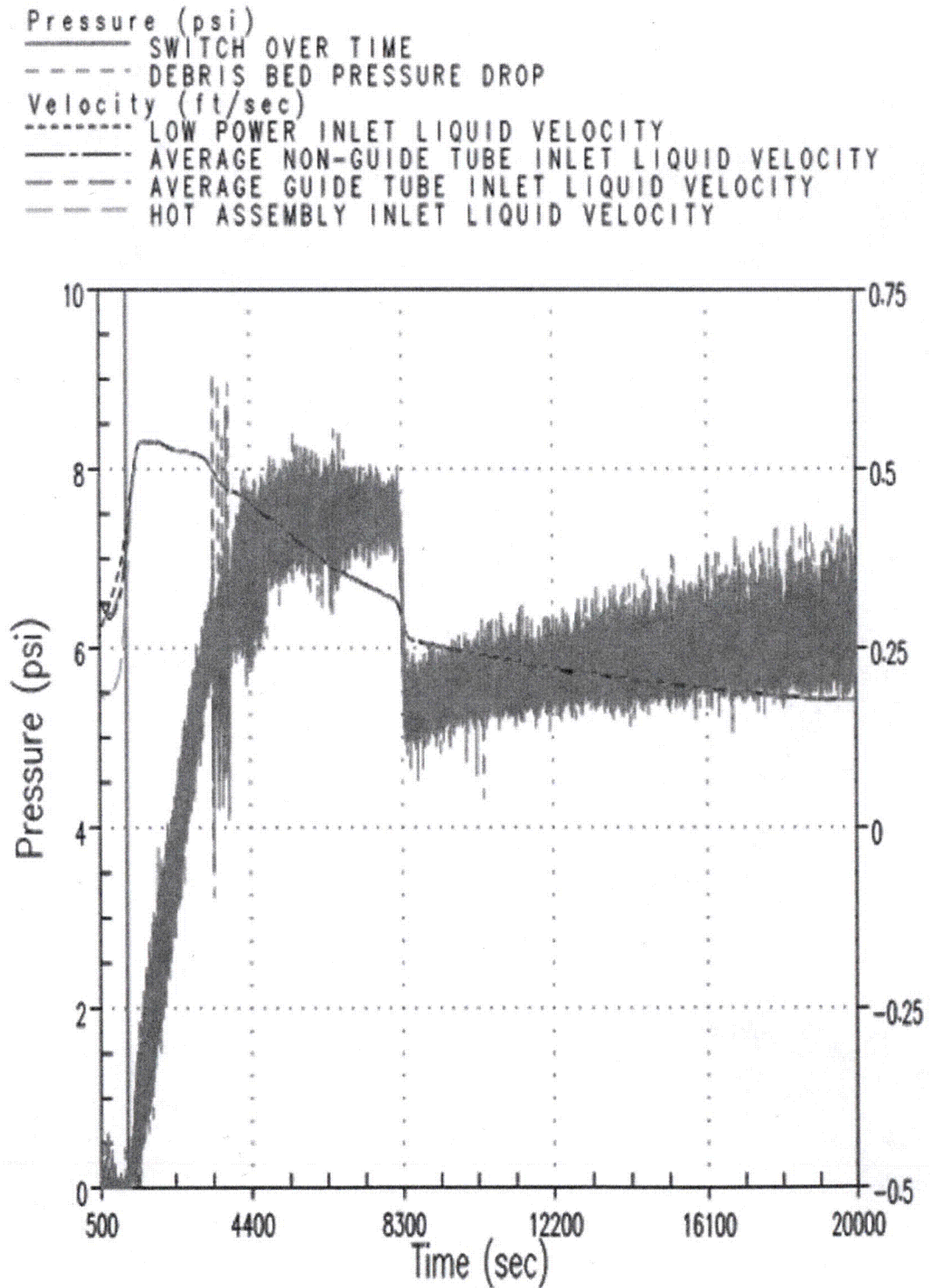
Pressure (psi)
——————— SWITCH OVER TIME
— · — · — DEBRIS BED PRESSURE DROP
Velocity (ft/sec)
·········· LOW POWER INLET LIQUID VELOCITY
— · · — AVERAGE NON-GUIDE TUBE INLET LIQUID VELOCITY
— · — · AVERAGE GUIDE TUBE INLET LIQUID VELOCITY
— — — HOT ASSEMBLY INLET LIQUID VELOCITY

Figure 9-31 K_{split} Case 1 – Debris Bed Pressure Drop and Core Inlet Liquid Velocity

9.2.4.2   Case 3 – 18 gpm/FA

Select transient plots from Case 3 are shown in Figures 9-32 through 9-35. The RCS response to core inlet blockage was expected and is generally consistent with the transient response shown in Section 9.2.3. Figure 9-32 shows the core inlet, UHSN, and guide tube flow rates compared to boil-off. The figure demonstrates that flow to the core is well above boil-off during the entire transient. The flow response to core inlet blockage is also shown by the figure. As core inlet blockage is applied, the pressure drop across the core inlet increases. Once K_{split} is reached, the UHSN and guide tube flow rate becomes positive and increases as the magnitude of core inlet blockage increases. As a result, the core inlet flow rate decreases consistent with the rate that the UHSN flow rate increases.

Figure 9-33 shows the transient downcomer and upper head collapsed liquid levels. As core inlet blockage is applied, the downcomer collapsed liquid level increases as expected. When K_{split} is reached, the downcomer collapsed liquid level has reached the UHSN elevation, and the upper head begins to flood. After a short delay, the upper head fills to the guide tube elevation, and coolant begins to enter the guide tubes and flows downward into the UP region of the RV. Comparing this flow response to the high-flow case described previously, it can be shown that reducing the ECCS flow results in a longer time period to reach K_{split}.

The PCT transient is shown in Figure 9-34. The figure indicates that the PCT remains well below 800°F and the lack of any significant heatups indicates that the core never uncovers after application of core inlet resistance.

Figure 9-35 shows the calculated pressure drop across the core inlet and the core inlet liquid velocity. As expected, the core inlet velocity decreases as the pressure drop across the simulated debris bed increases.
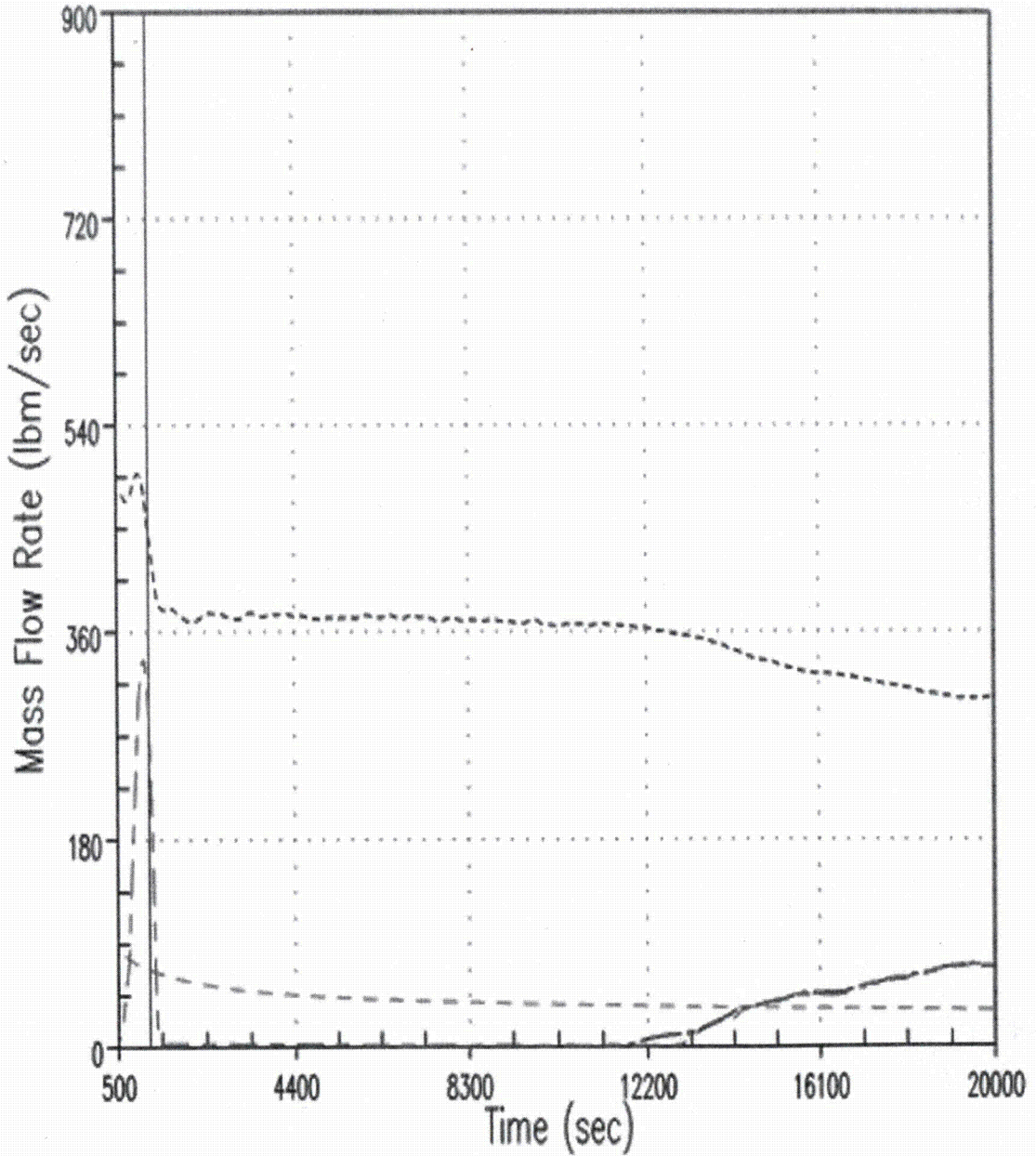
Figure 9-32 K$_{split}$ Case 3 – Core Inlet and Upper Head Spray Nozzle Flow Rates Compared to Boil-off
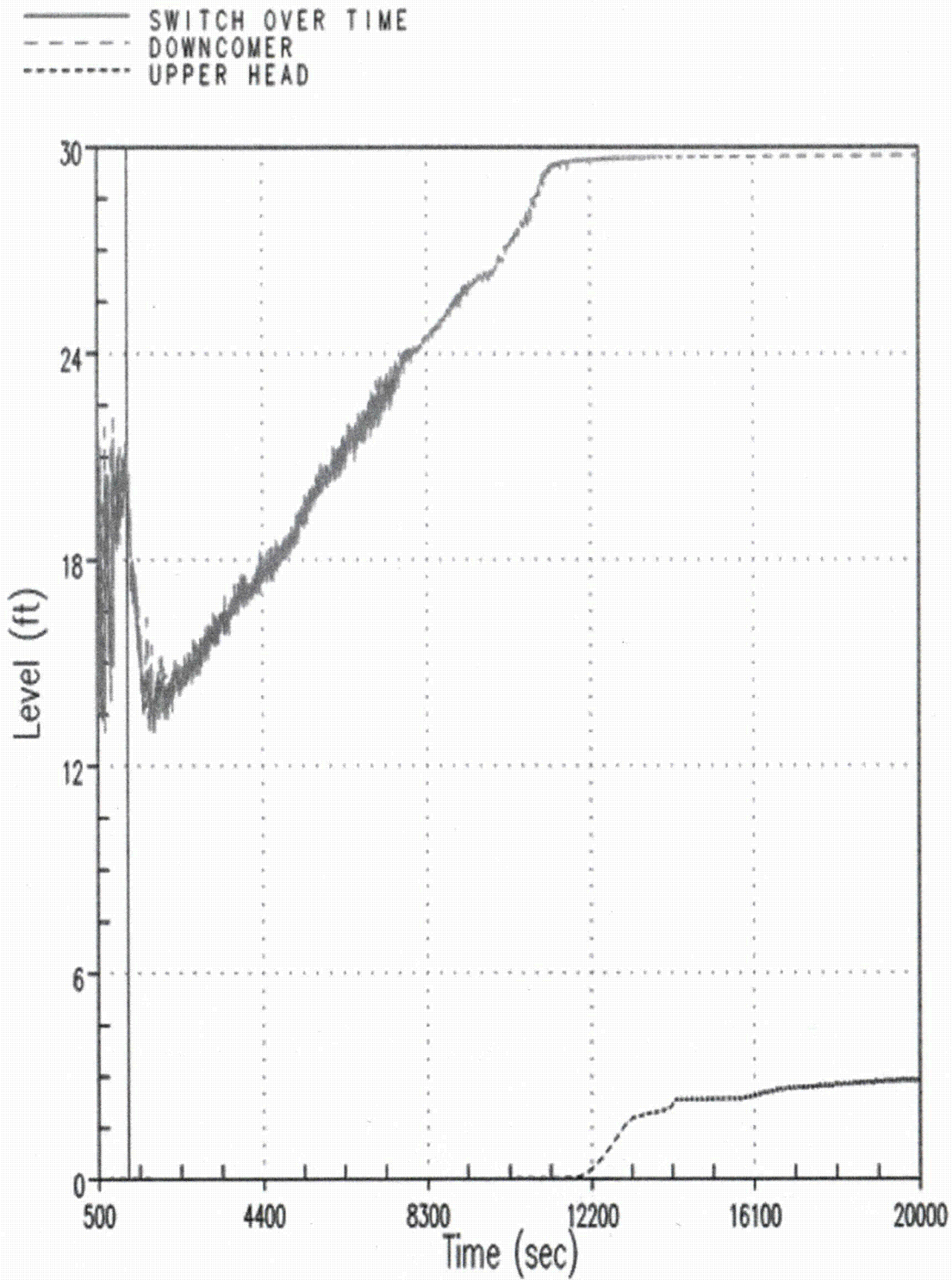
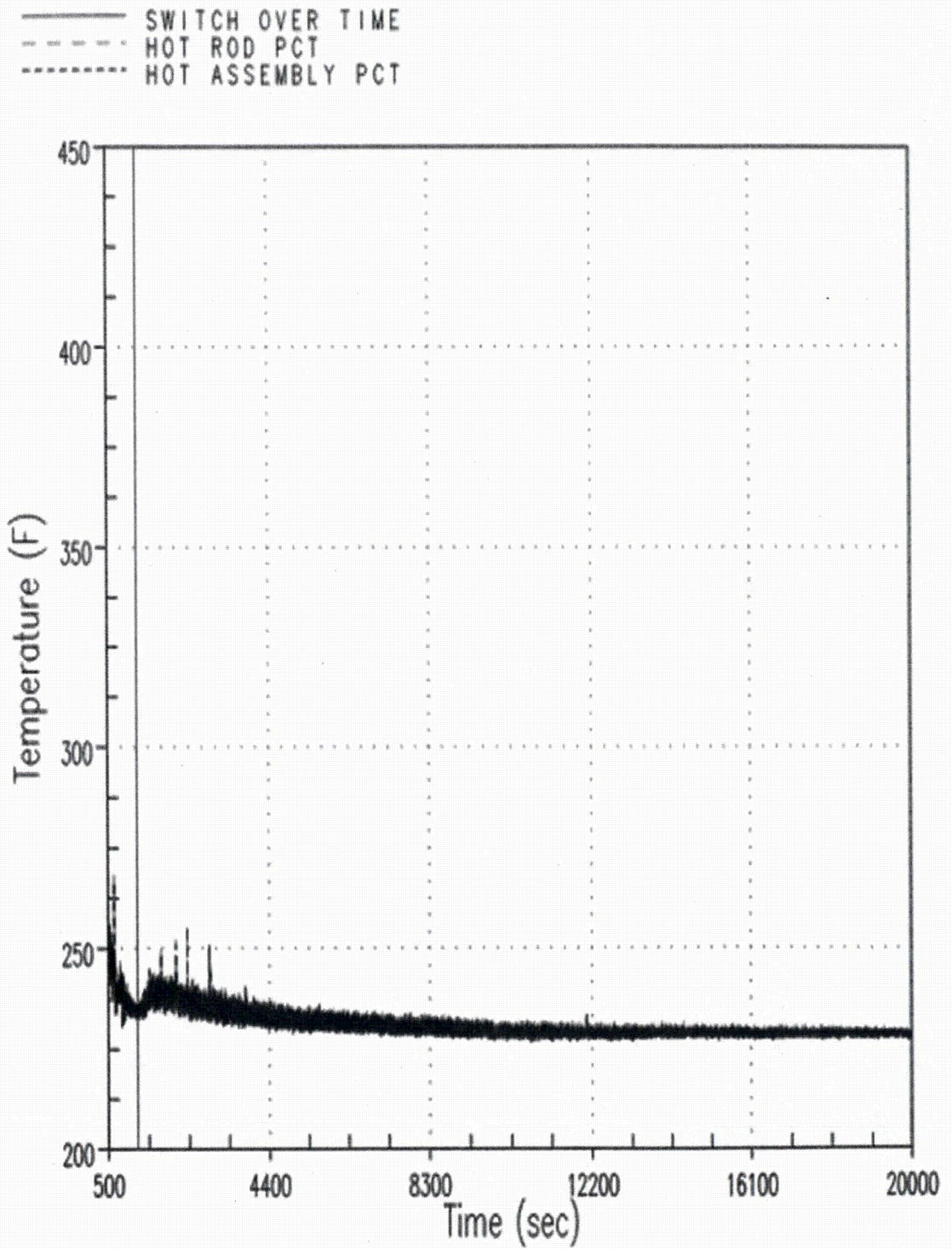**Figure 9-33 K_{split} Case 3 – Downcomer and Upper Head Collapsed Liquid Levels**

Figure 9-34 K_{split} Case 3 – Hot Rod and Hot Assembly Peak Cladding Temperatures

Pressure (psi)
——————— SWITCH OVER TIME
— — — — — DEBRIS BED PRESSURE DROP
Velocity (ft/sec)
———————— LOW POWER INLET LIQUID VELOCITY
— · — · — · AVERAGE NON-GUIDE TUBE INLET LIQUID VELOCITY
— — — — AVERAGE GUIDE TUBE INLET LIQUID VELOCITY
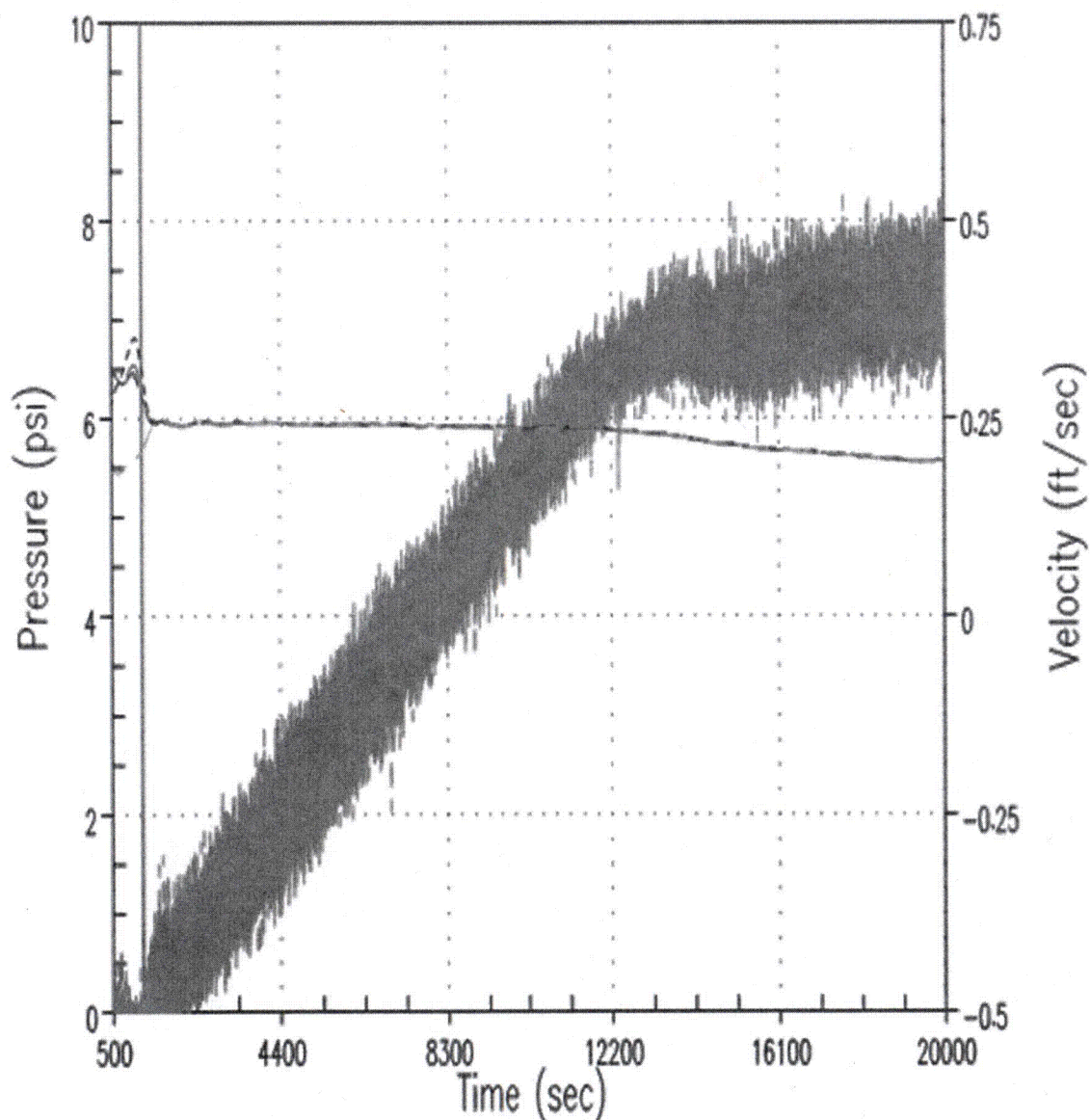———— ———— HOT ASSEMBLY INLET LIQUID VELOCITY

Figure 9-35 K$_{split}$ Case 3 – Debris Bed Pressure Drop and Core Inlet Liquid Velocity

9.2.4.3   Case 5 – 8 gpm/FA

Select transient plots from Case 5 are shown in Figures 9-36 through 9-39. The RCS response to core inlet blockage was expected and is generally consistent with the transient response shown in Section 9.2.3. Figure 9-36 shows the core inlet, UHSN, and guide tube flow rates compared to boil-off. The figure demonstrates that flow to the core is well above boil-off during the entire transient. The flow response to core inlet blockage is also shown by the figure. As core inlet blockage is applied, the pressure drop across the core inlet increases. Once K_{split} is reached, the UHSN and guide tube flow rate becomes positive and increases as the magnitude of core inlet blockage increases. As a result, the core inlet flow rate decreases consistent with the rate that the UHSN flow rate increases.

Figure 9-37 shows the transient downcomer and upper head collapsed liquid levels. As core inlet blockage is applied, the downcomer collapsed liquid level increases as expected. When K_{split} is reached, the downcomer collapsed liquid level has reached the UHSN elevation, and the upper head begins to flood. After a delay, the upper head fills to the guide tube elevation, and coolant begins to enter the guide tubes and flows downward into the UP region of the RV. Comparing this flow response to the high- and mid-flow cases described previously, it can be seen that further reducing the ECCS flow results in a longer time period to reach K_{split}.

The PCT transient is shown in Figure 9-38. The figure indicates that the PCT remains well below 800°F.

Figure 9-39 shows the calculated pressure drop across the core inlet and the core inlet liquid velocity. As expected, the core inlet velocity decreases after K_{split} and the pressure drop across the simulated debris bed continues to increase.
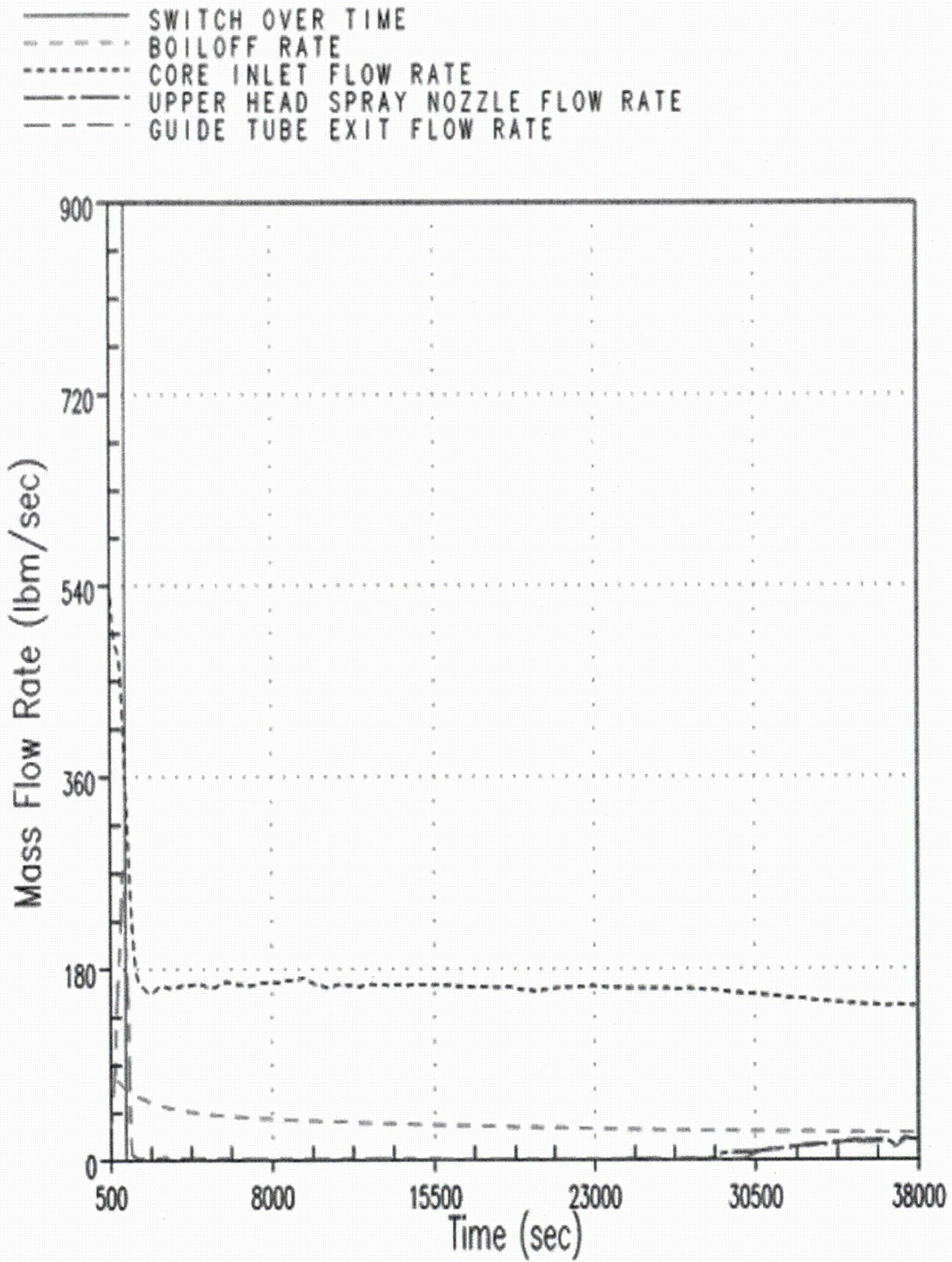
Figure 9-36 K$_{split}$ Case 5 – Core Inlet and Upper Head Spray Nozzle Flow Rates Compared to
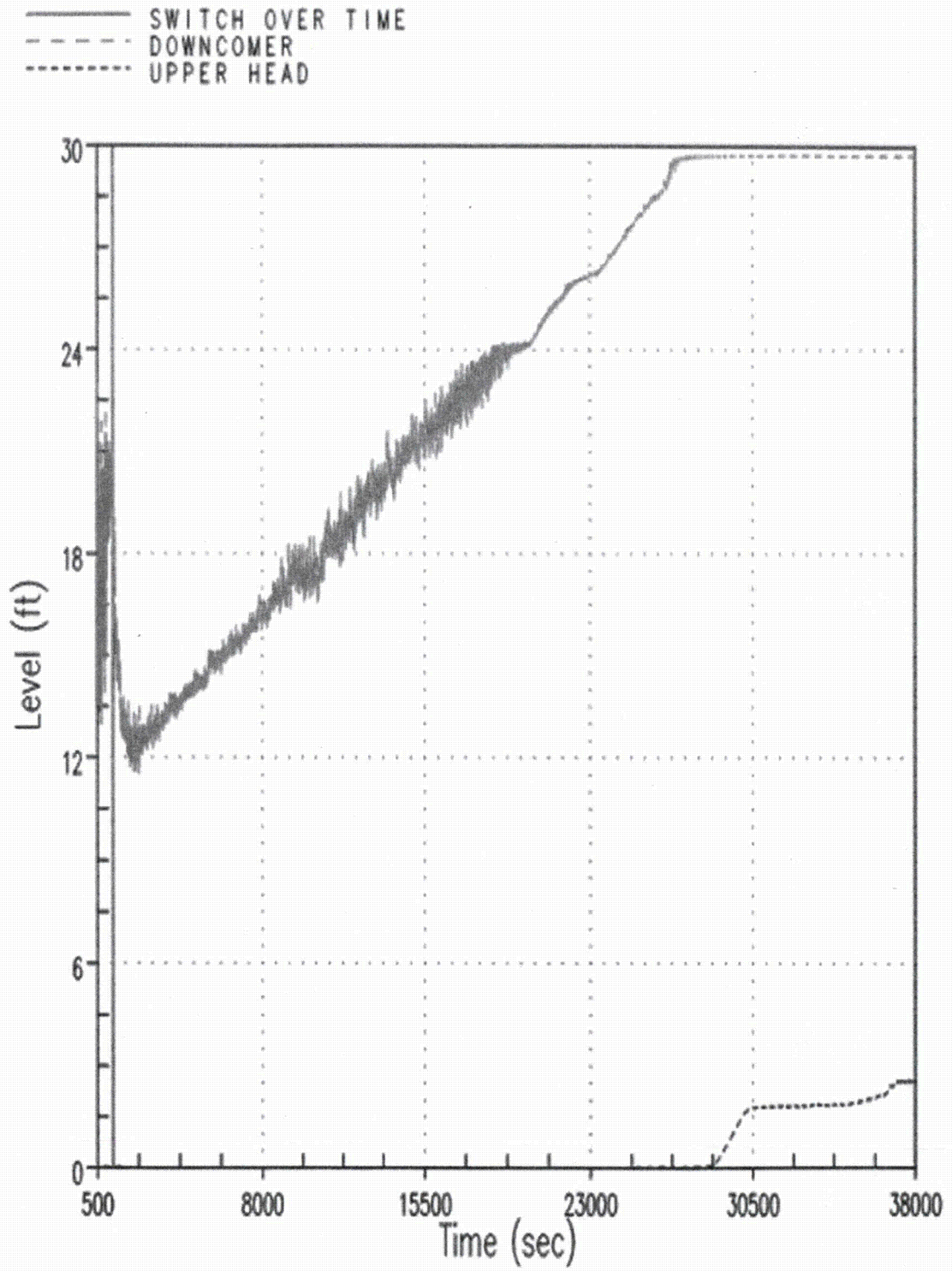Boil-off

Figure 9-37 K_{split} Case 5 – Downcomer and Upper Head Collapsed Liquid Levels
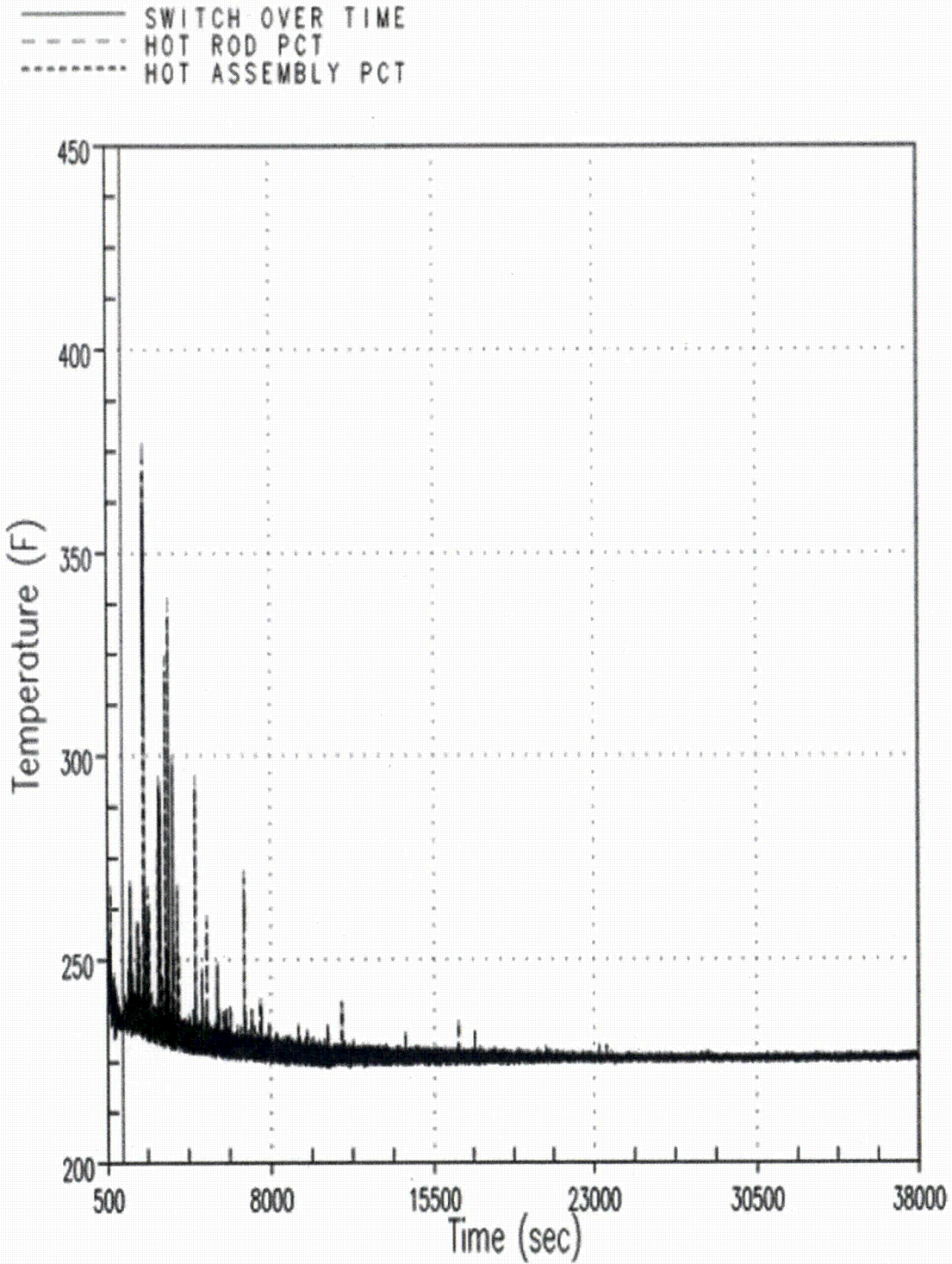
Figure 9-38 K$_{split}$ Case 5 – Hot Rod and Hot Assembly Peak Cladding Temperatures

Pressure (psi)
——————— SWITCH OVER TIME
– – – – – DEBRIS BED PRESSURE DROP
Velocity (ft/sec)
·············· LOW POWER INLET LIQUID VELOCITY
–·–·–·– AVERAGE NON-GUIDE TUBE INLET LIQUID VELOCITY
–··–··– AVERAGE GUIDE TUBE INLET LIQUID VELOCITY
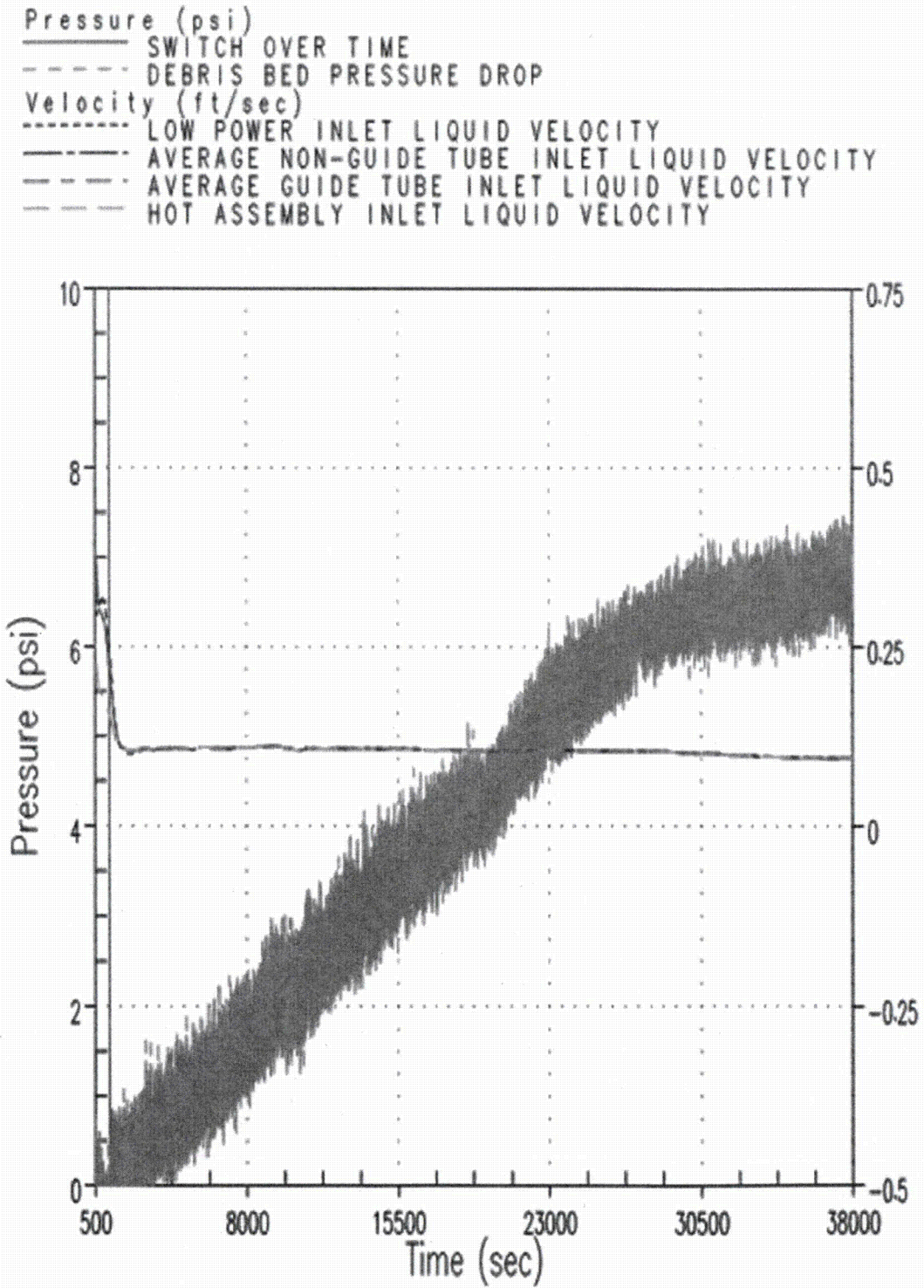——— ——— HOT ASSEMBLY INLET LIQUID VELOCITY

Figure 9-39 K$_{split}$ Case 5 – Debris Bed Pressure Drop and Core Inlet Liquid Velocity

9.3   DISCUSSION OF RESULTS

During the first 20 minutes of the transient (before debris arrives), the core region has completely reflooded and the cladding temperatures are just above the saturation temperature. During transfer to sump recirculation, the ECCS coolant temperature is set to 212°F. The core is boiling vigorously and the core average void fraction is approximately 50%. The downcomer is filling with coolant supplied to the cold legs via the ECCS and the downcomer collapsed liquid level is below the cold leg elevation. No liquid is flowing through the UHSNs and there is no liquid inventory in the upper head. There is a strong recirculation pattern within the core region in which the hot and average assemblies have predominately upflow while the peripheral assemblies have downflow. Vapor generated in the core flows toward the break and liquid carryover to the break is significant.

The first set of core inlet blockage simulations (Section 9.2.2) examined a scenario in which the core inlet was instantaneously completely blocked at some finite time after transfer to sump recirculation by applying a large form-loss coefficient at the core inlet. For this scenario, no partial blockage is applied prior to applying complete core inlet blockage. These simulations showed that the application of an instantaneous complete core inlet blockage resulted in a short-duration heatup within the core that was a result of core uncovery at the top of the core. When the blockage was applied, flow through the core inlet ceased and the ECCS began to fill the downcomer. The downcomer liquid level reached the UHSNs and began to flood the upper head. Eventually, the liquid level in the upper head reached the upper guide tube elevation and liquid began to flow into the UP and into the top of the core. This process resulted in recovery of the core two-phase mixture level and return of the cladding temperatures to values near the saturation temperature. It was found that the duration and magnitude of the heatup were heavily dependent on the timing of complete core inlet blockage and the ECCS flow rate. Applying the blockage earlier in the transient resulted in a longer-duration heatup with a higher PCT because the decay heat is higher and the core boiling more vigorous. Similarly, a lower ECCS flow rate resulted in a longer time to fill the downcomer and flood the upper head to the upper guide tube elevation. For the range of ECCS flow rates investigated, it was determined that complete blockage of the core inlet had to be delayed until at least 260 minutes after the postulated LOCA to maintain a secondary heatup of less than 800°F.

It is recognized that the complete core inlet blockage scenario used to determine t_{block} is unrealistic relative to the prototypic system. In reality, the arrival of fibrous and particulate debris to the core inlet prior to the formation of chemical products will create a lower resistance partial blockage well before the core inlet is expected to block completely. The resulting partial blockage will aid in filling the downcomer and activating the UHSN AFP prior to reaching complete core inlet blockage. However, neglecting this effect in the determination of t_{block} leads to a conservative value, as demonstrated by the second core inlet blockage scenario described next.

The second set of core inlet blockage simulations (Section 9.2.3) examined a scenario in which the core inlet was first partially blocked prior to applying complete core inlet blockage. For this scenario, a form-loss coefficient was applied instantaneously at the time of transfer to sump recirculation to simulate the collection of fibrous and particulate debris. The magnitude of the form-loss coefficient was such that flow through the core inlet is reduced but not stopped completely. The RCS response to the partial blockage was very similar to the response after complete core inlet blockage, other than the fact that flow through the core inlet continued. The partial blockage resistance was held constant until t_{block} was reached. At this point, a higher form-loss coefficient was applied to block the core inlet completely.

Since the partial blockage applied at the time of transfer to sump recirculation was sufficient to fill the downcomer and activate the UHSN, no significant heatups were observed when complete core inlet blockage was applied. This demonstrates the inherent conservatism in t_{block}.

The value of the form-loss coefficient applied to simulate partial blockage was iterated upon to determine the maximum value that could be tolerated and maintain the PCT below 800°F. For the range of ECCS flows investigated, it was determined that a constant form-loss coefficient of $6x10^5$ produced acceptable results.

In the prototypic system, it is unrealistic to expect all the fibrous and particulate debris to arrive at the core inlet instantaneously. It is expected that the arrival of debris will occur over some finite period of time that is on the order of hours. Since the exact timing of debris arrival is complex and will vary from plant-to-plant, the approach for determining K_{max} via application of an instantaneous ramp simplifies the approach by taking the timing of debris arrival out of the solution. Taking this approach inherently leads to a conservative K_{max} value. This is demonstrated by comparing K_{max} to the final form-losses applied to the Westinghouse upflow plant category Series 3 cases which applied a linear ramp. From Table 8-3, the final form-loss applied to the Series 3 cases was $4x10^6$, which is almost an order of magnitude higher than the K_{max} value determined from the Westinghouse downflow plant category instantaneous cases.

The third set of core inlet blockage simulations (Section 9.2.4) examined a scenario in which a gradual build-up of debris was applied at the core inlet. These are considered the most realistic cases relative to how fibrous and particulate debris is expected to arrive at the core inlet; however, these cases do not simulate complete core inlet blockage. The gradual addition of resistance at the core inlet slowly increases the downcomer level and delays the activation of the UHSN AFP. Eventually, the downcomer fills to the UHSN elevation and the upper head floods to the upper guide tube elevation. After this point, flow into the RV is split between the core inlet and the UHSNs and, as the core inlet resistance continues to build, the flow fraction to the UHSNs continues to increase while the flow fraction to the core inlet decreases. From these simulations, the core inlet resistance necessary to activate the UHSN AFP (K_{split}) was determined to be a strong function of the ECCS flow. K_{split} plotted as a function of ECCS flow rate is provided in Figure 9-3, and the corresponding flow split between the core inlet and the UHSNs (m_{split}) following K_{split} is shown in Figure 9-4.

10   COMBUSTION ENGINEERING DESIGNS

In this section, results from the CE plant category are presented and discussed. The range of conditions and case matrix are provided in Section 10.1. Results from the analysis are presented in Section 10.2. This section is broken into several subsections and the material contained in each subsection is summarized as follows:

- In Section 10.2.1, results from the beginning of the case used to determine K_{max} are used to describe the RCS state at the time of transfer to sump recirculation and the arrival of debris. Since all simulations are identical prior to that point in time, the discussion in this section is applicable to all cases. In the simulations, transfer to sump recirculation occurs 20 minutes after the postulated LOCA.

- In Section 10.2.2, results from the case used to determine t_{block} are presented. This case did not apply partial blockage to the core inlet prior to the application of complete core inlet blockage. Complete core inlet blockage was applied instantaneously at time t_{block} and was applied uniformly across all core channels.

- In Section 10.2.3, results from the case used to determine a value for K_{max} are presented. This case applies a conservative representation of partial blockage across the core inlet beginning at 1800 seconds (Figure 10-2). The blockage was applied uniformly across all core channels. Complete core inlet blockage was not applied during this case.

- In Section 10.2.4, results from additional cases used to determine K_{split} and m_{split} are presented. For these cases, a linear ramp in resistance was applied uniformly across the core inlet and complete core inlet blockage was not simulated. Since these cases were used to assess the timing of the activation of the BB channel, the build-up of core inlet resistance was applied more slowly compared to the cases used to determine K_{max}. As a result, the RCS response to core inlet blockage was much slower in that the downcomer fill rate and the activation of the BB channel occurred over a longer period of time. These simulations are more realistic with regard to the timing at which debris is expected to arrive at the core inlet.

Section 10.3 summarizes and discusses the key analysis results.

10.1   RANGE OF CONDITIONS AND CASE MATRIX

The simulation matrix used to determine t_{block} and K_{max} is shown in Table 10-1. For these cases, a maximum BB flow resistance was used. In the table, the loss coefficient column identifies the core inlet losses applied at the designated initiation times to simulate the collection of debris. All cases applied a step change or a timewise ramp to the loss coefficient applied at the core inlet. The core inlet resistances applied for these cases are presented graphically in Figure 10-1 and Figure 10-2.

Step changes in loss coefficients are applied over a 60 second interval. In Case 1, a step change from zero to 1×10^9 is applied from 15,000 to 15,060 seconds. A ramp of the loss coefficient with time was applied to Case 2 as a conservative representation of debris build-up. For all simulations, the sump recirculation flow rate is applied 1200 seconds after the initiation of the event.

The simulation matrix used to determine K_{split} and m_{split} is shown in Table 10-2. For these cases, a minimum BB flow resistance was used. In the table, the loss coefficient column identifies the core inlet losses applied starting at the designated initiation time and ending at the designated end time. For example, in Case 3a, a linear ramp of the loss coefficient at a rate of 180,000 /hr is applied starting at 1200 seconds and ending at 12,000 seconds. The ending value of the loss coefficient is 540,000. Complete core inlet blockage is not applied to these cases. The core inlet resistances applied for these cases are presented graphically in Figure 10-3. For all simulations, the sump recirculation flow rate is applied at 1200 seconds after the initiation of the event.

Table 10-1   Simulation Matrix for t_{block} and K_{max} – CE Plant Design

Case	Sump Recirculation Flow Rate (gpm/FA)	Debris Bed Model	
		Loss Coefficient	Initiation Time (sec)
1	3.7	1×10^9	1200 / 15,000
2	3.7	Figure 10-2	1800

Table 10-2   Simulation Matrix for K_{split} and m_{split} – CE Plant Design

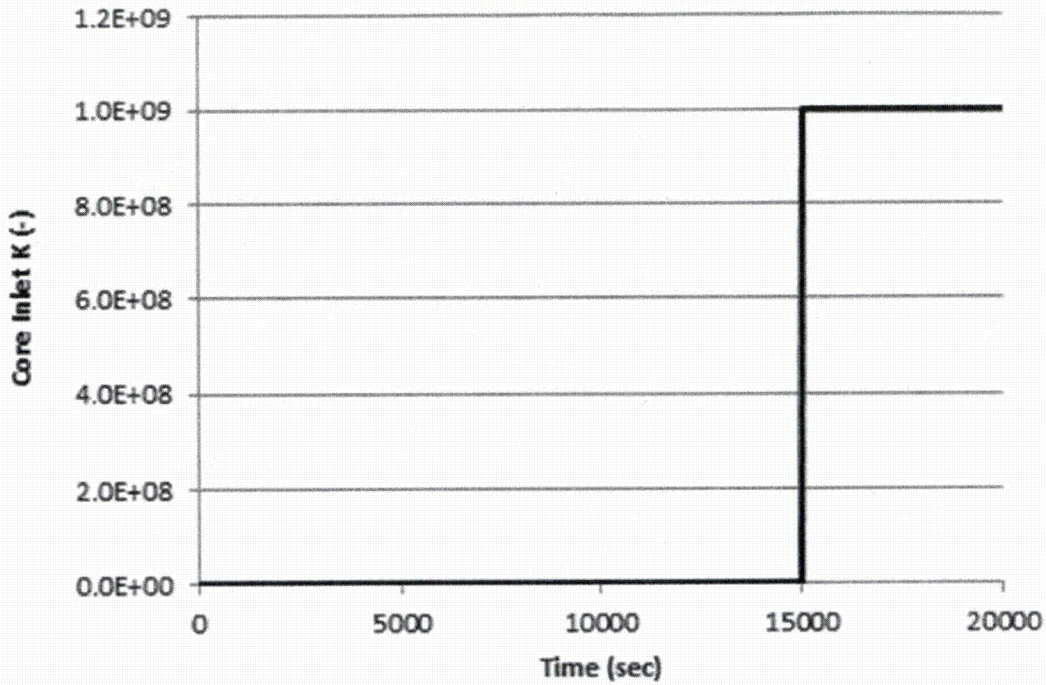| Case	Sump Recirculation Flow Rate (gpm/FA)	Debris Bed Model (Linear Ramp)		
		Loss Coefficient	Initiation Time (sec)	End Time (sec)
3a	3.7	180,000/hr	1200	12,000
3b	7.4	120,000/hr	1200	12,000
3c	11.1	120,000/hr	1200	12,000

Figure 10-1 Core Inlet Resistance Transient Applied to Case 1 Simulations from CE Analysis
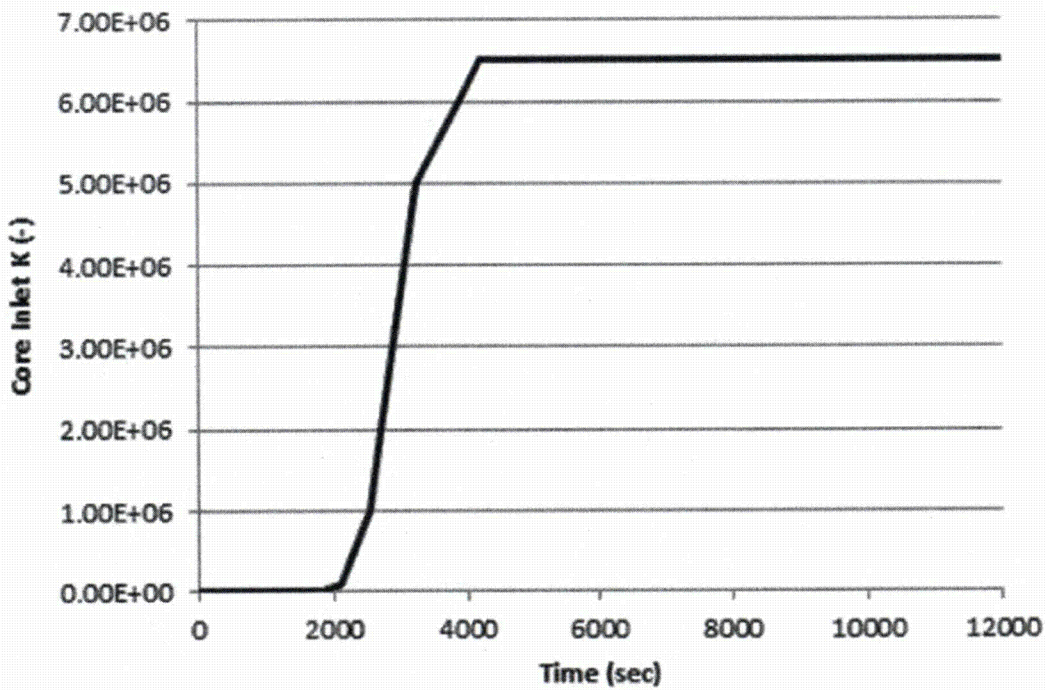

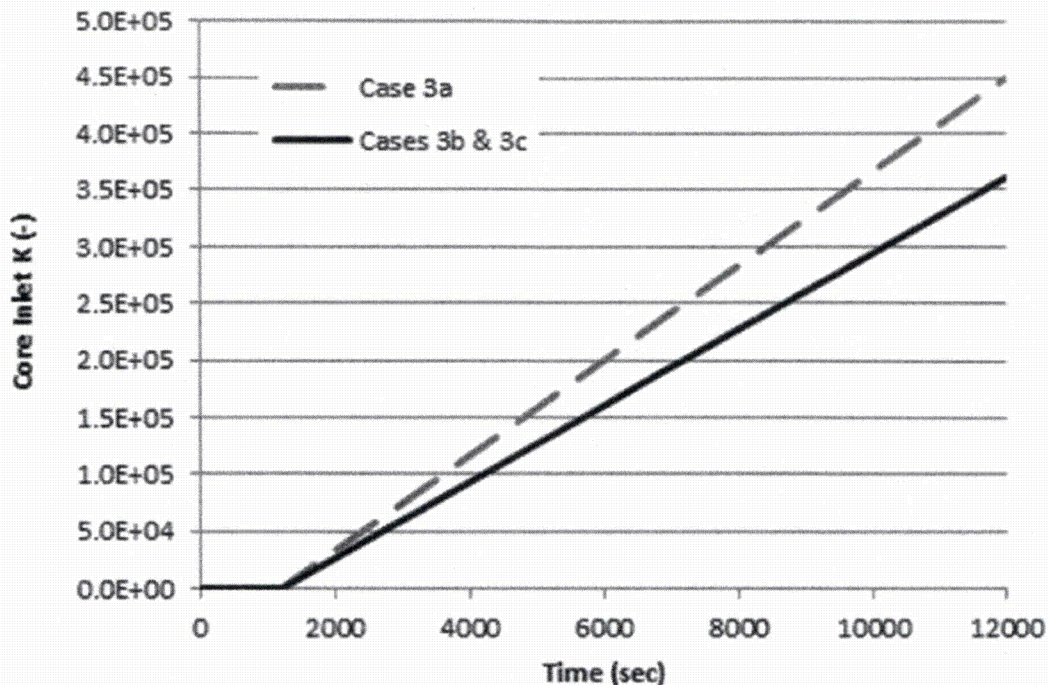**Figure 10-2 Core Inlet Resistance Transient Applied to Case 2 Simulations from CE Analysis**

Figure 10-3 Core Inlet Resistance Transient Applied to Case 3 Simulations from CE Analysis

10.2 RESULTS OF ANALYSIS

Key results from the t_{block} and K_{max} simulations are summarized in Table 10-3. From these results, it is concluded that LTCC can be maintained if complete core inlet blockage occurs 250 minutes (15,000 sec), or later, after the initiation of the LOCA event. Prior to reaching complete core inlet blockage, a maximum supportable K_{max} value of 6.5×10^6, corresponding to a pressure drop of 4.3 psid across the core inlet, is determined to be the limiting value when a uniform resistance is applied that conservatively represents debris build-up (Figure 10-2). Both of these results are based on cases with minimum ECCS recirculation flow. As shown in Section 8 for the Westinghouse upflow plant design, higher ECCS flow rates will fill the downcomer more quickly, leading to more favorable results and the use of the minimum ECCS flow rate bounds the range of recirculation flows expected.

With regard to BAPC, all cases demonstrate that, after core inlet blockage, the break exit quality remains sufficiently low such that boron is flushed from the core and concentrations are expected to remain well below the solubility limit. Further, all cases demonstrate that the core mixing patterns are such that the core can be considered well-mixed and no localized regions containing higher boron concentration are expected to form.

Key results from the K_{split} and m_{split} simulations are summarized in Table 10-4. The K_{split} values shown in the table are used in conjunction with various ECCS sump recirculation flow rates to generate the curve shown in Figure 10-4. The time that K_{split} occurs is determined by examination of the BB exit flow rate. The time at which the BB exit flow rate becomes positive is defined as the K_{split} time. The transient flow split between the core inlet and BB is shown in Figure 10-5 for the three ECCS recirculation flow rates

investigated. The flow split is represented as the fraction of total ECCS recirculation flow through the BB and is plotted as a function of the core inlet resistance following K_{split}.

Table 10-3	Summary of Results for t_{block} and K_{max} – CE Plant Design						
Case	Time Core Inlet Resistance Applied	Core Inlet Loss Coefficient (K)	Core Inlet Average Mass Flow Rate per FA	Core Inlet Average Velocity	Pressure Drop across Debris Bed	Break Exit Quality	PCT
---	seconds	---	lbm/sec	ft/s	psid	---	°F
1	15,000	1×10^9	0.029	0.00197	5.7	Figure 10-22	< 260
2	1800	Figure 10-2	0.143	0.00964	4.3	~0.6	< 260

Table 10-4	Summary of Results for K_{split} and m_{split} – CE Plant Design	
Case	Time of K_{split}	K_{split}
---	seconds	---
3a	10,320	4.56×10^5
3b	4840	1.21×10^5
3c	2680	4.93×10^4
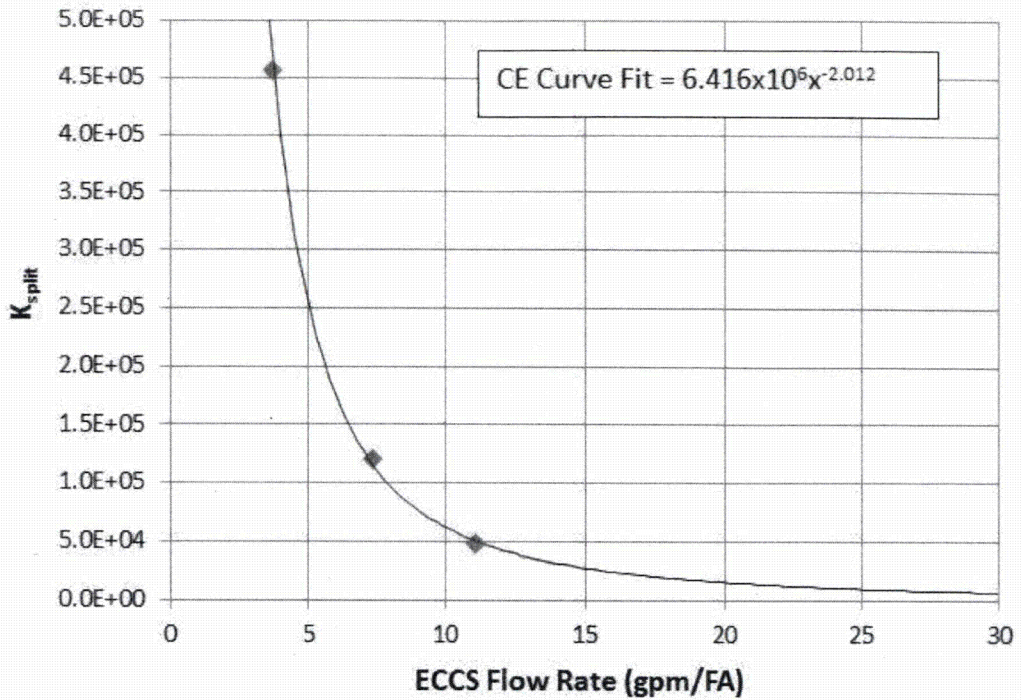
Figure 10-4 K_{split} as a Function of ECCS Recirculation Flow Rate from CE Analysis
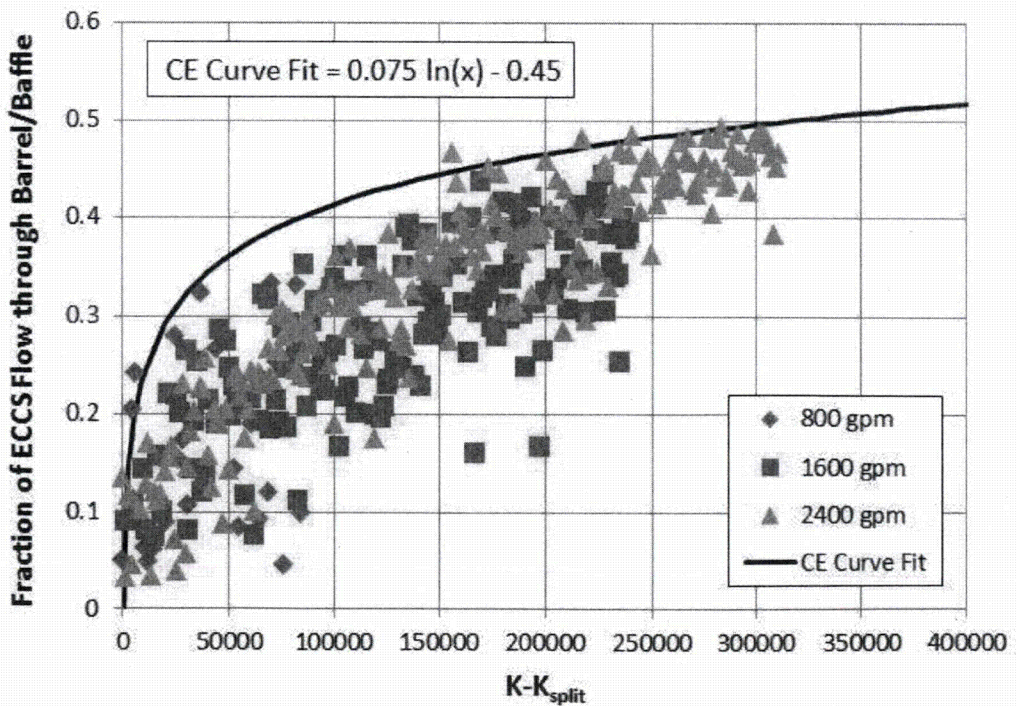
Figure 10-5 Fraction of ECCS Recirculation Flow through the BB following K_{split} from CE Analysis

10.2.1 All Cases – Before Debris Introduction

The results from Case 2 (up to 1200 seconds) are used to describe the RCS state at the point of transfer to sump recirculation and the arrival of debris. Since all simulations are identical prior to that point in the transient, the discussion in this section is applicable to all cases. In the simulations, transfer to sump recirculation occurs 20 minutes after the postulated LOCA.

Just before transfer to sump recirculation, the RCS loop piping and SGs are mostly voided. The entire core has quenched and the cladding temperatures are just above saturation temperature as shown in Figure 10-6. The core region is covered with a two-phase mixture and the core collapsed liquid level is roughly six feet into the active fuel region. Figure 10-7 shows the average core collapsed liquid level (the data in this figure represents a running average of the case data) and Figure 10-8 shows the downcomer average collapsed liquid level. The difference between the collapsed liquid levels in the downcomer and the inner RV is expected given the additional two-phase pressure losses in the boiling core. It is also noted that the downcomer collapsed liquid level is well below the cold leg elevation which limits the available driving head at the start of sump recirculation.

Figure 10-9 shows the mass flux at the core inlet for each of the four core channels. Just prior to sump recirculation, all but the core periphery indicate flow from the LP into the core (i.e., upflow). In the periphery of the core, there is flow from the core to the LP. Figure 10-10 shows the mass flux near the core outlet. All channels indicate flow from the core to the UP. Figure 10-11 shows the flow rate from the UP to the BB region (the data in this figure represents a running average of the case data). The figure shows that the top of the BB channel is experiencing flow into the channel from the UP.

The break exit quality is shown in Figure 10-12 (the data in this figure represents a running average of the case data). The figure shows that the nominal break exit quality is less than 40% upon transfer to sump recirculation which indicates a substantial amount of liquid carryover out the break. At transfer to sump recirculation, the ECCS liquid temperature is increased, which increases the break quality. Note that the increase in break quality prior to the time of sump recirculation is an artifact of the running average scheme used during post-processing of the results.

Due to the large amount of liquid carryover prior to sump recirculation, BAP is controlled and boron concentration levels in the RV upon entry to sump recirculation are expected to be comparable to the ECCS source concentration.
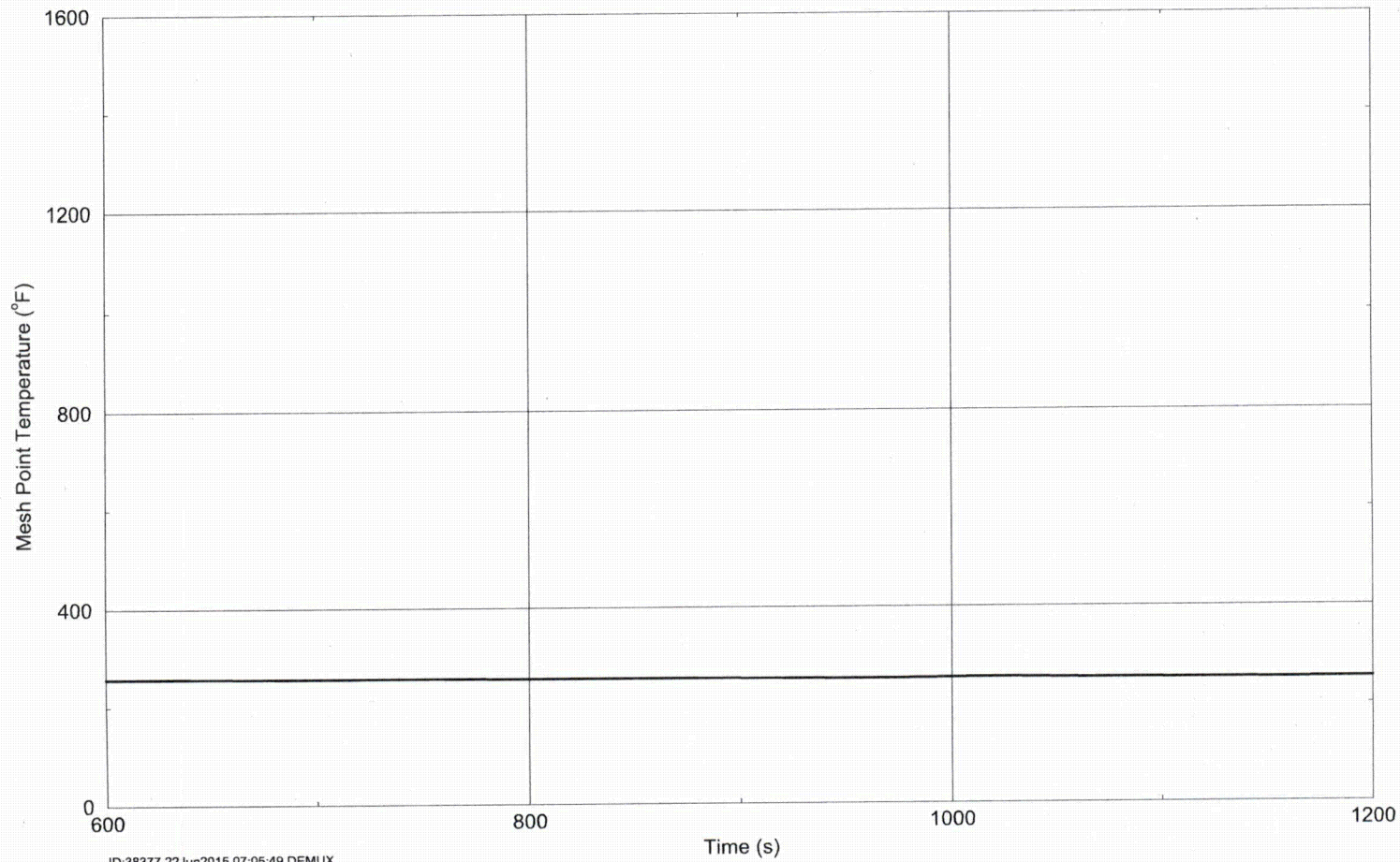
PCT Trace

ID:38377 22Jun2015 07:05:49 DEMUX

Figure 10-6 Case 2 – Hot Assembly Peak Cladding Temperature

Average Core Liquid Level

ID:38377 22Jun2015 07:05:49 DEMUX
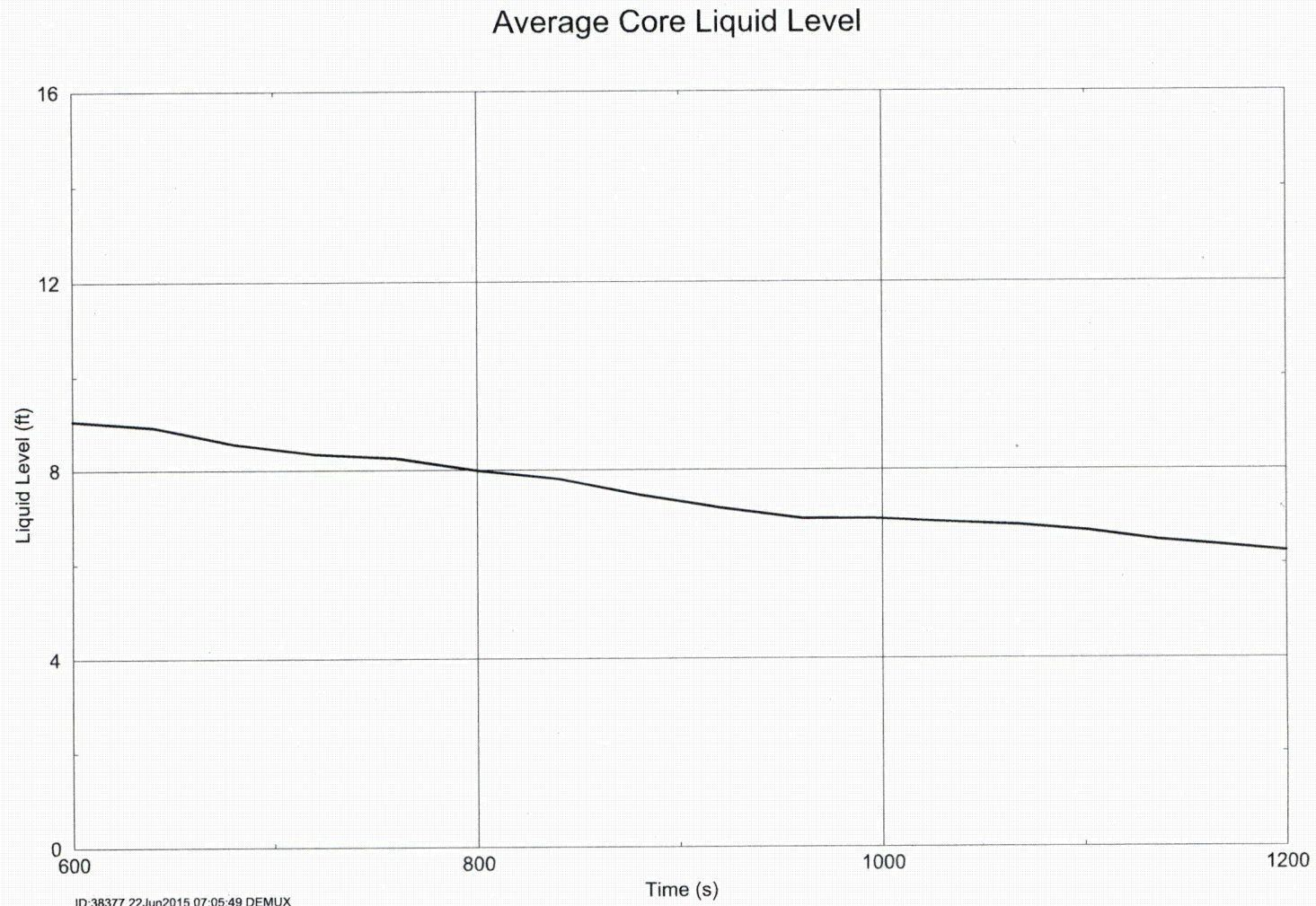
Figure 10-7 Case 2 – Average Core Collapsed Liquid Level

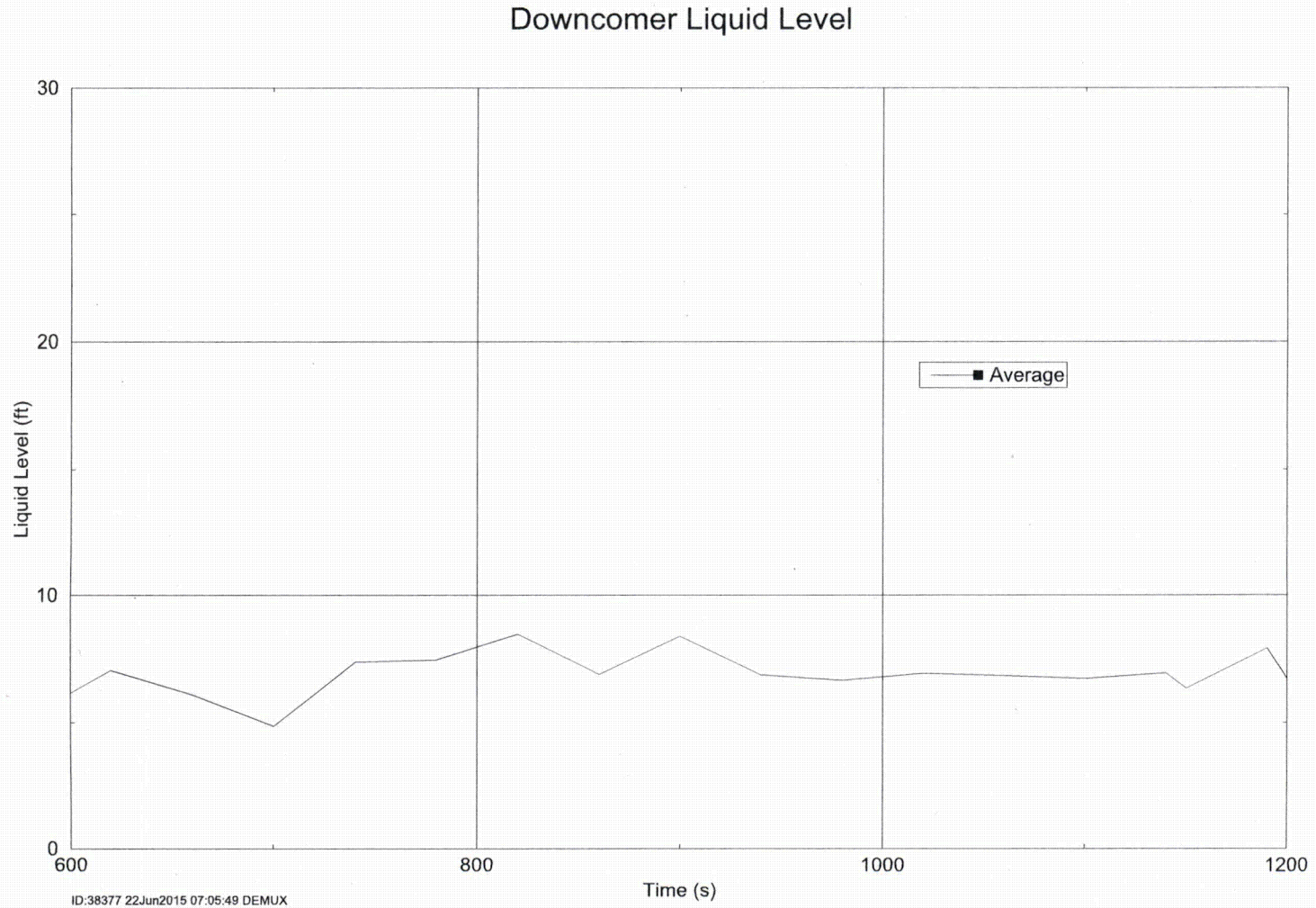## Downcomer Liquid Level

Figure 10-8 Case 2 – Downcomer Collapsed Liquid Level

Core Mass Flux at Core Elevation 0.26 ft
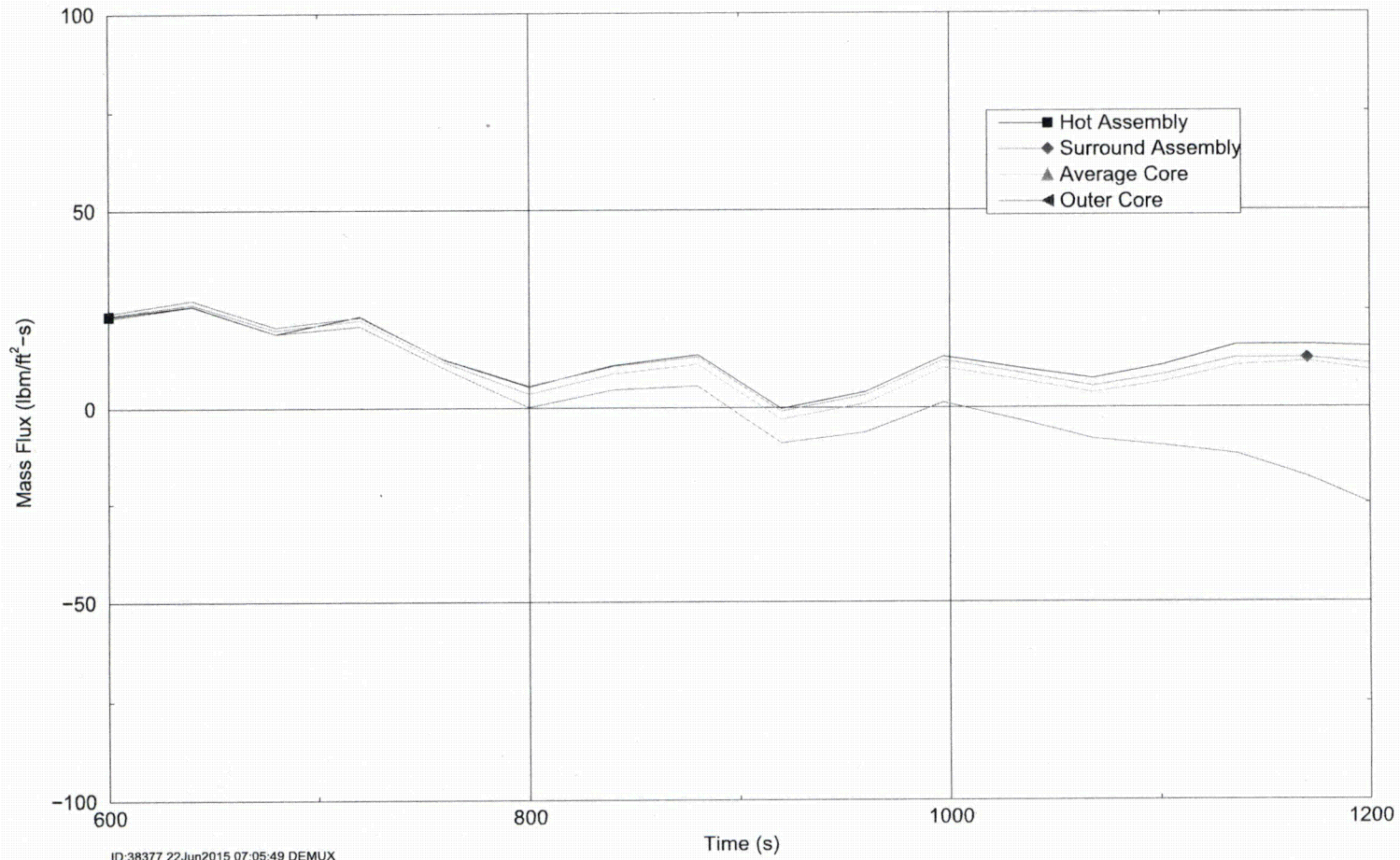
Figure 10-9 Case 2 – Core Inlet Mass Flux
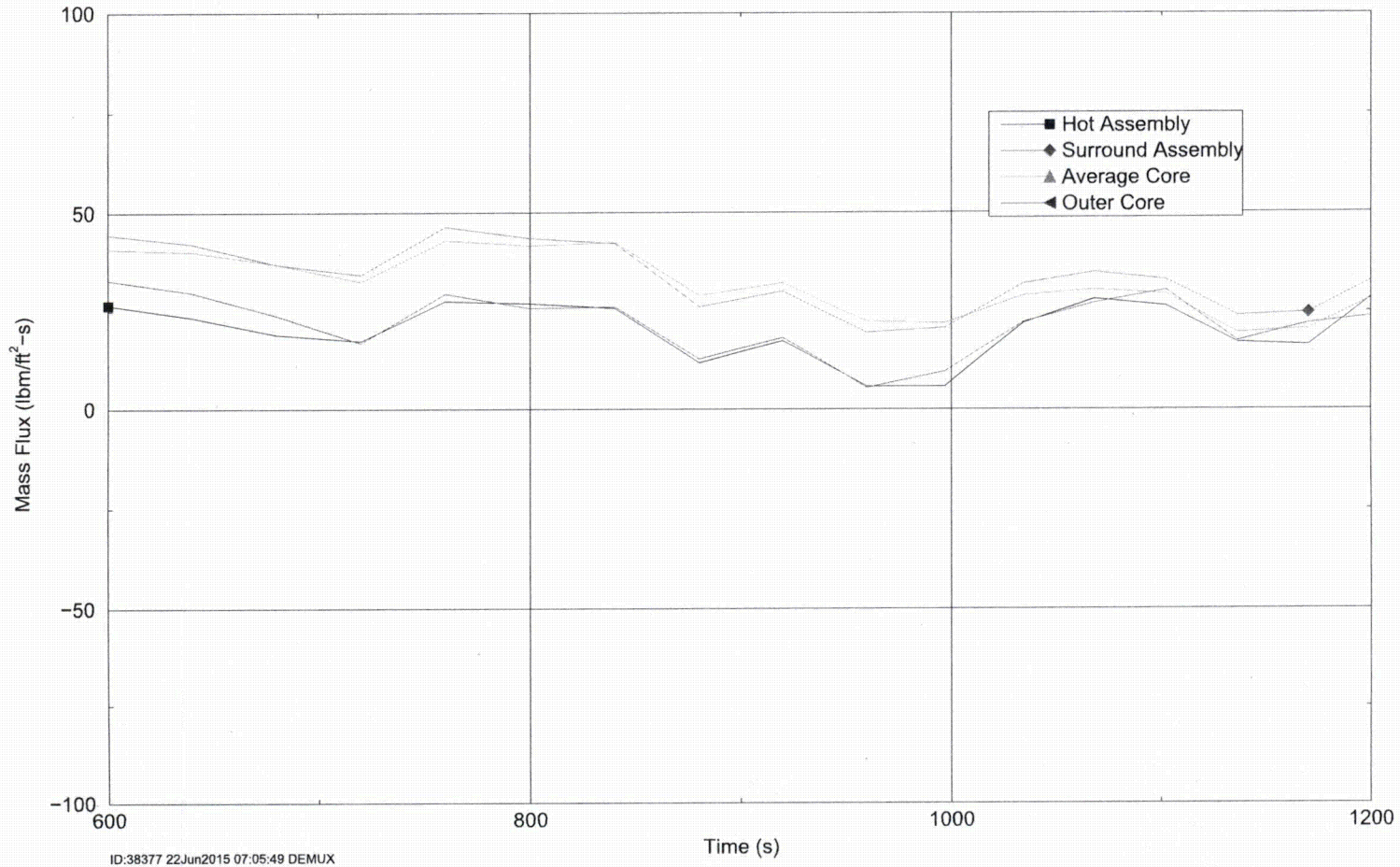
Core Mass Flux at Core Elevation 13.47 ft

ID:38377 22Jun2015 07:05:49 DEMUX

Figure 10-10 Case 2 – Core Exit Mass Flux

Baffle Exit Flow

ID:38377 22Jun2015 07:05:49 DEMUX
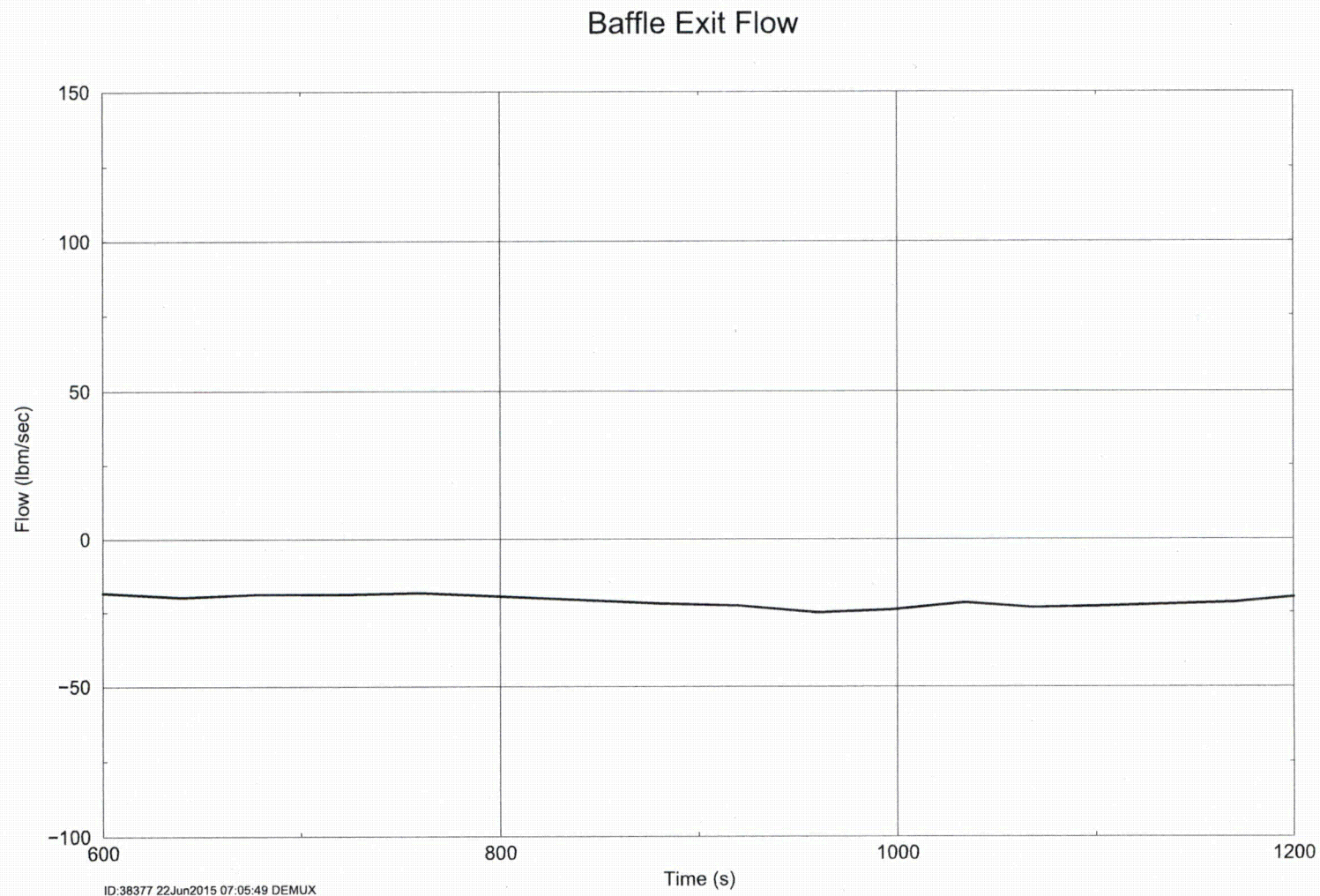
Figure 10-11 Case 2 – Barrel/Baffle Channel Exit Mass Flow Rate
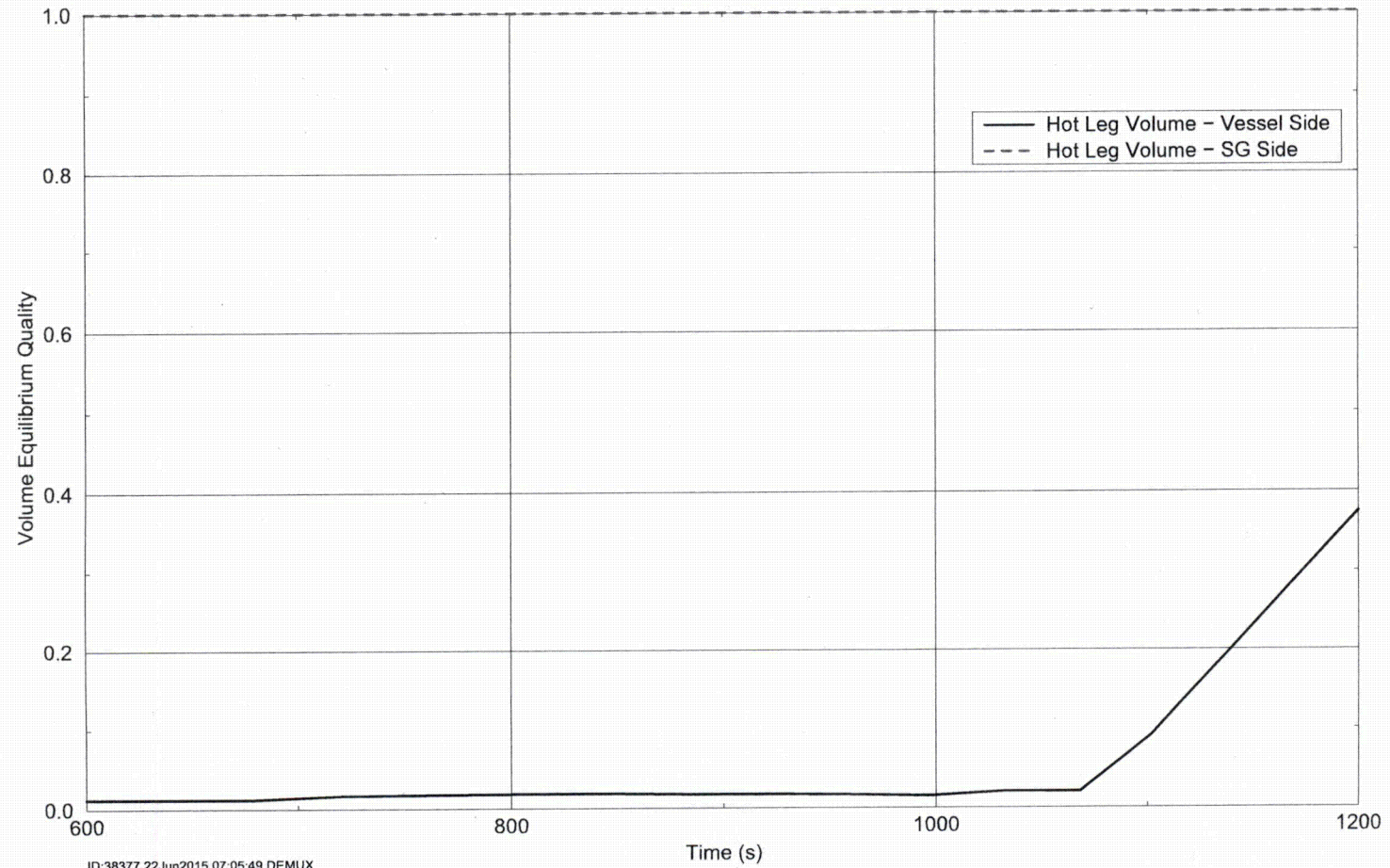
Figure 10-12 Case 2 – Break Exit Quality

10.2.2 After Debris Introduction – Calculation of t_{block}

Case 1 is used to determine t_{block}. This case does not apply any partial blockage to the core inlet prior to the application of complete core inlet blockage.

Throughout the duration of the transient, more-than-adequate core cooling flow is provided through the ECCS to the cold legs. Complete core inlet blockage is applied at 250 min (15,000 seconds). After this time, coolant from the ECCS backs-up and fills the downcomer until adequate driving head is achieved such that flow can be provided to the core via the exit of the BB channel. Figure 10-13 shows that no temperature excursion occurs after the application of complete core inlet blockage, which indicates that the delay time associated with filling the downcomer (to provide adequate driving head such that coolant can flow through the BB channel to the top of the core) is short enough to ensure that the core does not uncover. Once the BB channel is active in providing coolant to the top of the core, the two-phase mixture level in the core continues to be above the heated core.

The RV fluid mass is shown in Figure 10-14 (the data in this figure represents a running average of the case data). The average channel collapsed liquid level is shown in Figure 10-15 (the data in this figure represents a running average of the case data). When complete core inlet blockage is applied, the RV inventory increases quickly, which can be attributed to the downcomer filling. At the same time, the average channel collapsed liquid level decreases, which reflects the lack of flow to the core to make up for boil-off. Once the downcomer fills and the BB channel becomes an active flow path, the RV fluid mass eventually stabilizes and remains fairly constant for the remainder of the transient. Similarly, the average channel collapsed liquid level recovers. The collapsed liquid levels in the other core channels show similar trends. The downcomer collapsed liquid level is shown in Figure 10-16. When the blockage is applied, the downcomer collapsed liquid level quickly increases due to the blockage at the core inlet. As a result, the BB channel is filled with coolant and flow through the channel provides coolant to the top of the core.

The core inlet mass flow rate and the BB exit flow rate are compared to 120 percent of boil-off in Figure 10-17 and Figure 10-18, respectively (the data in these figures represents a running average of the case data). Figure 10-17 indicates that flow into the core is well in excess of boil-off prior to the application of complete core inlet blockage. After the blockage is applied, flow through the core inlet ceases and flow in excess of boil-off from the BB exit enters the top of the core and provides coolant for DHR.

The majority of the flow that exits the BB flows into the peripheral core channel and the flow direction is predominately downward. Figure 10-19 shows the integrated mass flow rate near the top of the core and Figure 10-20 shows the integrated mass flow rate near the bottom of the core. These plots indicate that the flow of liquid is predominately downward along the entire length of the peripheral core channel.

With the bulk of the liquid exiting the BB channel and flowing downward in the periphery of the core, cross flow provides liquid to the average channels and hot assembly channel. This behavior is illustrated in Figure 10-21, which shows the integrated mass flow rate from the central core to the average core near the top of the core. The negative slope in the figure indicates that flow is going into the central core from the average assembly channel. Similar cross flows are observed from the peripheral channel into the average channels along the entire axial elevation of the core.

The break exit quality is shown in Figure 10-22 (the data in this figure represents a running average of the case data). This figure shows that, prior to the application of complete core inlet blockage, the quality remains around 50%. After the application of blockage, the case shows a spike in the break quality, which quickly recovers and trends downwards thereafter. The spike is due to the reduction in core flow rate, which decreases the core heat removal and core collapsed liquid level as shown in Figure 10-15. Due to the large amount of liquid carryover out the break before and after complete core inlet blockage, BAP is controlled and boron concentrations in the RV will remain well below the solubility limit for the duration of the transient.

PCT Trace
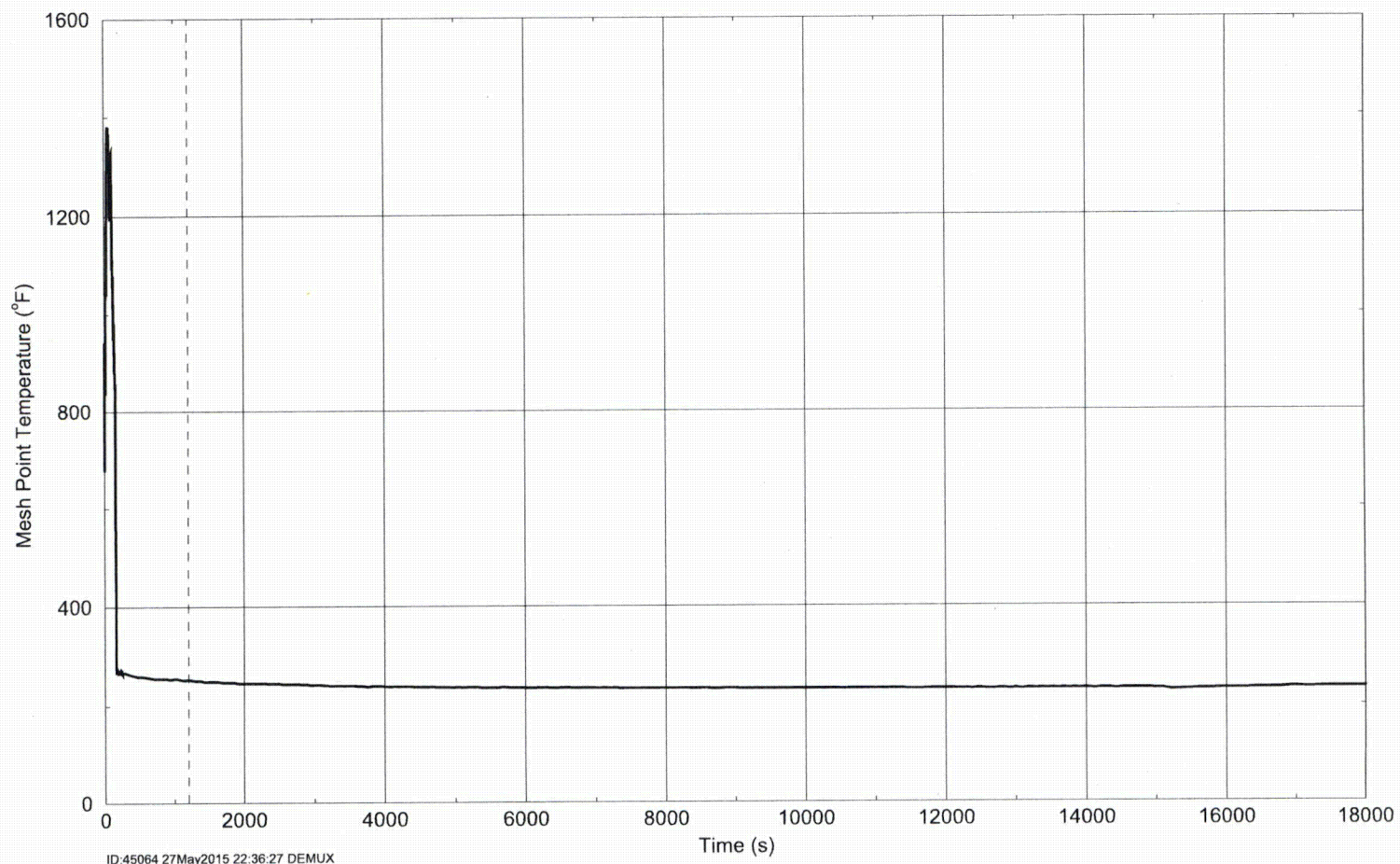
Figure 10-13 Case 1 – Hot Assembly Peak Cladding Temperature

Reactor Vessel Mass

ID:45064 27May2015 22:36:27 DEMUX
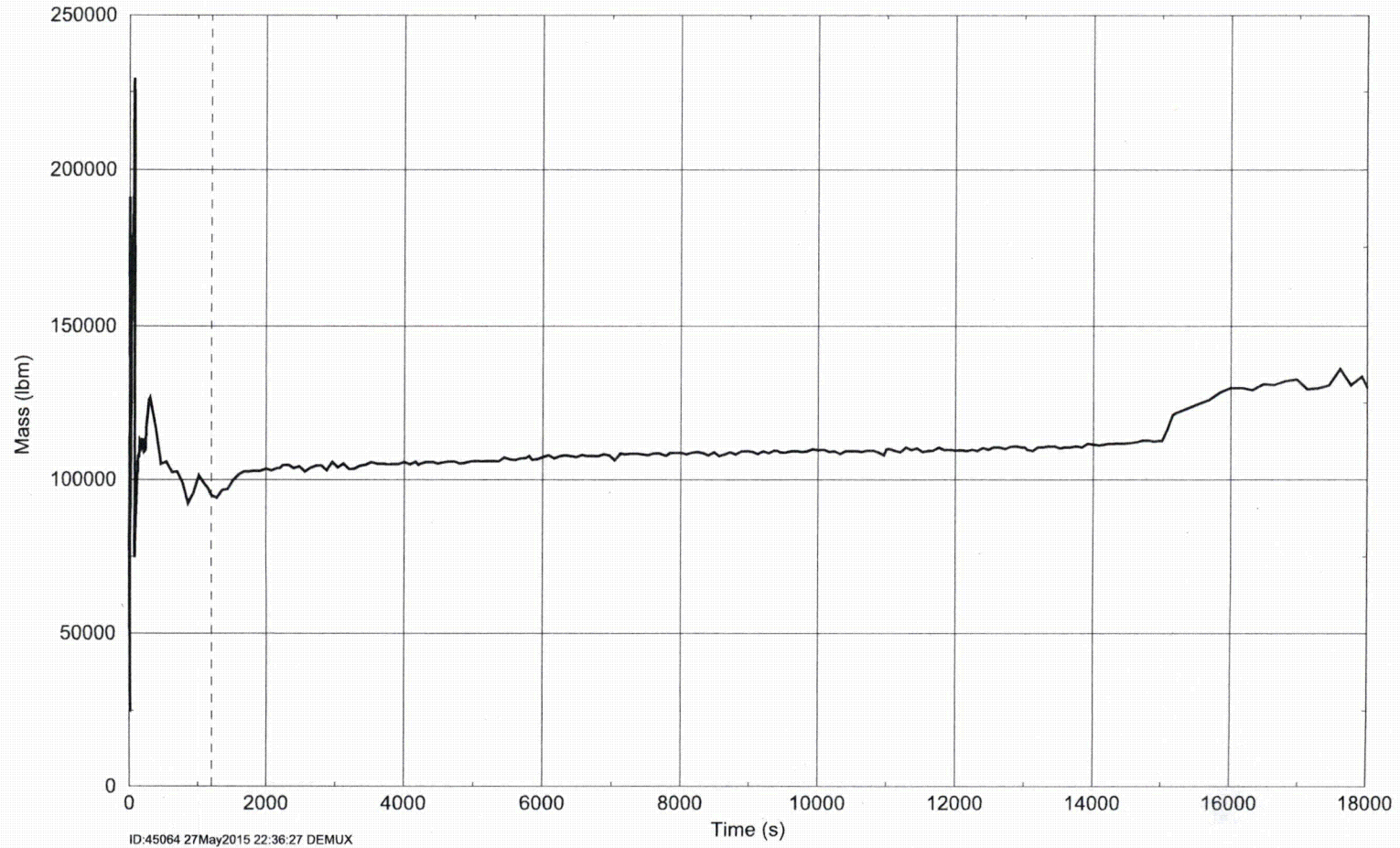
Figure 10-14 Case 1 – Reactor Vessel Fluid Mass

Average Core Liquid Level

ID:45064 27May2015 22:36:27 DEMUX
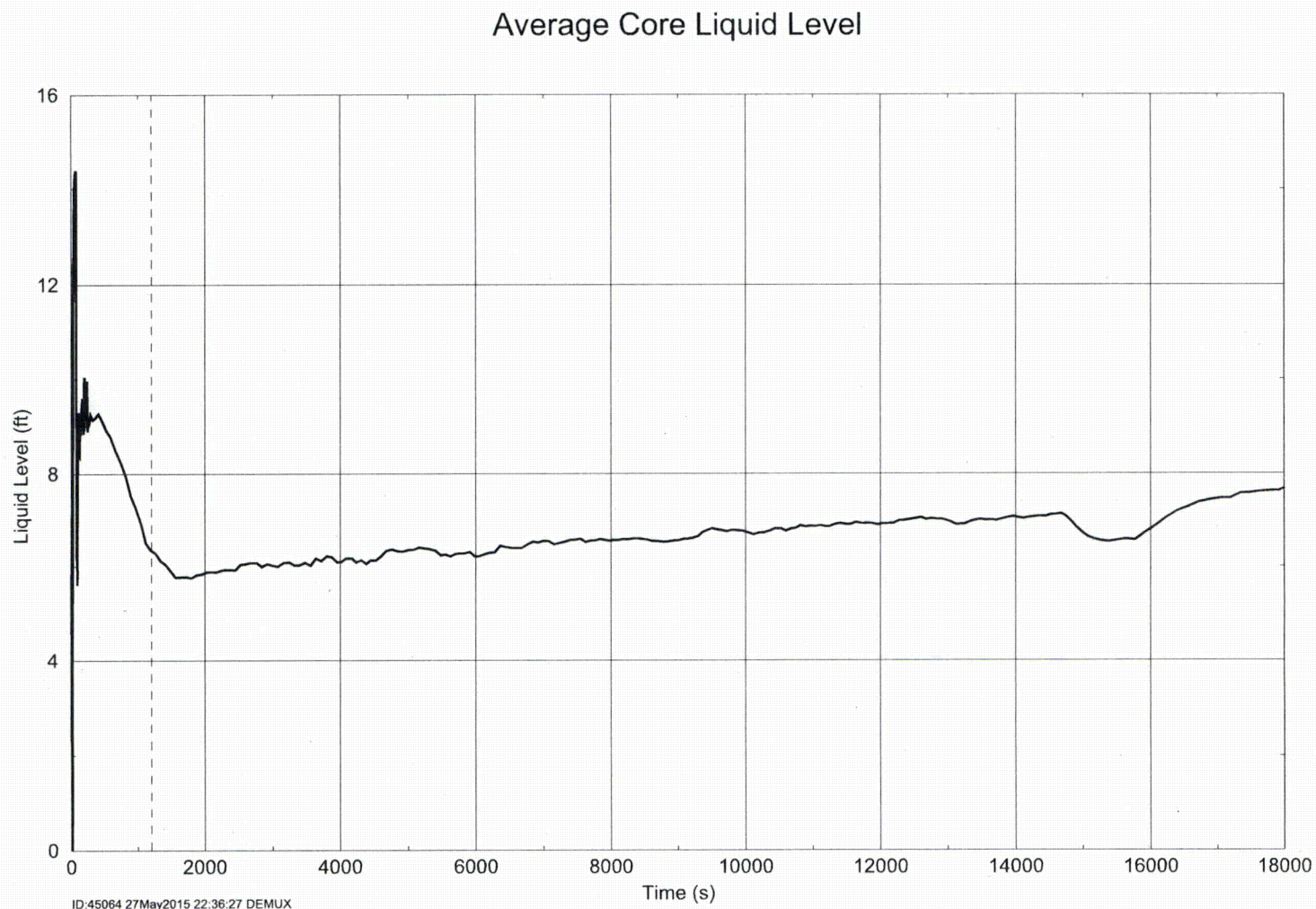
Figure 10-15 Case 1 – Average Core Collapsed Liquid Level

Downcomer Liquid Level

ID:45064 27May2015 22:36:27 DEMUX
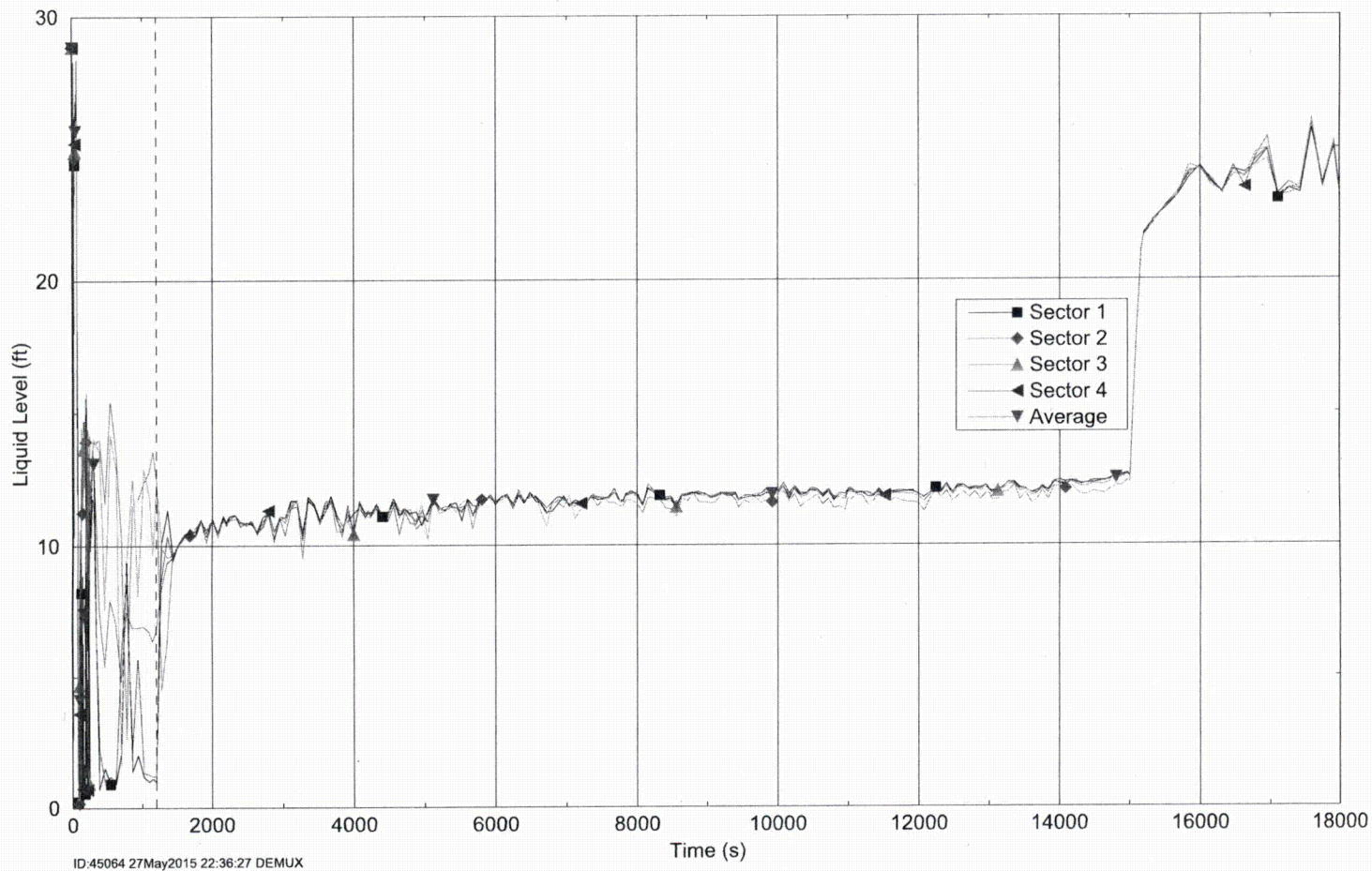
Figure 10-16 Case 1 – Downcomer Collapsed Liquid Level
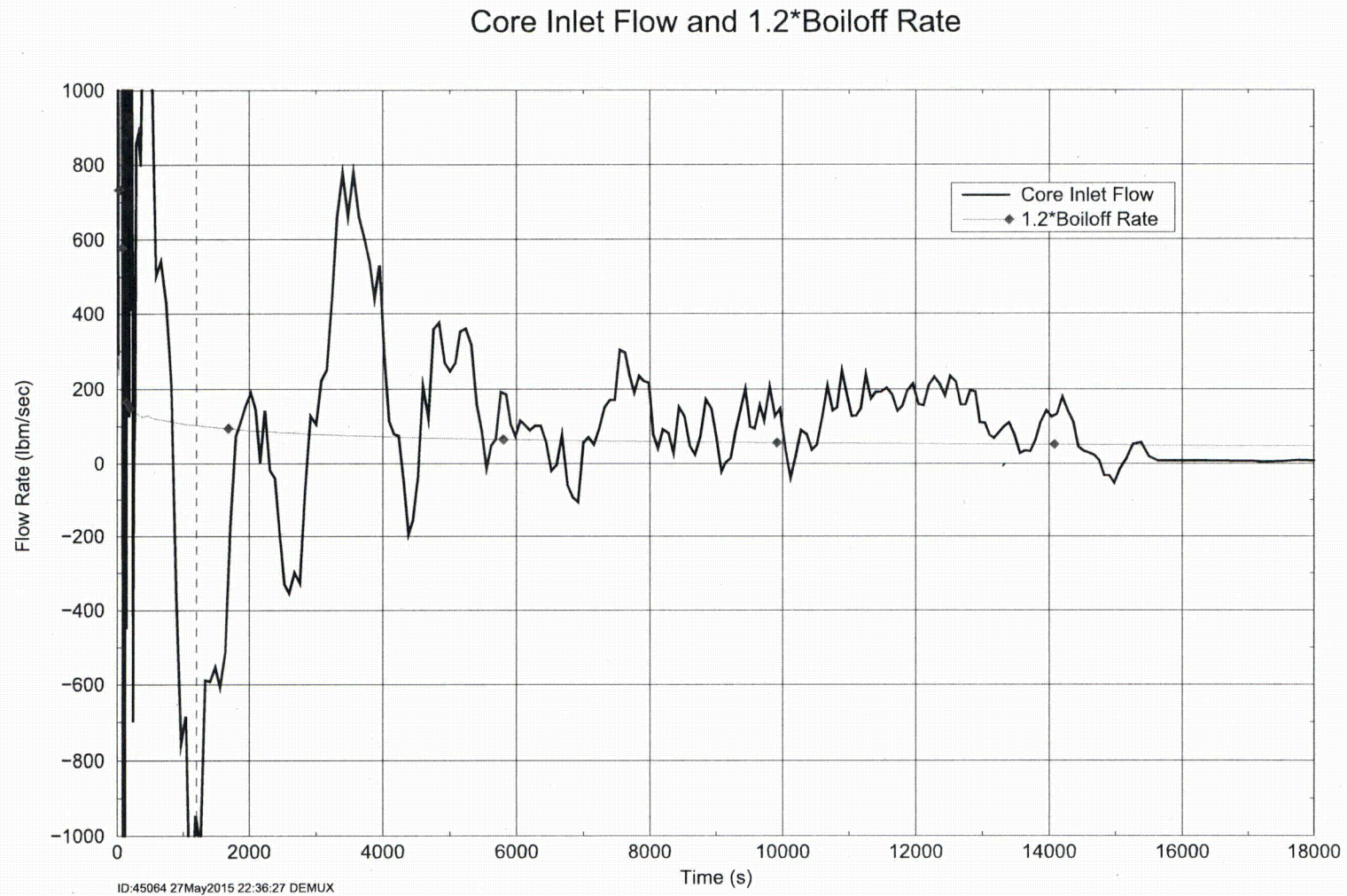
Figure 10-17 Case 1 – Core Inlet Flow Rate Compared to Boil-off
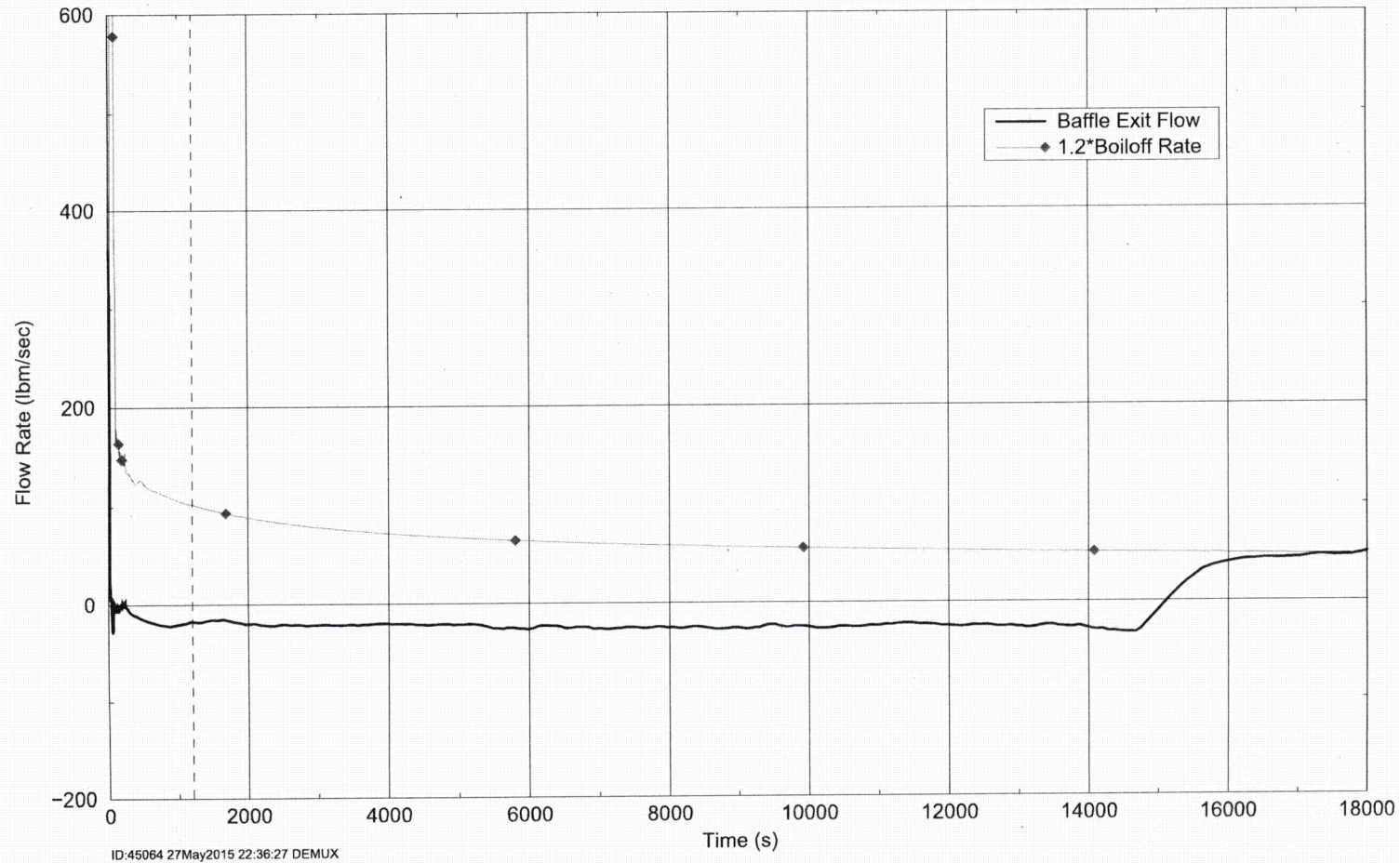
Figure 10-18 Case 1 – Barrel/Baffle Channel Exit Flow Rate Compared to Boil-off

Integrated Flow Rate at 11.14 ft

ID:45064 27May2015 22:36:27 DEMUX
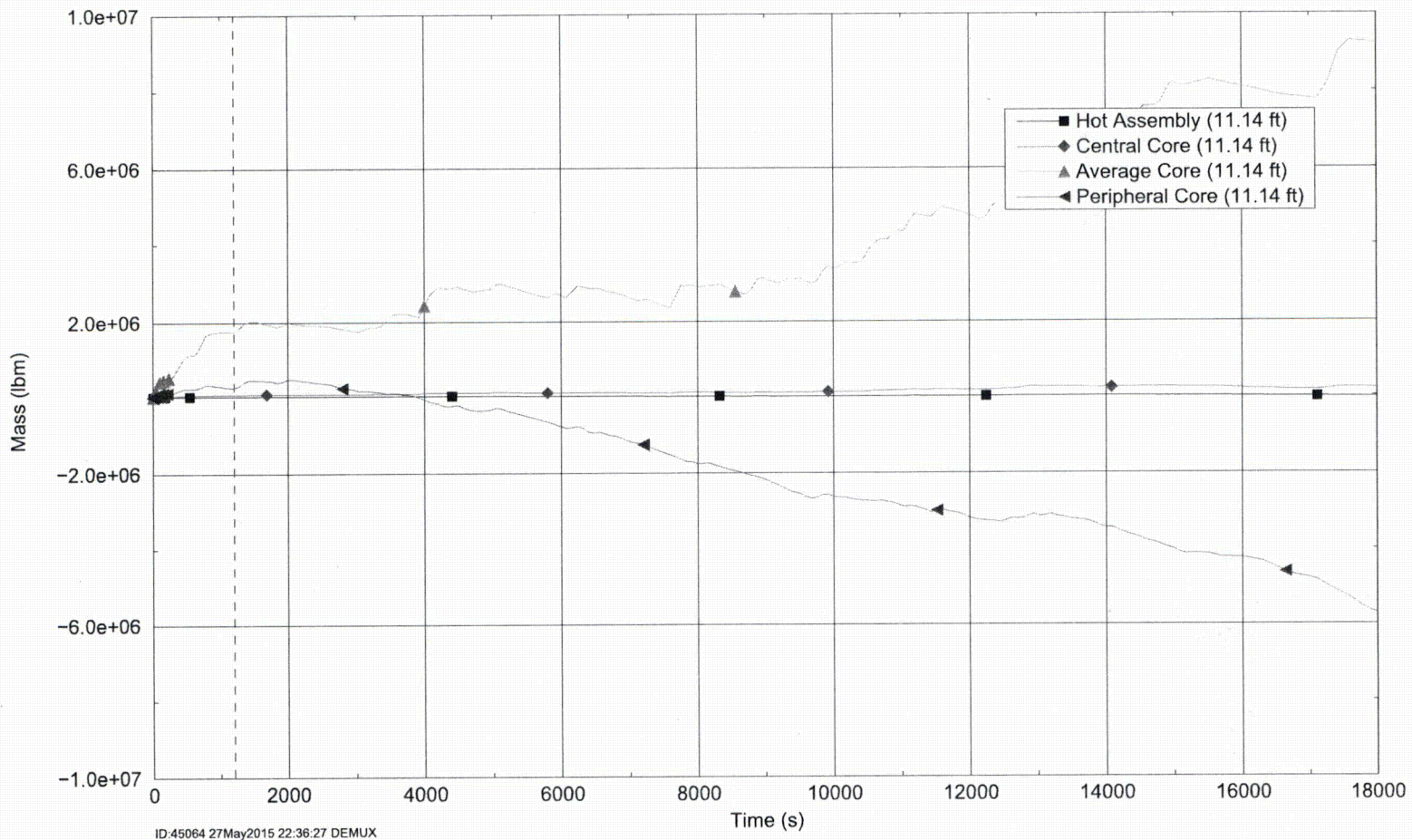
Figure 10-19 Case 1 – Integrated Flow Rate Near the Top of the Core

Integrated Flow Rate at 1.97 ft
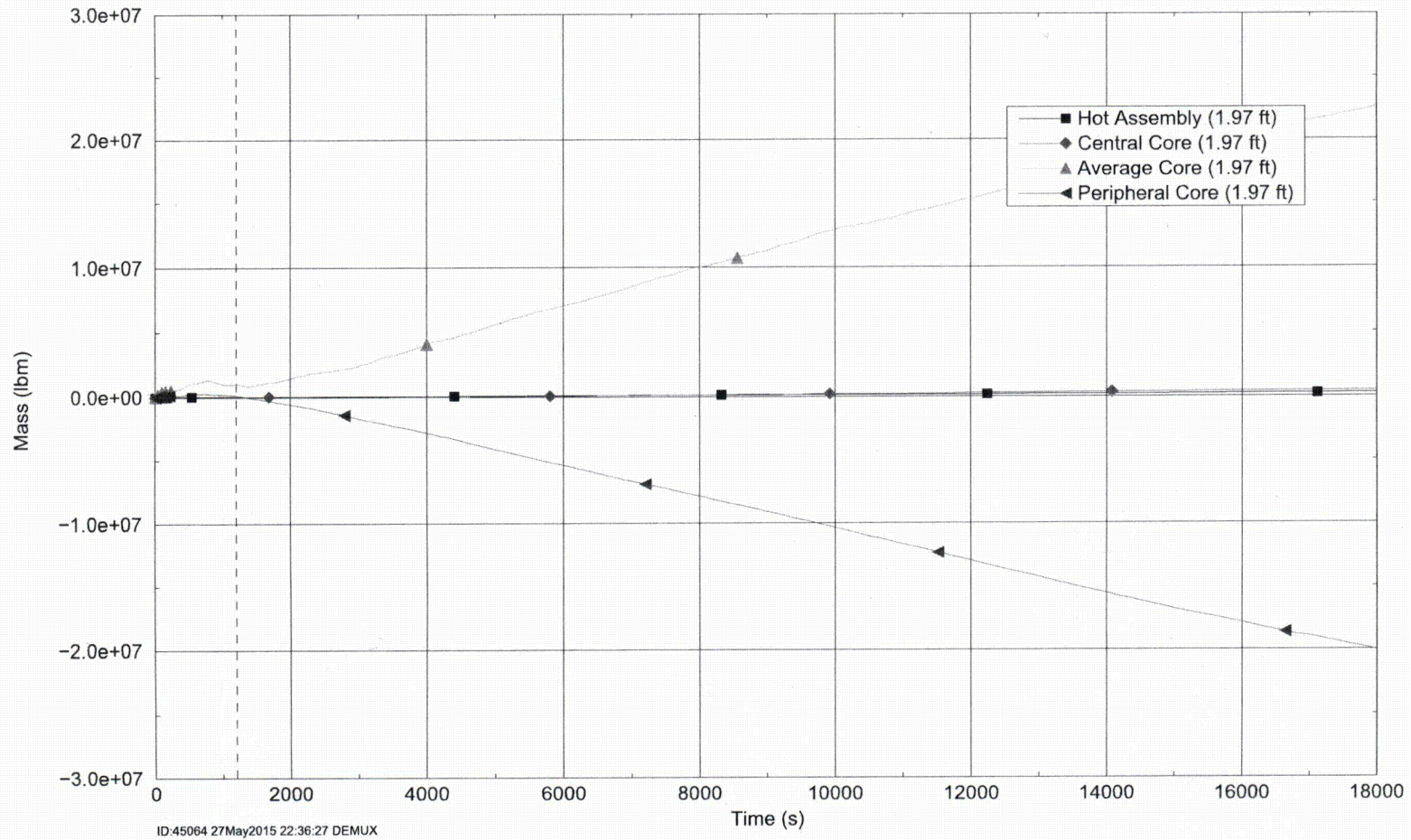
Figure 10-20 Case 1 – Integrated Flow Rate Near the Bottom of the Core

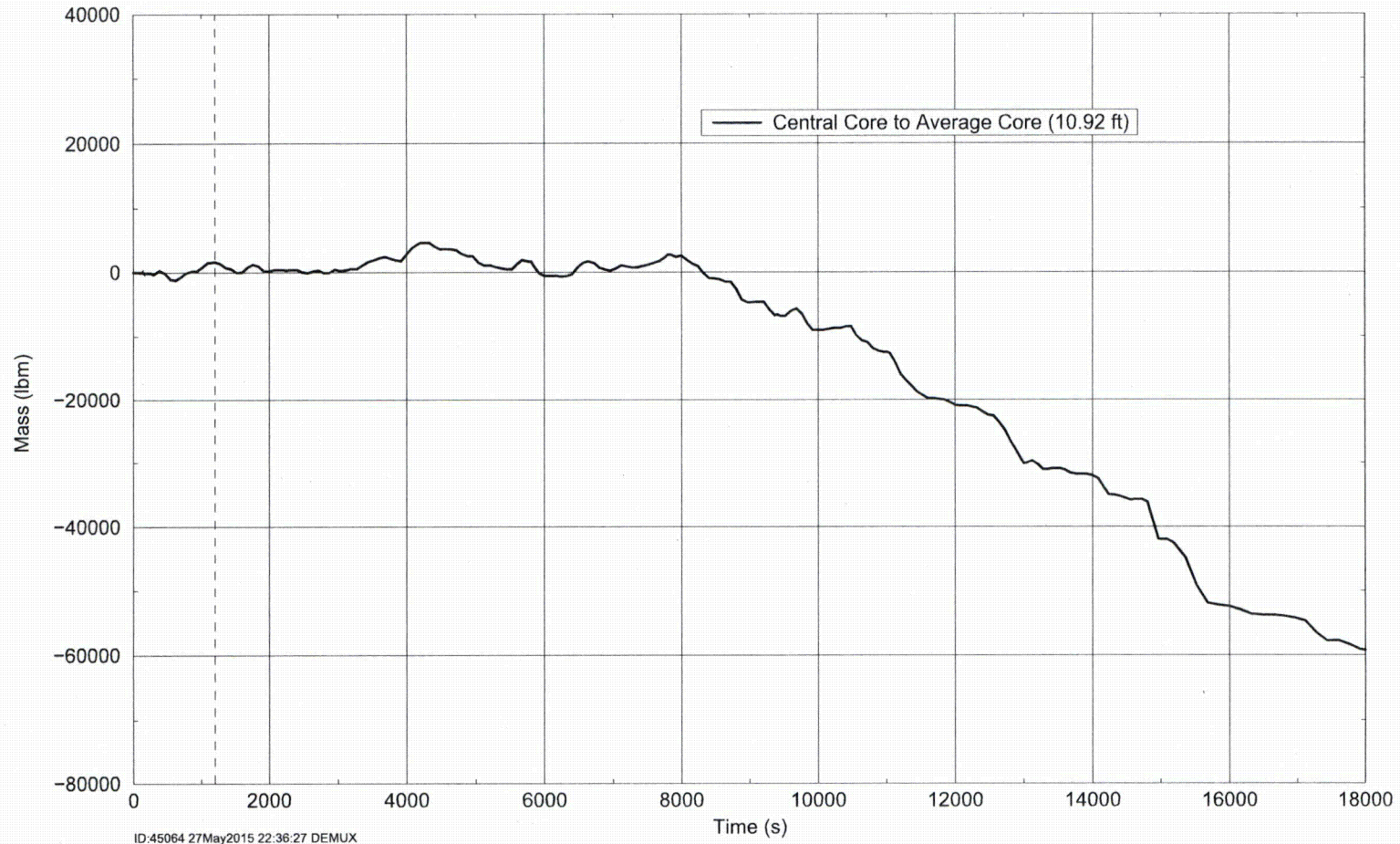## Integrated Crossflow CC to AC at 10.92 ft

ID:45064 27May2015 22:36:27 DEMUX

Figure 10-21 Case 1 – Cross Flow from Central Core to Average Core Near the Top of the Core
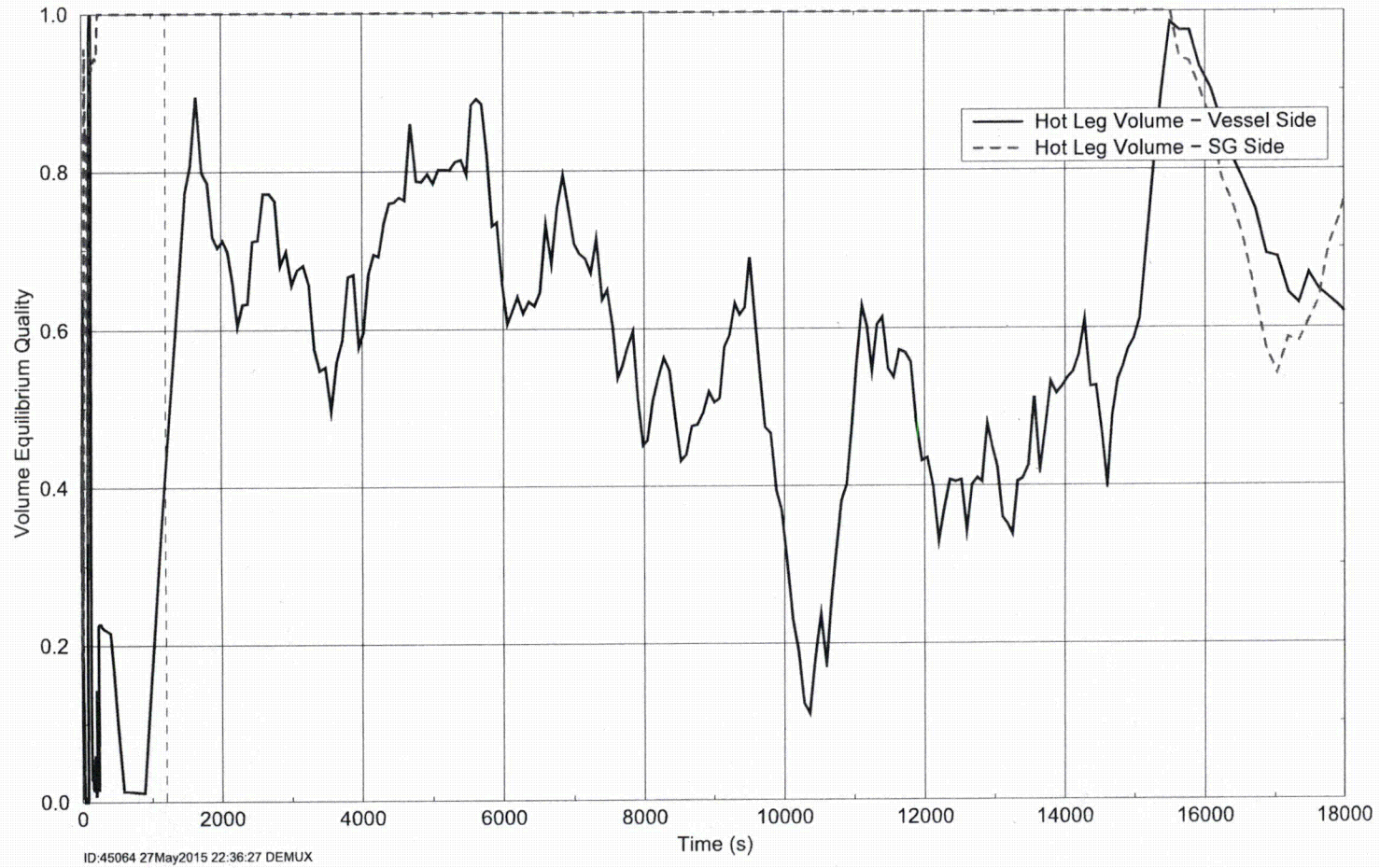
Volume Equilibrium Break Quality

Figure 10-22 Case 1 – Break Exit Quality

10.2.3 After Debris Introduction – Calculation of K_{max}

Case 2 is used to determine a value for K_{max}. This case applies a ramped blockage to the core inlet beginning at 1800 seconds (Figure 10-2).

Throughout the duration of the transient, more-than-adequate core cooling flow is provided through the ECCS to the cold legs. After the blockage is applied, the RCS response is very similar to the response seen after complete core inlet blockage (as described in Section 10.2.2), except that flow continues through the core inlet at a reduced rate. Coolant from the ECCS backs-up and fills the downcomer until adequate driving head is achieved such that flow through the BB channel begins. From this point forward, the total flow entering the LP is split between the core inlet and the BB channel. Figure 10-23 shows that the core did not experience a temperature excursion after the application of the core inlet blockage. DHR is maintained by a combination of flow through the core inlet and flow through the BB channel to the top of the core.

The RV fluid mass is shown in Figure 10-24 (the data in this figure represents a running average of the case data). As the core inlet blockage is applied, the RV inventory increases, which can be credited to filling of downcomer. Once the downcomer fills and the BB channel becomes an active flow path, the RV fluid mass eventually stabilizes and remains fairly constant for the remainder of the transient. These trends are consistent with the behavior of the average channel core collapsed liquid level as shown in Figure 10-25 (the data in this figure represents a running average of the case data). The collapsed liquid levels in the other core channels show similar trends. The downcomer collapsed liquid levels are shown in Figure 10-26. When the blockage is applied, the downcomer collapsed liquid level quickly increases due to the increased resistance to flow through the core inlet. As a result, the BB channel is filled with coolant and flow through the channel provides coolant to the top of the core.

The core inlet mass flow rate and the BB exit flow rate are compared to 120 percent of the boil-off in Figure 10-27 and Figure 10-28, respectively (the data in these figures represents a running average of the case data). These figures indicate that flow into the core exceeds boil-off after the application of core inlet blockage. Figure 10-29 shows the pressure drop across the debris bed (the data in this figure represents a running average of the case data), and Figure 10-30 shows the core inlet liquid velocities. These figures confirm that flow through the core inlet continues after the application of the blockage.

The majority of the flow that exits the BB flows into the peripheral core channel and the flow direction is predominately downward. Figure 10-31 shows the integrated mass flow rate near the top of the core and Figure 10-32 shows the integrated mass flow rate near the bottom of the core. These plots indicate that the flow of liquid is predominately downward along the entire length of the peripheral core channel.

With the bulk of the liquid exiting the BB channel and flowing downward in the periphery of the core, cross flow provides liquid to the average channels and hot assembly channel. This behavior is illustrated in Figure 10-33, which shows the integrated mass flow rate from the central core to the average core near the top of the core.   The negative slope in the figure indicates that flow is going into the central core from the average assembly channel. Similar cross flows are observed from the peripheral channel into the average channels along the entire axial elevation of the core.

The break exit quality is shown in Figure 10-34 (the data in this figure represents a running average of the case data). After the application of the blockage, the case shows an increase in the break quality which stabilizes near 75%. Due to the large amount of liquid carryover out the break during the transient, BAP is controlled and boron concentrations in the RV will remain well below the solubility limit.
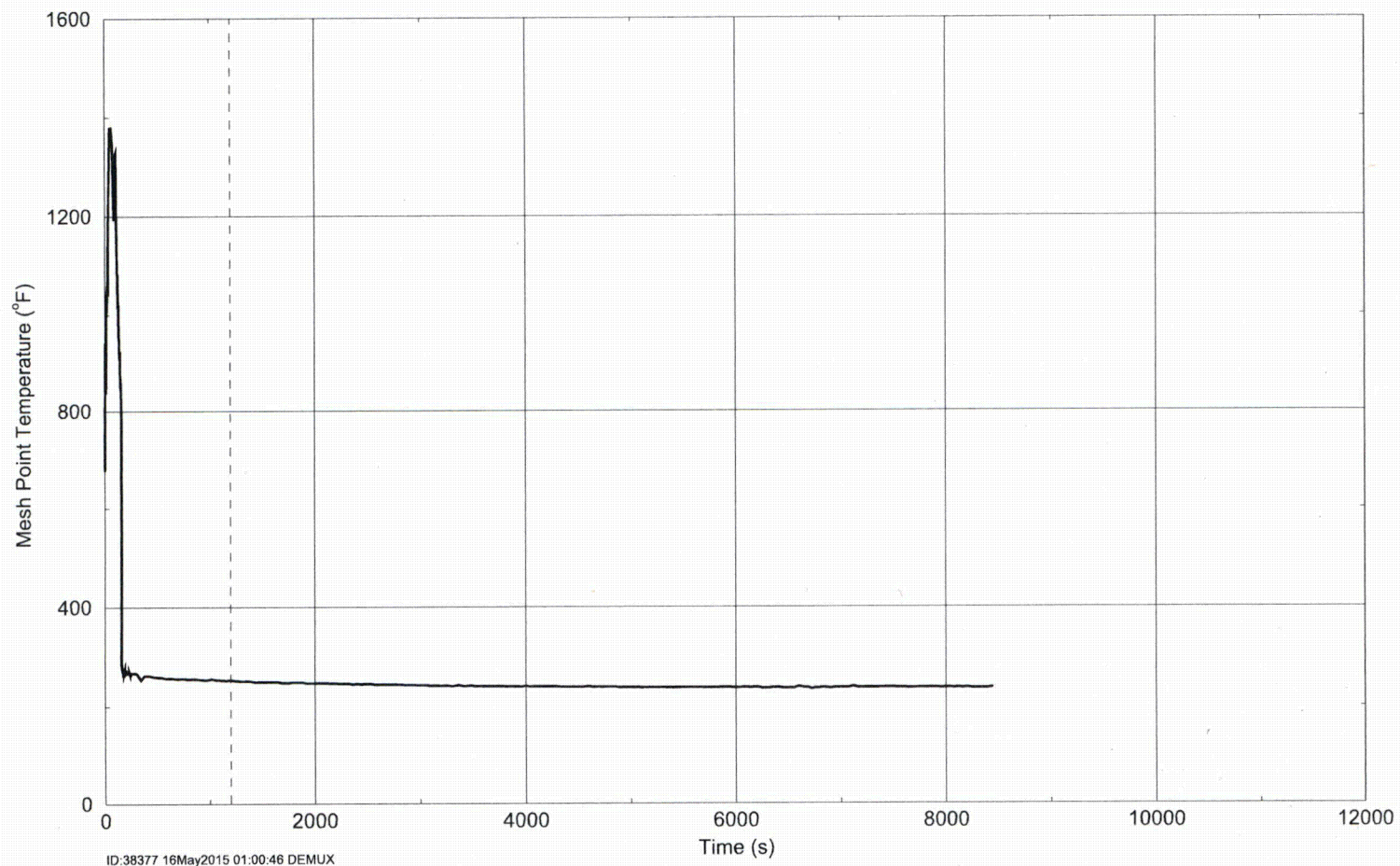
PCT Trace

ID:38377 16May2015 01:00:46 DEMUX

Figure 10-23 Case 2 – Hot Assembly Peak Cladding Temperature

Reactor Vessel Mass

ID:38377 16May2015 01:00:46 DEMUX
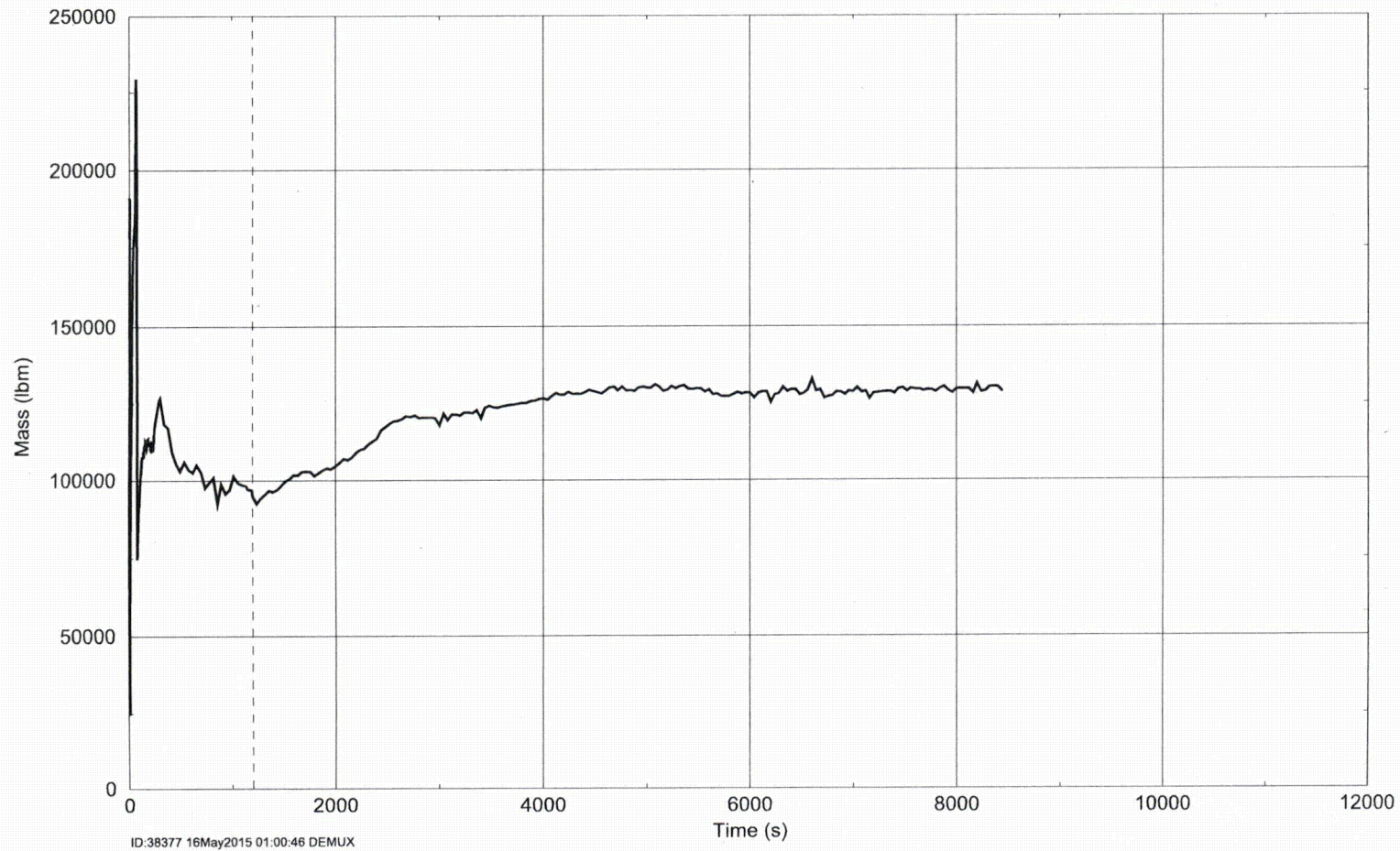
Figure 10-24 Case 2 – Reactor Vessel Fluid Mass

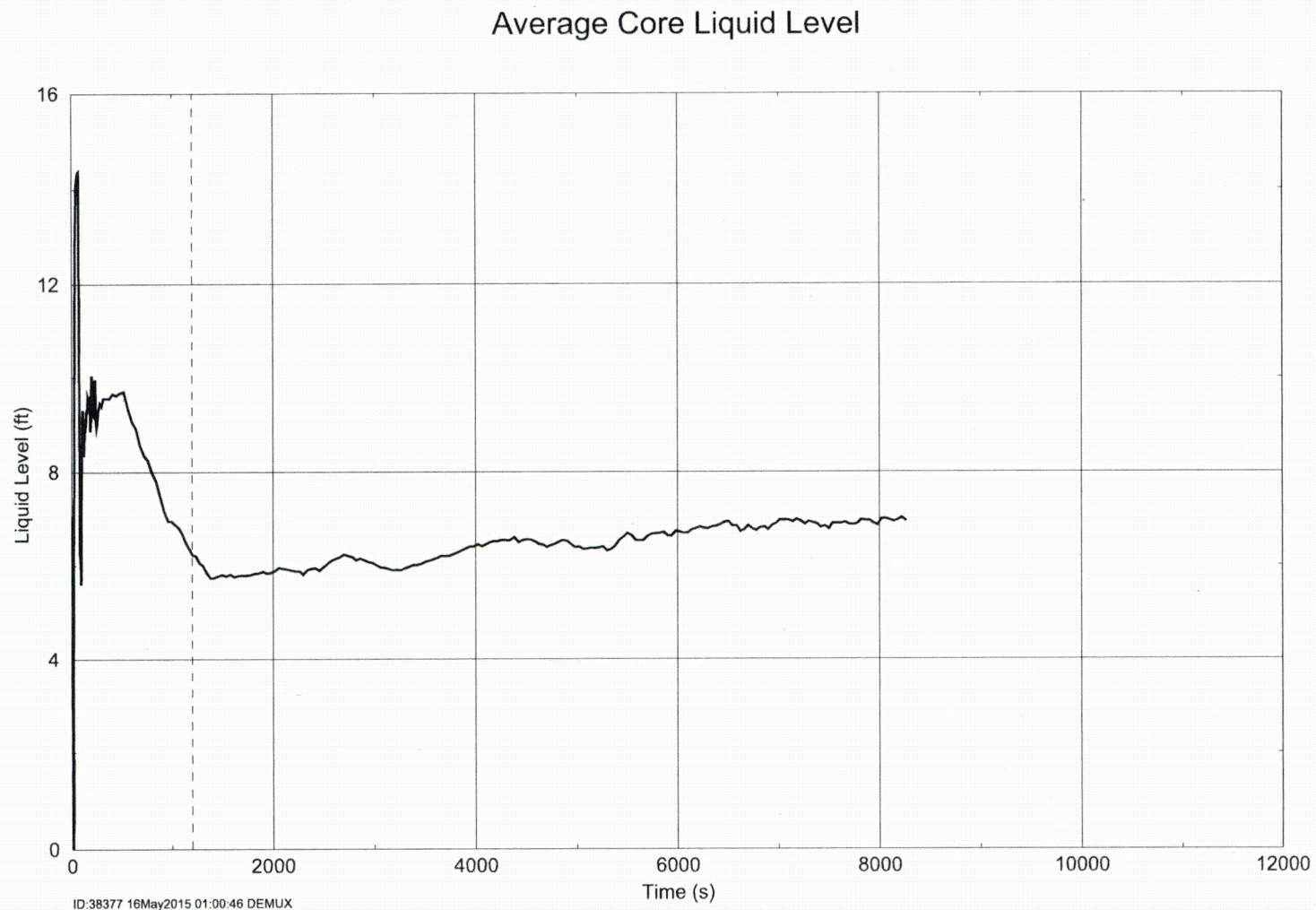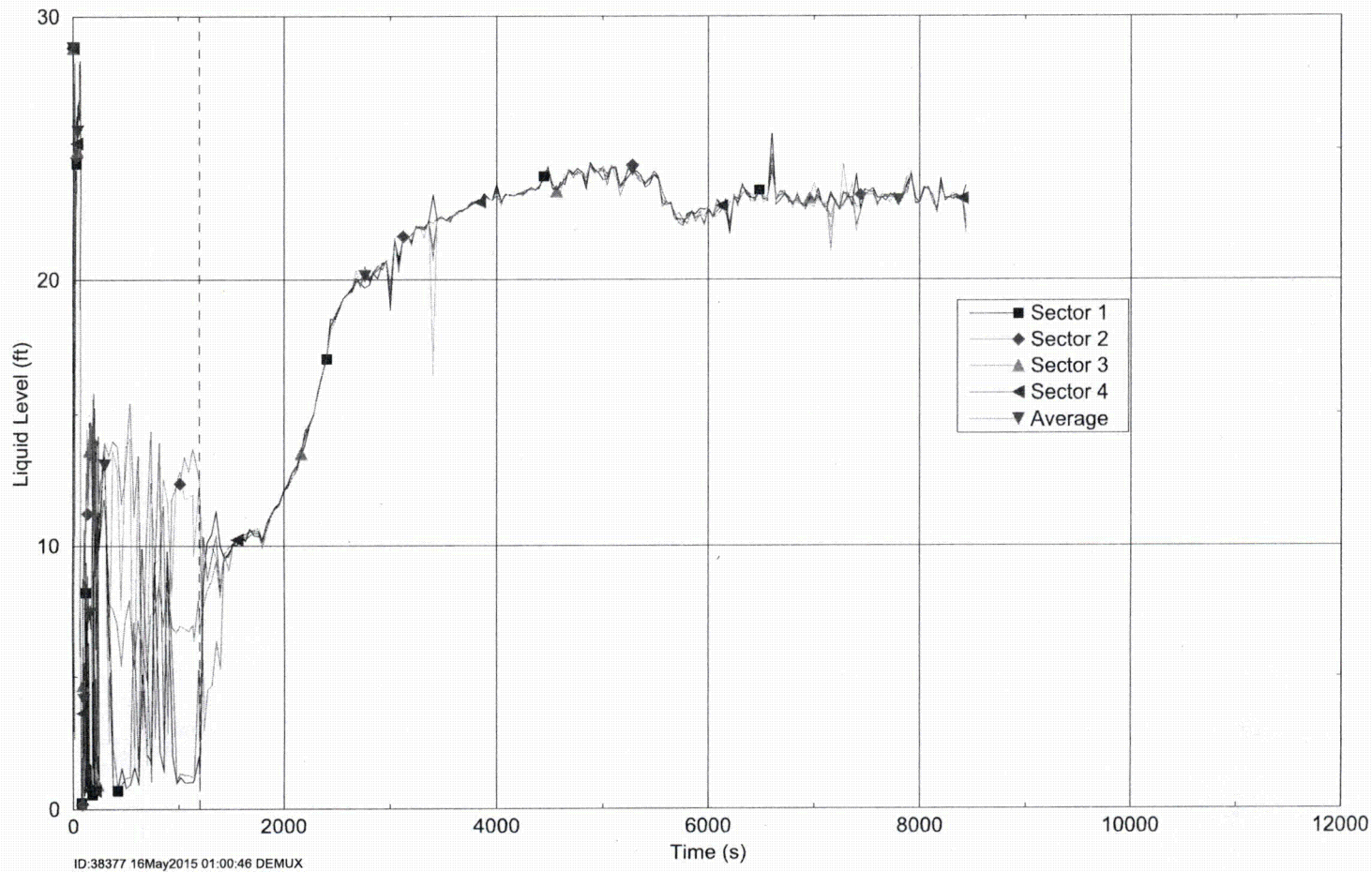Average Core Liquid Level

ID:38377 16May2015 01:00:46 DEMUX

Figure 10-25 Case 2 – Average Core Collapsed Liquid Level

Downcomer Liquid Level

ID:38377 16May2015 01:00:46 DEMUX

Figure 10-26 Case 2 – Downcomer Collapsed Liquid Levels
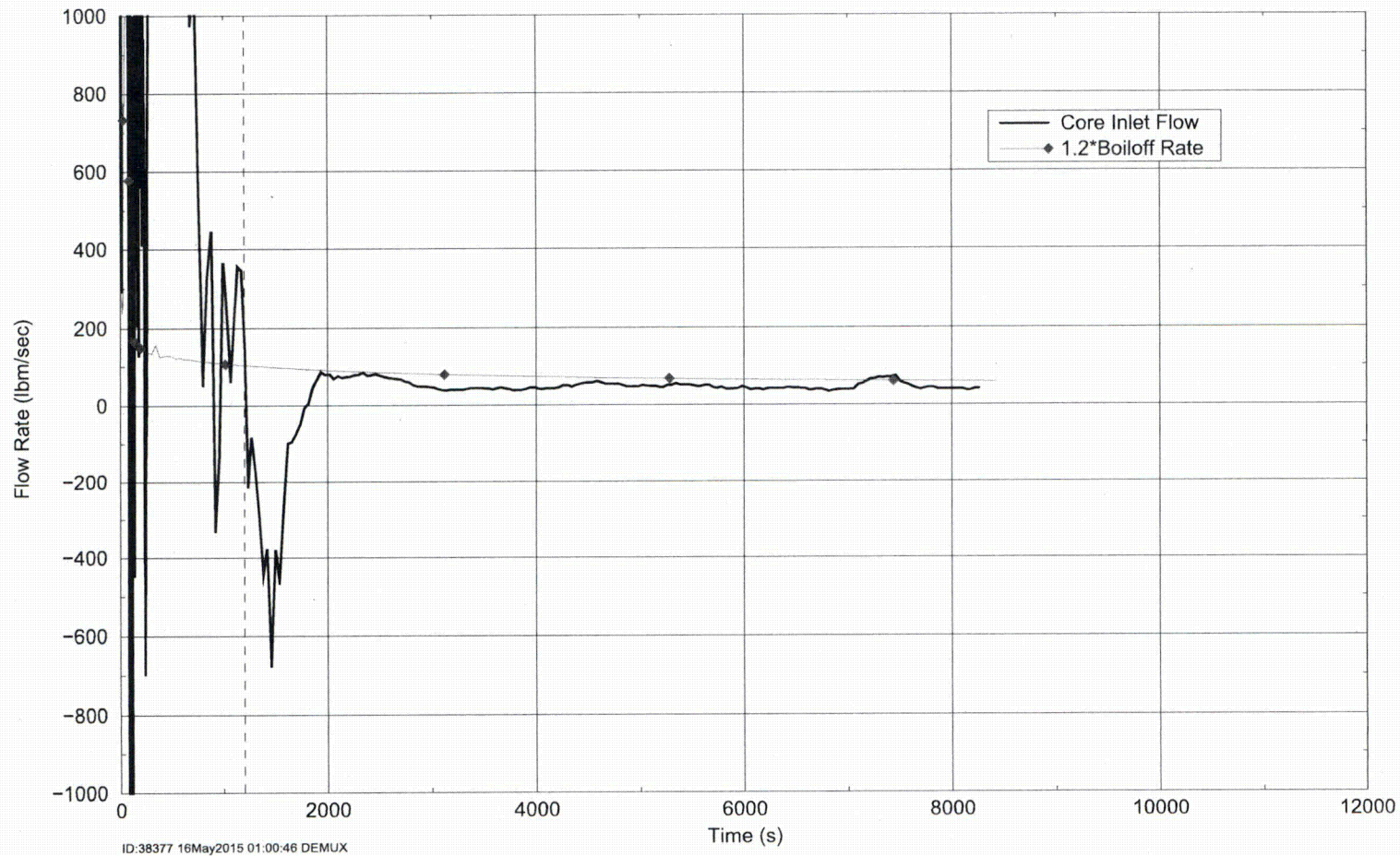
Core Inlet Flow and 1.2*Boiloff Rate

Figure 10-27 Case 2 – Core Inlet Flow Rate Compared to Boil-off
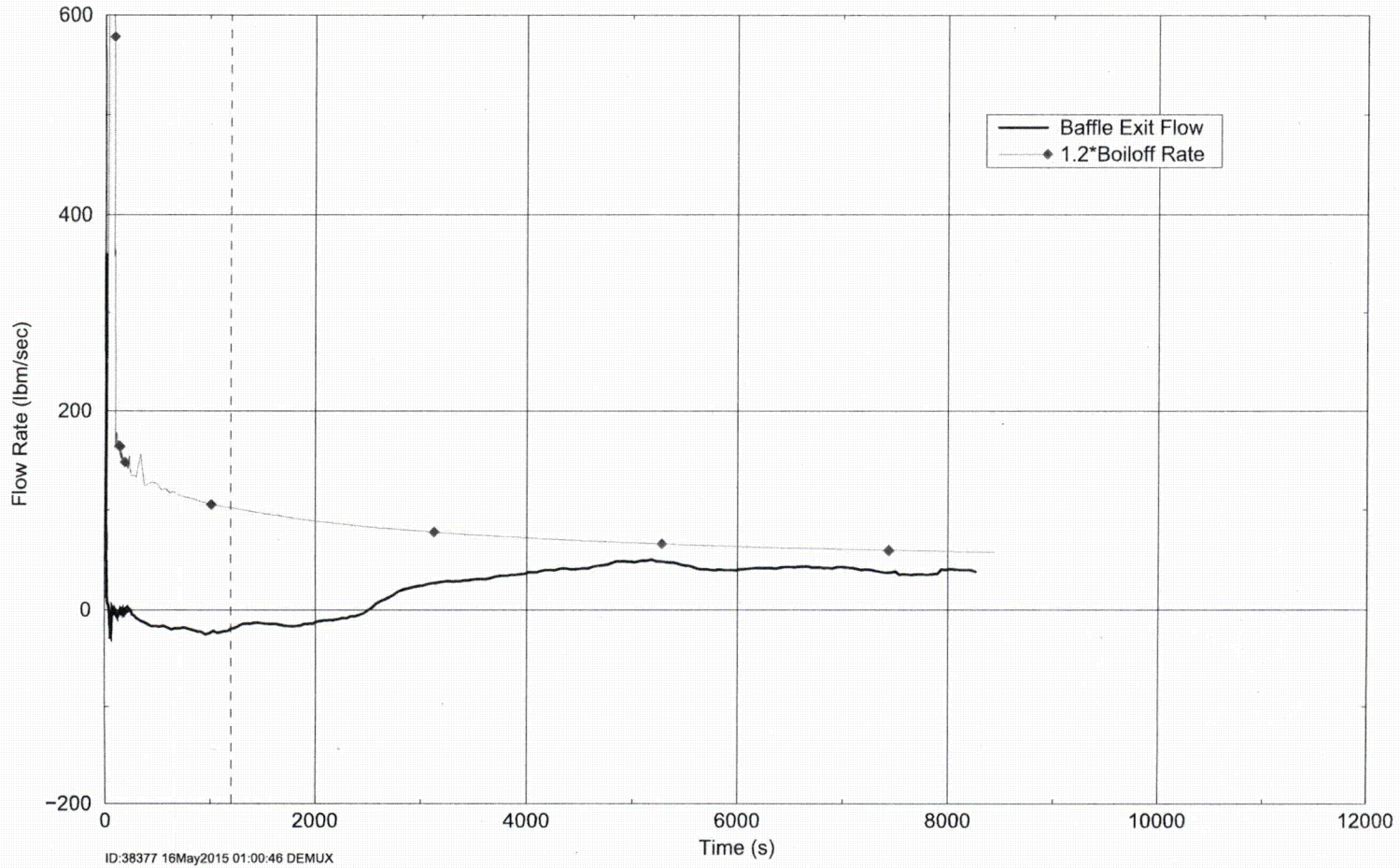
Figure 10-28 Case 2 – Barrel/Baffle Channel Exit Flow Rate Compared to Boil-off

Total Core Inlet DP

ID:38377 16May2015 01:00:46 DEMUX
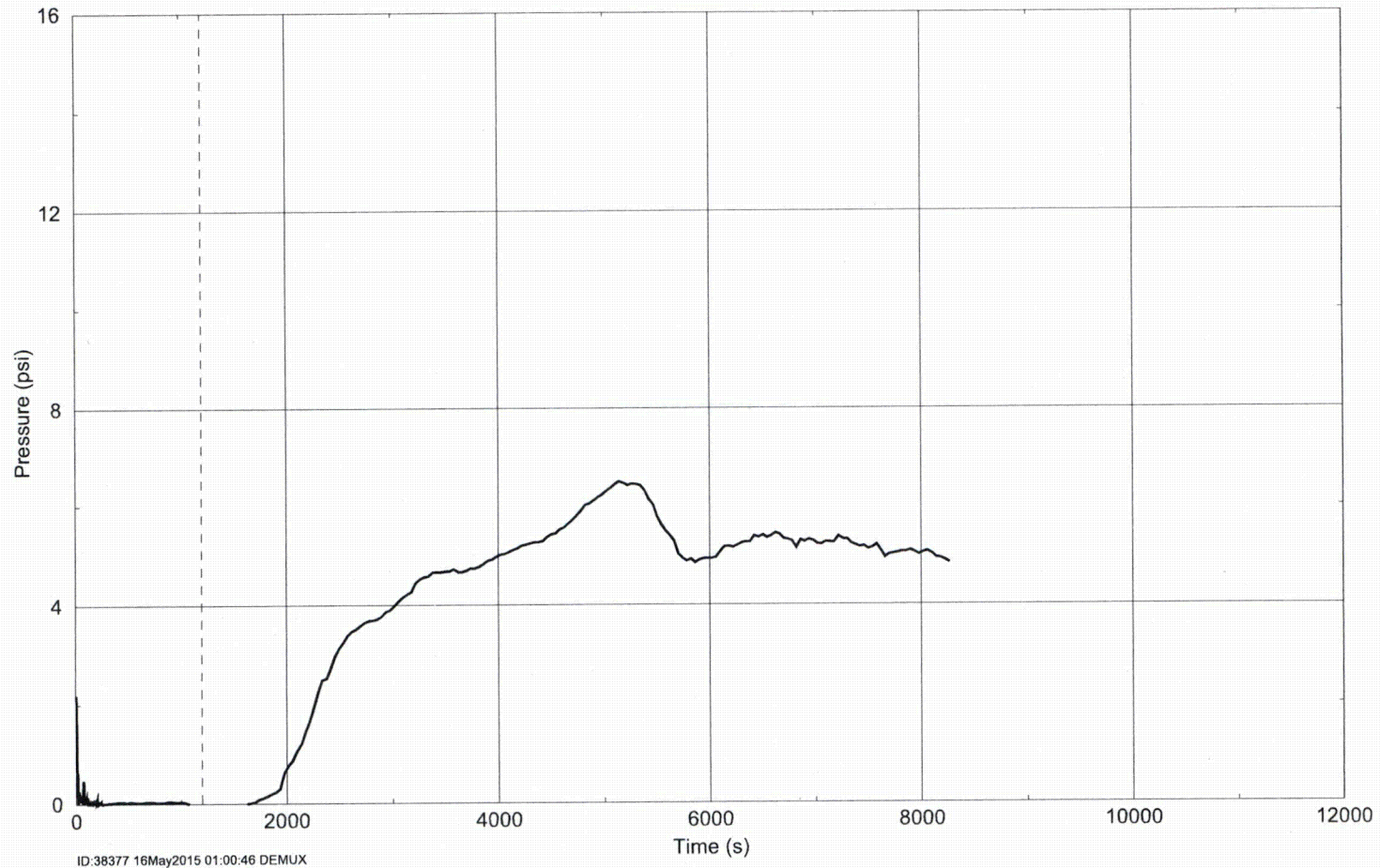
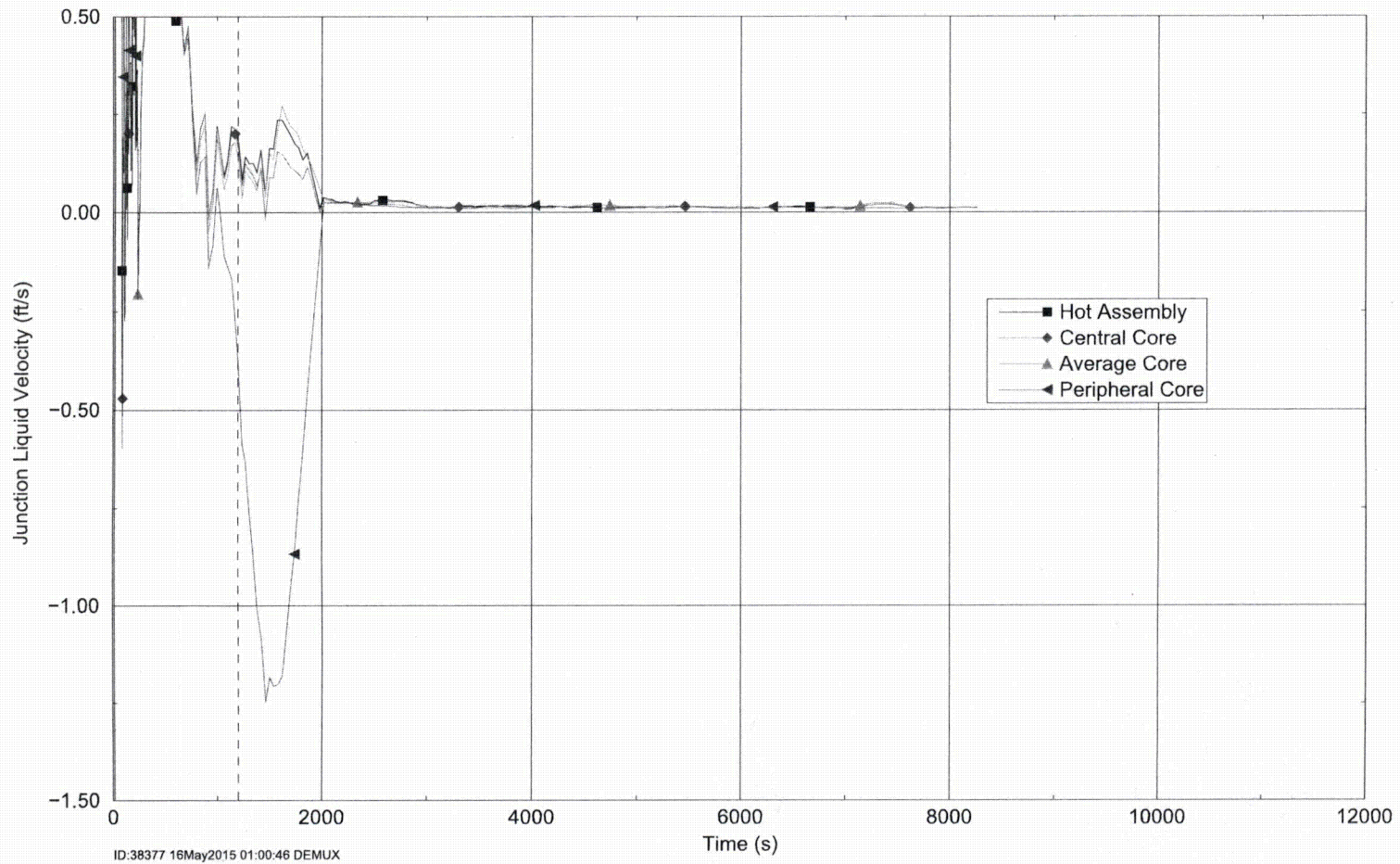**Figure 10-29 Case 2 – Pressure Drop across Debris Bed**

Figure 10-30 Case 2 – Core Inlet Liquid Velocities
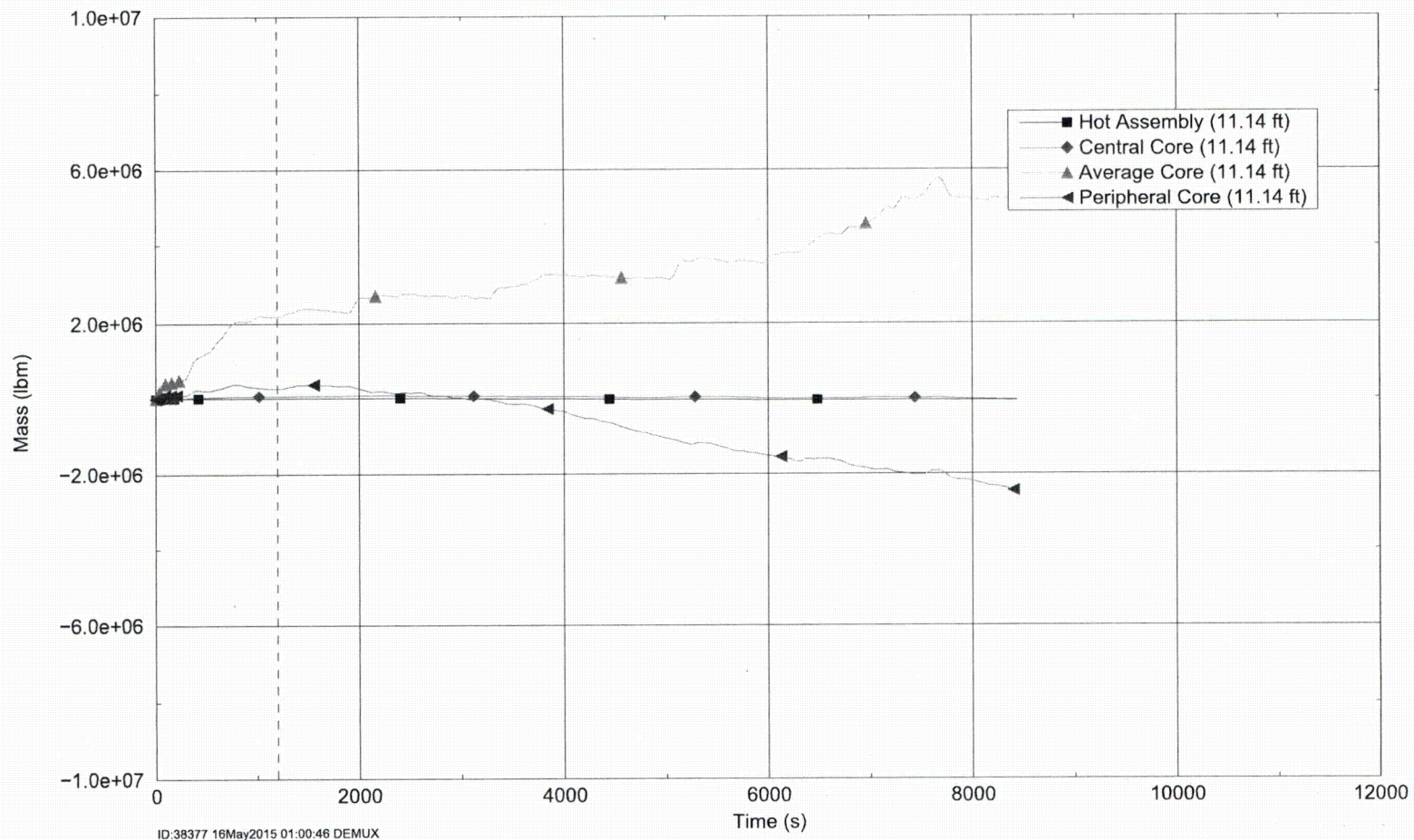
Integrated Flow Rate at 11.14 ft

Figure 10-31 Case 2 – Integrated Flow Rate Near the Top of the Core
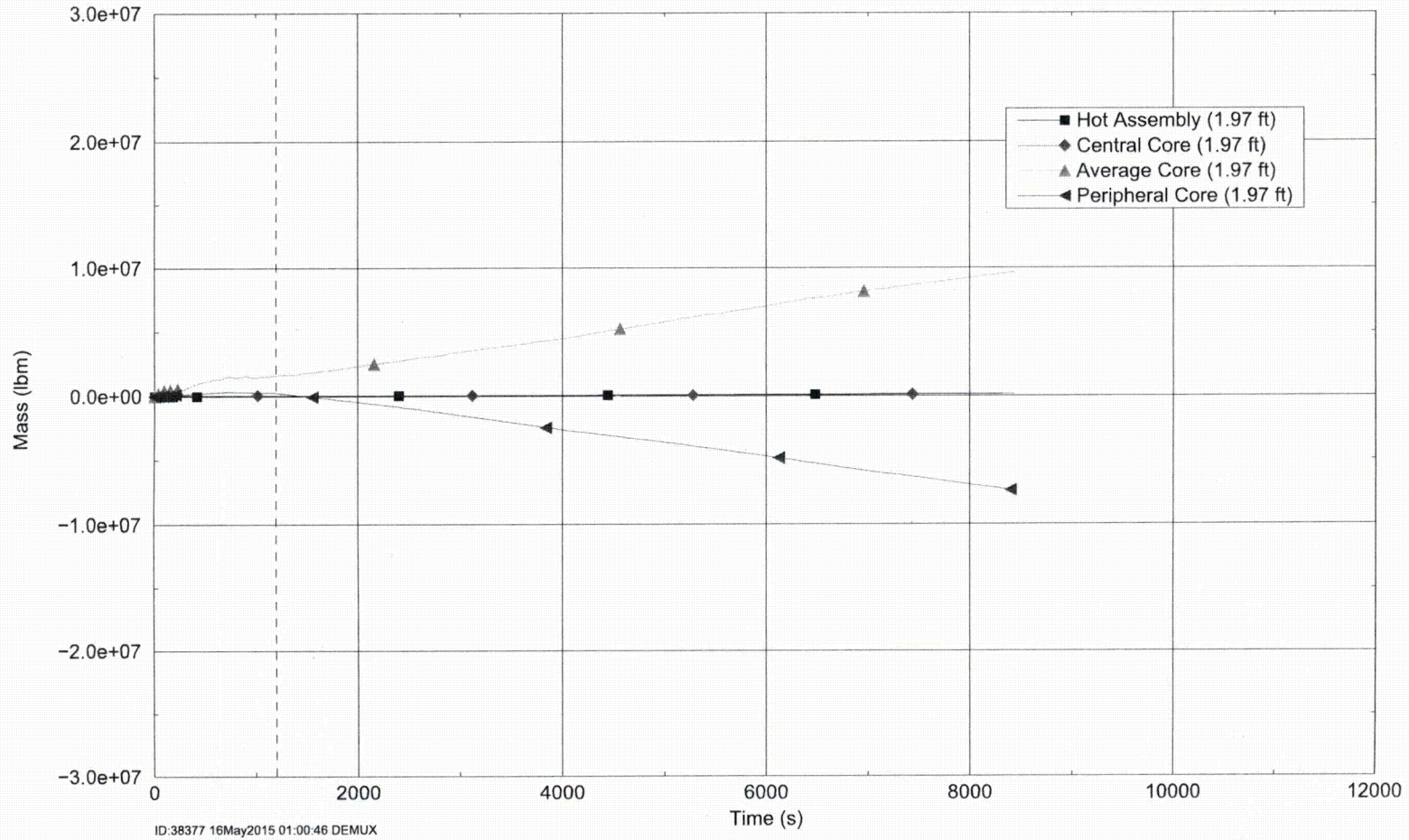
Integrated Flow Rate at 1.97 ft

Figure 10-32 Case 2 – Integrated Flow Rate Near the Bottom of the Core
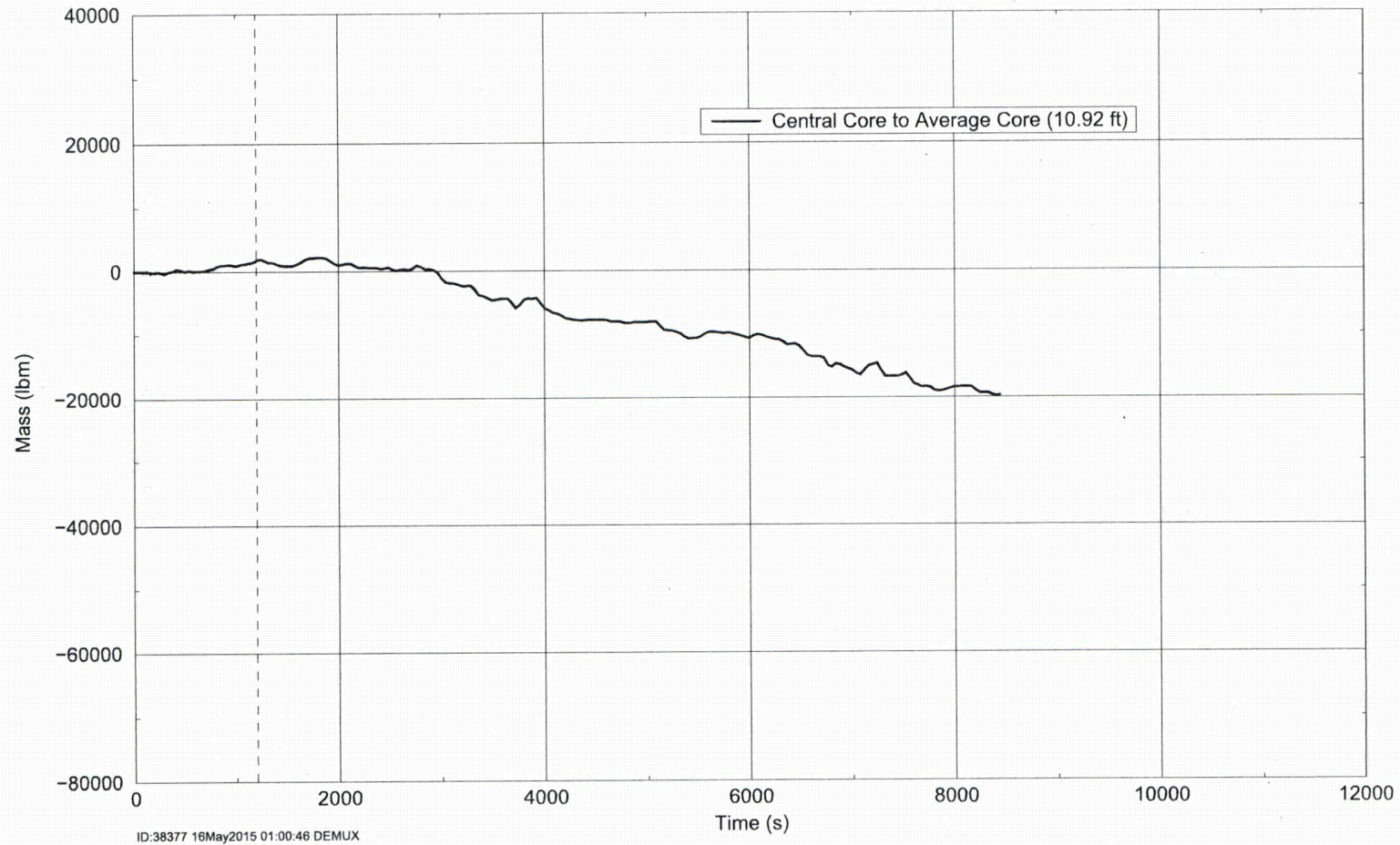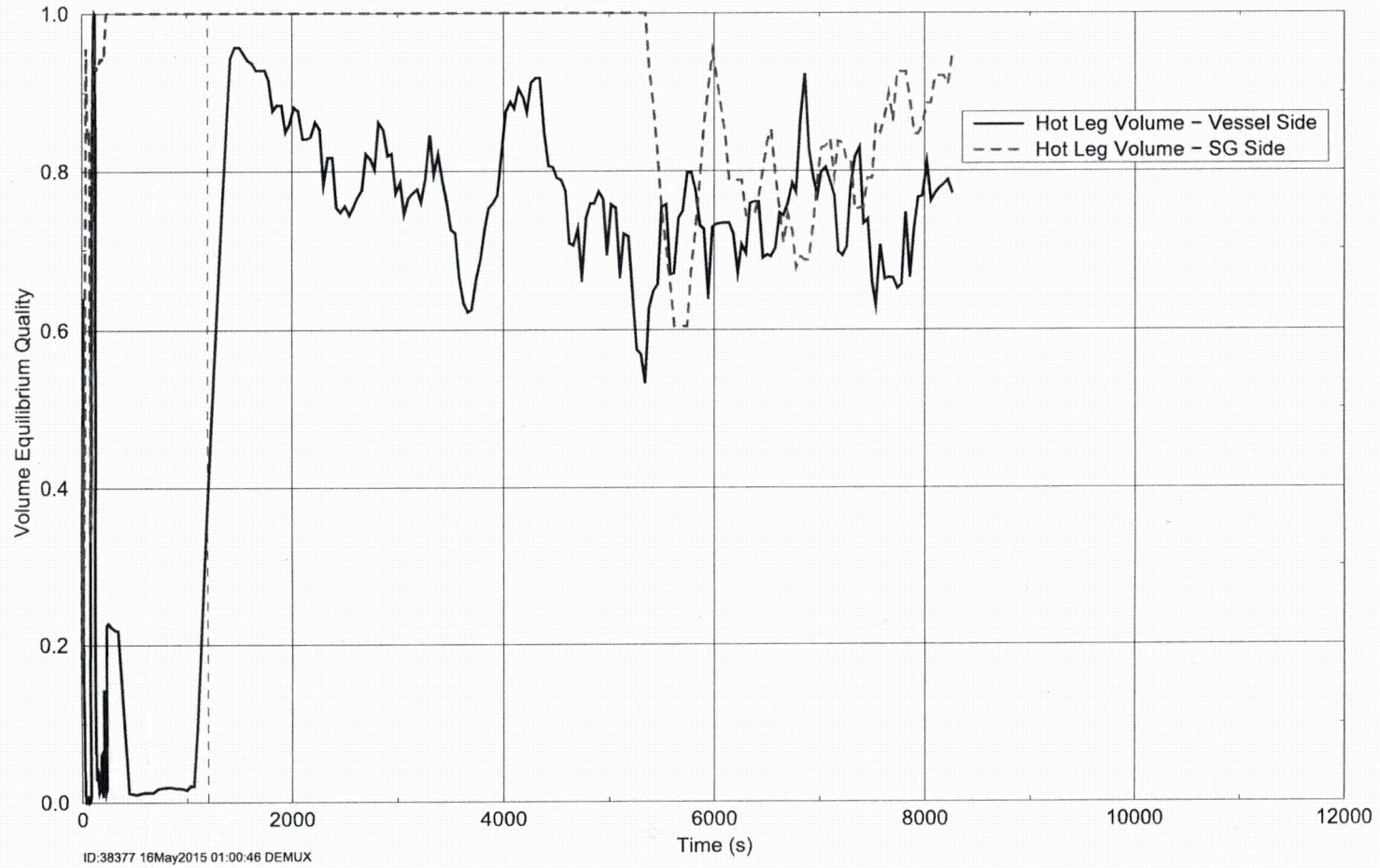
Integrated Crossflow CC to AC at 10.92 ft

Figure 10-33 Case 2 – Cross Flow from Central Core to Average Core Near the Top of the Core

Figure 10-34 Case 2 – Break Exit Quality

10.2.4 After Debris Introduction – Calculation of K_{split} and m_{split}

Three additional cases were run to determine K_{split} and m_{split}. For these cases, a linear ramp in resistance was applied at the core inlet and complete core inlet blockage was not simulated. Since these cases were used to assess the timing of the activation of the BB channel, the build-up of core inlet resistance was applied more slowly compared to the cases used to determine K_{max}. As a result, the RCS response to core inlet blockage was much slower in that the downcomer fill rate and the activation of the BB channel occurred over a longer period of time. It is noted that these simulations are more realistic with regard to the timing at which debris is expected to arrive at the core inlet.

Even though three simulations were completed to cover the full range of ECCS flows expected during sump recirculation, only the mid-flow case is discussed in this section. Similar trends were observed in the two cases not discussed.

Select transient plots from Case 3b are shown in Figures 10-35 through 10-40. The RCS response to core inlet blockage was expected and is generally consistent with the transient response discussed in Section 10.2.3. Figure 10-35 and Figure 10-36 show the core inlet flow rate and BB exit flow rate compared to 120 percent of boil-off, respectively (the data in these figures represents a running average of the case data). The figures demonstrate that flow to the core is well above boil-off during the entire transient. The flow response to core inlet blockage is also shown by the figure. As core inlet blockage is applied, the pressure drop across the core inlet increases. Once K_{split} is reached, the BB exit flow rate becomes positive and increases as the magnitude of core inlet blockage increases. As a result, the core inlet flow rate decreases consistent with the rate that the BB flow rate increases.

Figure 10-37 shows the transient downcomer collapsed liquid levels. As core inlet blockage is applied, the downcomer collapsed liquid level increases as expected. When K_{split} is reached, the BB channel is completely flooded. As core inlet blockage continues to increase, the downcomer continues to flood and eventually fills.

The PCT transient is shown in Figure 10-38. The figure indicates that the PCT remains well below 800°F and the lack of any significant heatups indicates that the core never uncovers after application of core inlet resistance.

Figure 10-39 (the data in this figure represents a running average of the case data) and Figure 10-40 show the pressure drop across the core inlet and the core inlet liquid velocity, respectively. As expected, the core inlet velocity decreases as the pressure drop across the simulated debris bed increases.

Core Inlet Flow and 1.2*Boiloff Rate
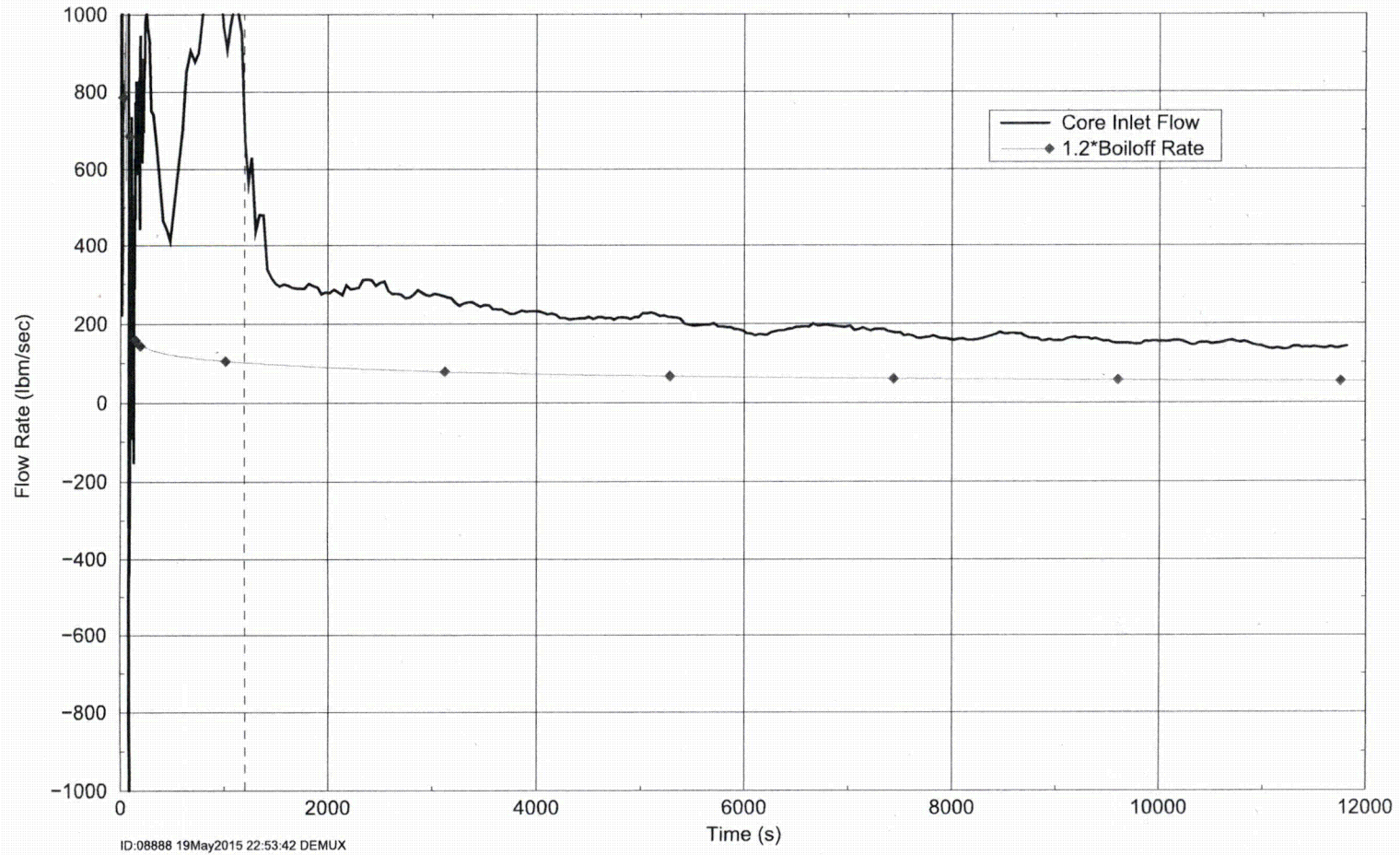
Figure 10-35 K_{split} Case 3b – Core Inlet Flow Rates Compared to Boil-off
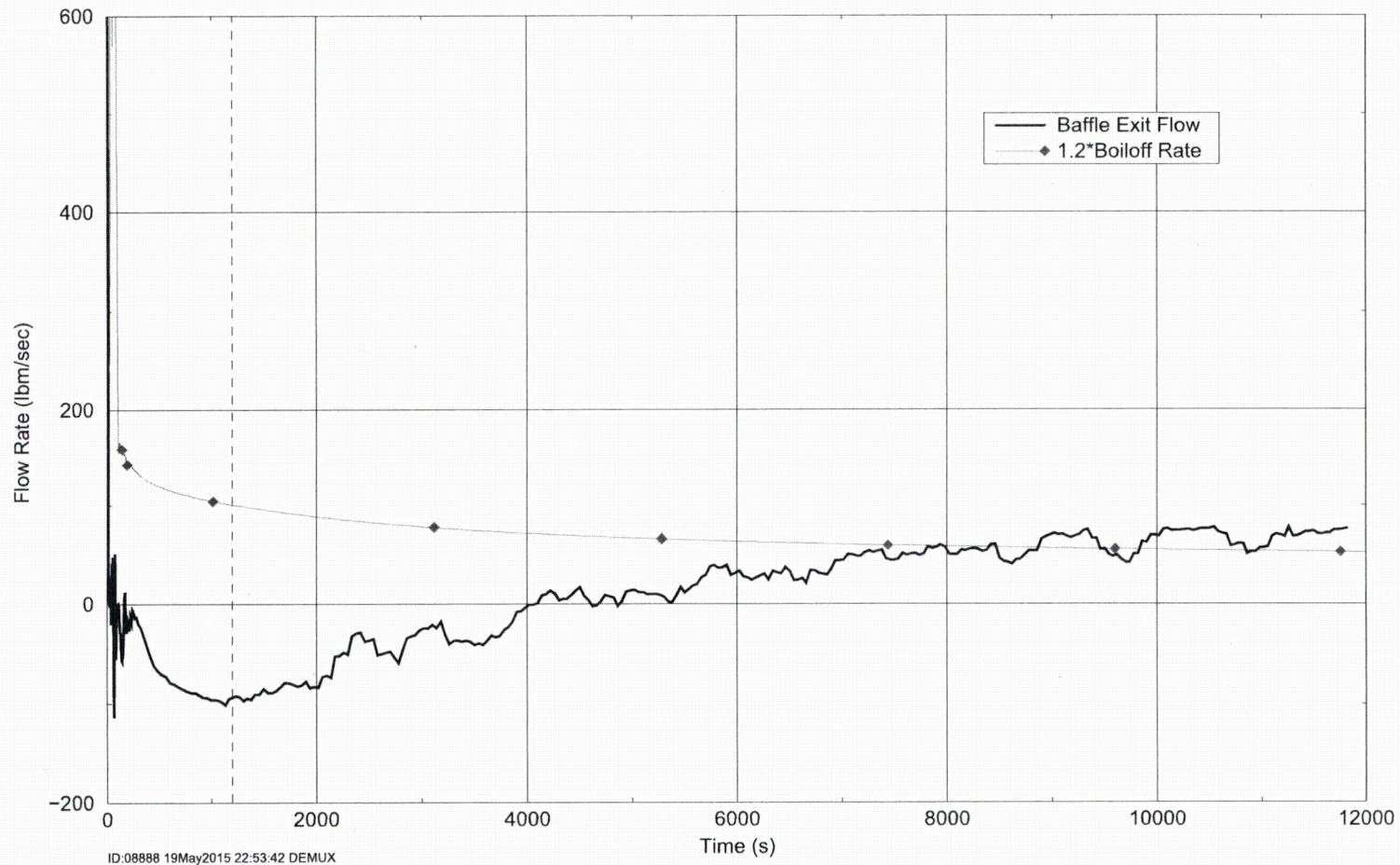
Figure 10-36 K_{split} Case 3b – Barrel/Baffle Exit Flow Rates Compared to Boil-off
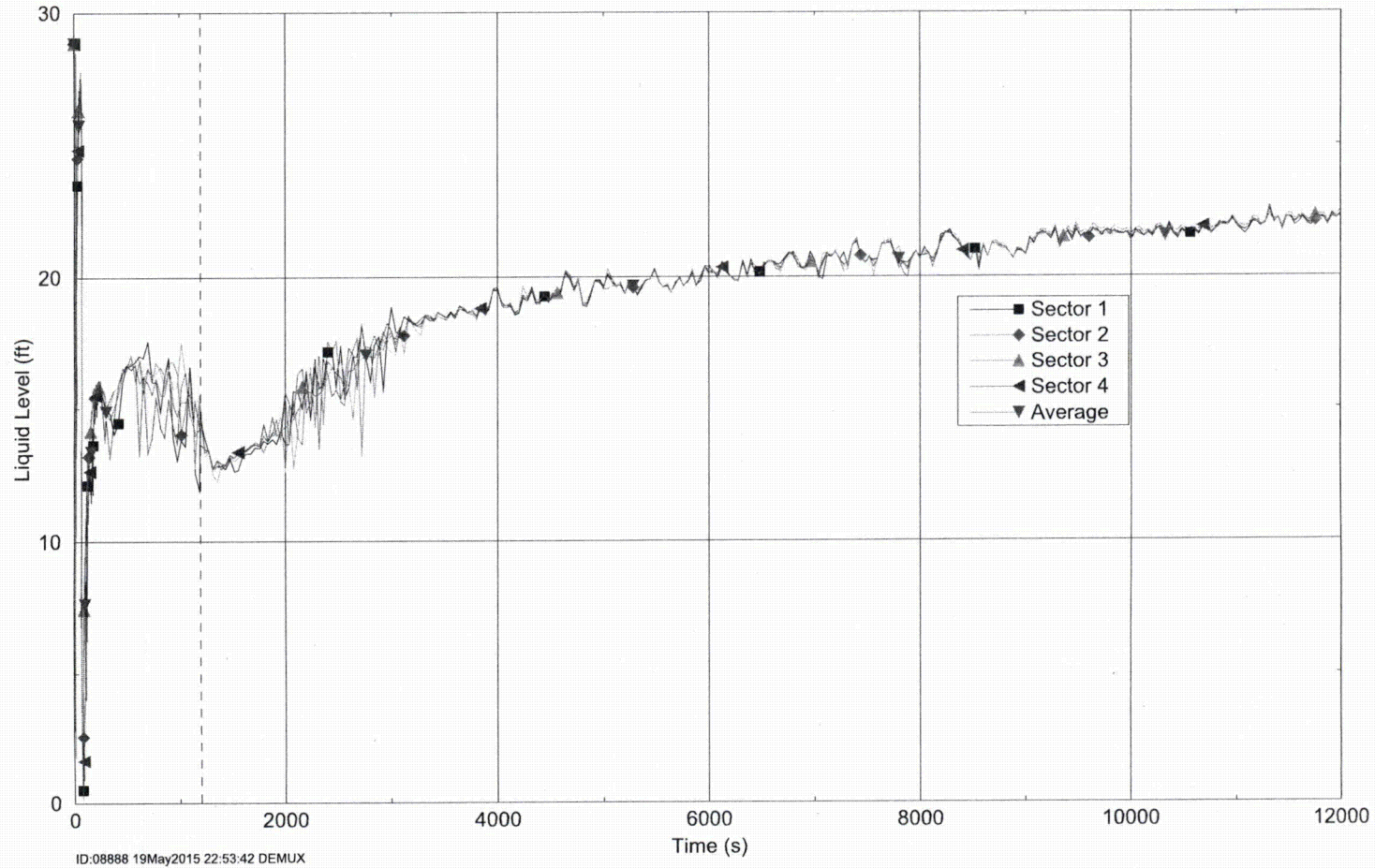
Figure 10-37 K$_{split}$ Case 3b – Downcomer Collapsed Liquid Levels

PCT Trace

ID:08888 19May2015 22:53:42 DEMUX

Figure 10-38 K$_{split}$ Case 3b – Hot Assembly Peak Cladding Temperature

Total Core Inlet DP
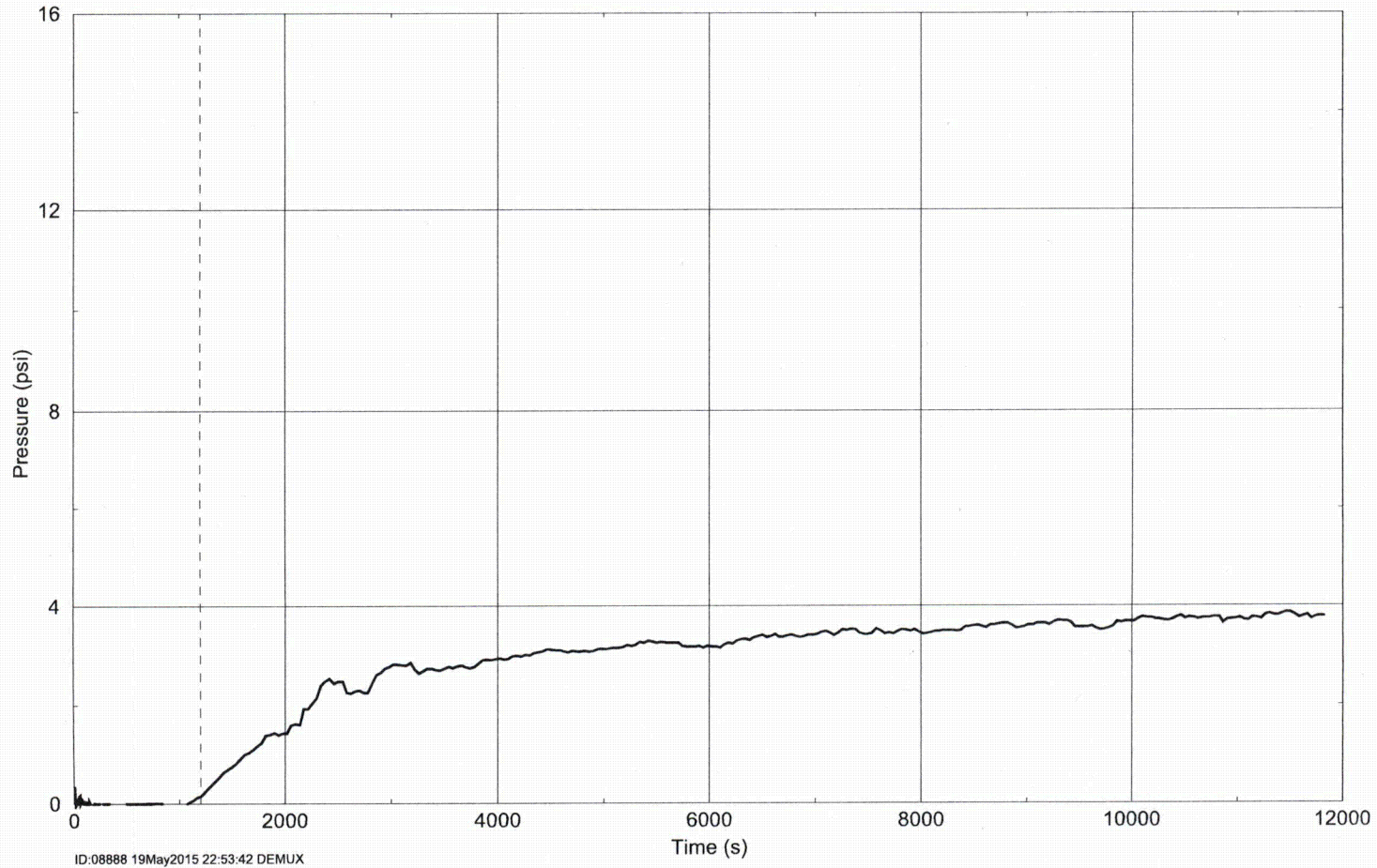
Figure 10-39 K_split Case 3b – Pressure Drop across Debris Bed

Core Inlet Velocity

ID:08888 19May2015 22:53:42 DEMUX

Figure 10-40 K$_{split}$ Case 3b – Core Inlet Liquid Velocities

10.3   DISCUSSION OF RESULTS

During the first 20 minutes of the transient (before debris arrives), the core region has completely reflooded and the cladding temperatures are just above the saturation t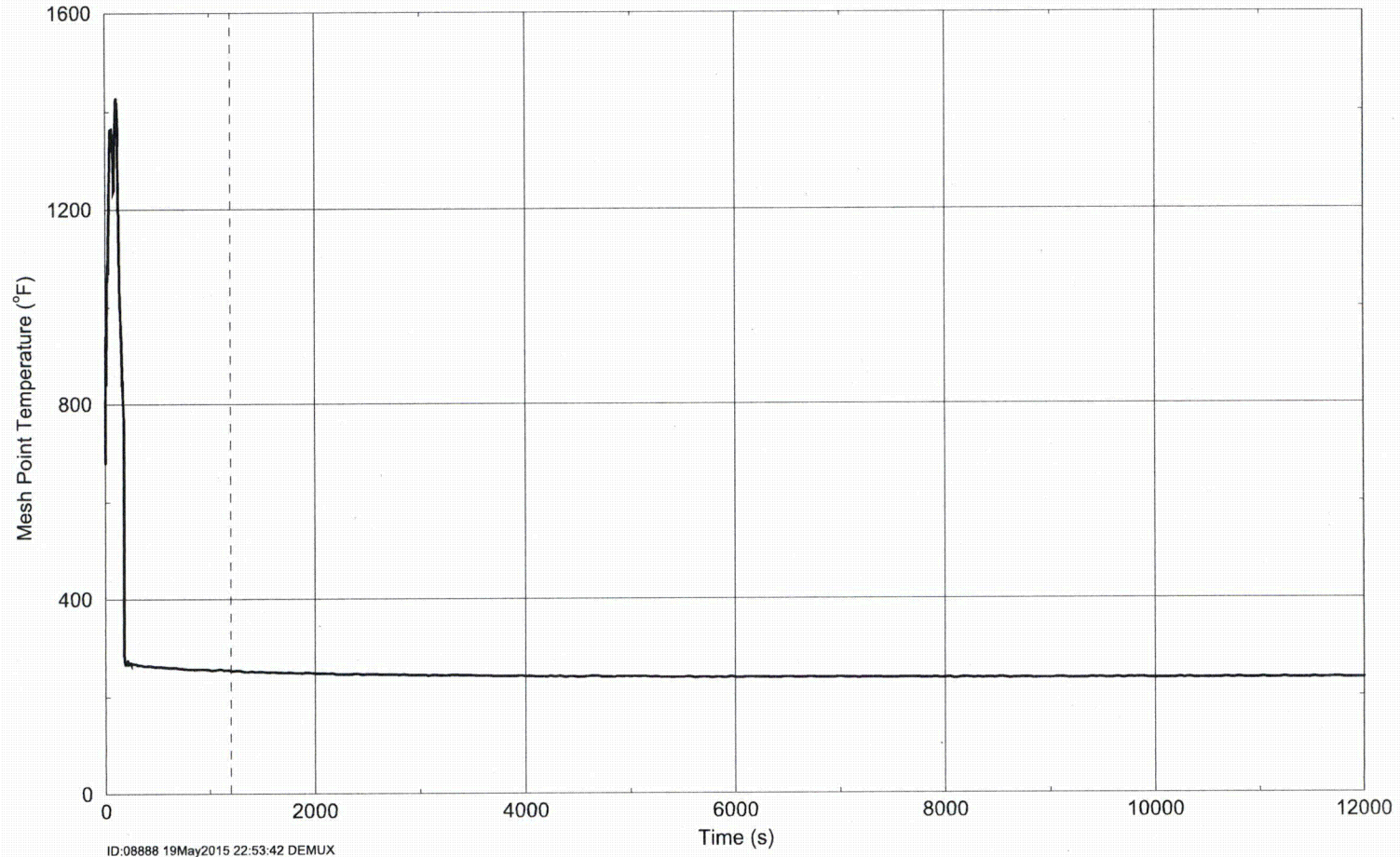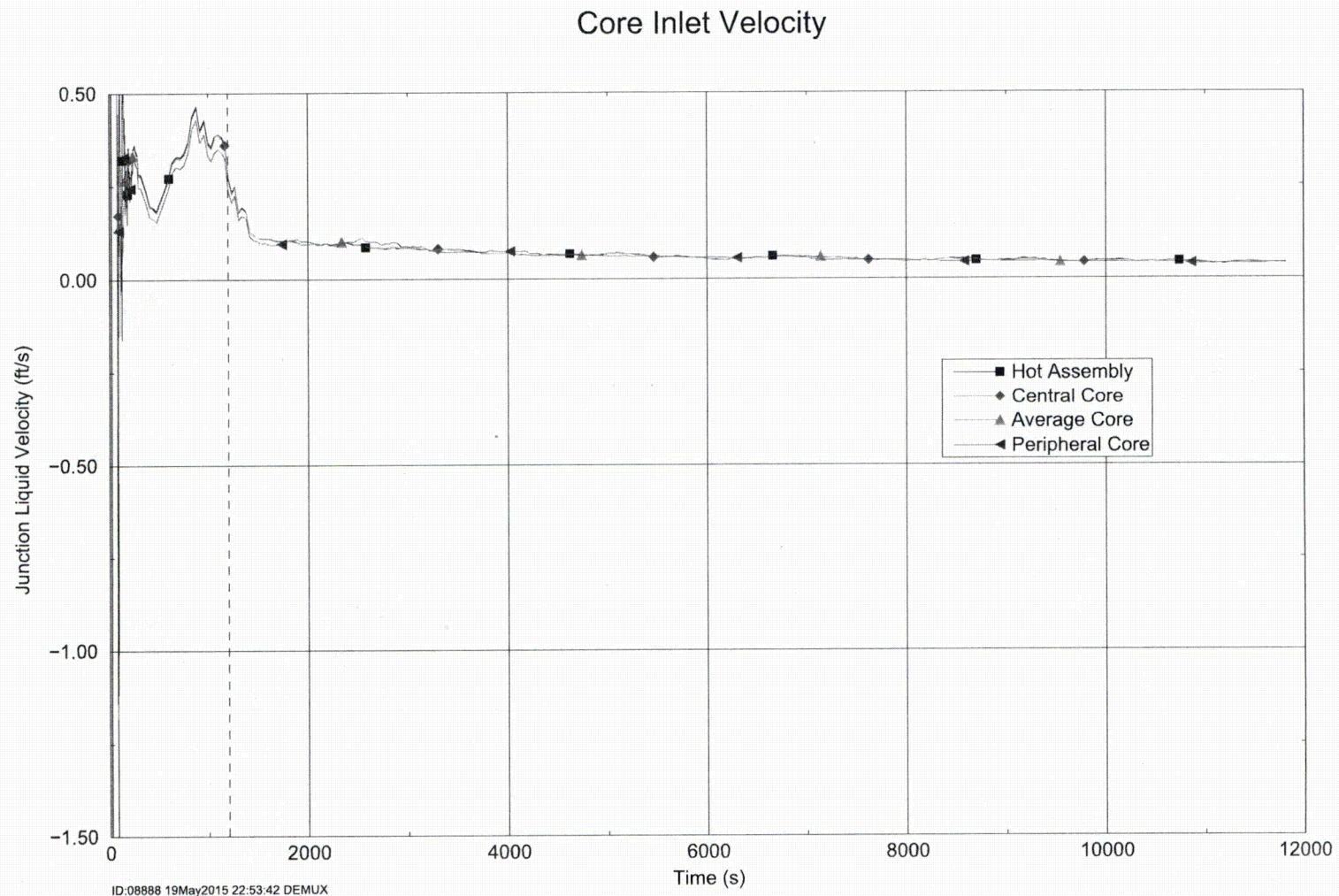emperature. The core is boiling vigorously and the core average void fraction is approximately 50%. The downcomer is filling with coolant supplied to the cold legs via the ECCS. At 20 minutes, the downcomer collapsed liquid level is well below the cold leg elevation. Similarly, the BB is not liquid solid and is filling with liquid supplied from the UP region. There is a strong recirculation pattern within the core region in which the hot and average assemblies have predominately upflow while the peripheral assemblies have downflow. Vapor generated in the core flows toward the break and liquid carryover to the break is significant.

The first core inlet blockage simulation (Section 10.2.2) examined a scenario in which the core inlet was instantaneously completely blocked at some finite time after transfer to sump recirculation by applying a large form-loss coefficient at the core inlet. For this scenario, no partial blockage is applied prior to applying complete core inlet blockage. These simulations showed that the application of an instantaneous complete core inlet blockage resulted in no heatup within the core. When the blockage was applied, flow through the core inlet ceased and the ECCS began to fill the downcomer. Eventually, the downcomer liquid level reached a point where the driving head was sufficient to push coolant through the BB channel to the top of the core. This process resulted in recovery of the core two-phase mixture level and return of the cladding temperatures to values near the saturation temperature. A lower ECCS flow rate resulted in a longer time to fill the downcomer and increase the driving head to a value high enough to push flow through the BB channel to the top of the core. It was determined that complete blockage of the core inlet had to be delayed until at least 250 minutes after the postulated LOCA to maintain a secondary heatup of less than 800°F.

It is recognized that the complete core inlet blockage scenario used to determine t_{block} is unrealistic relative to the prototypic system. In reality, the arrival of fibrous and particulate debris to the core inlet prior to the formation of chemical products will create a lower resistance partial blockage well before the core inlet is expected to block completely. The resulting partial blockage will aid in filling the downcomer and activating the BB channel prior to reaching complete core inlet blockage. Higher ECCS flow rates would also fill the downcomer faster and generate an earlier time that complete core inlet blockage could be tolerated.

The second core inlet blockage simulation (Section 10.2.3) applied a ramped blockage to the core inlet beginning at 1800 seconds. The magnitude of the form-loss coefficient was such that flow through the core inlet is reduced but not stopped completely. The RCS response to the partial blockage was very similar to the response after complete core inlet blockage, other than the fact that flow through the core inlet continued. No significant heatups were observed in this case.

The value of the form-loss coefficient applied to simulate partial blockage was iterated upon to determine the maximum value that could be tolerated and maintain the PCT below 800°F. For the minimum ECCS flow, it was determined that a constant form-loss coefficient of 6.5×10^6 produced acceptable results. Similar to the Westinghouse cases discussed in Section 8, as ECCS flow increases, this value is expected to increase.

The third set of core inlet blockage simulations (Section 10.2.4) examined a scenario in which a gradual build-up of debris was applied at the core inlet. These are considered the most realistic cases relative to how fibrous and particulate debris is expected to arrive at the core inlet; however, these cases do not simulate complete core inlet blockage. The gradual addition of resistance at the core inlet slowly increases the downcomer level and delays the activation of the BB channel. Eventually, the downcomer driving head becomes sufficiently large to change the flow direction in the BB channel. After this point, flow from the LP is split between the core inlet and the BB and, as the core inlet resistance continues to build, the flow fraction to the BB continues to increase while the flow fraction to the core inlet decreases. From these simulations, the core inlet resistance necessary to activate the BB channel (K_{split}) was determined to be a strong function of the ECCS flow. K_{split} plotted as a function of ECCS flow rate is provided in Figure 10-4 and the corresponding flow split between the core inlet and the BB channel (m_{split}) following K_{split} is shown in Figure 10-5.

11   BABCOCK AND WILCOX DESIGNS

In this section, results from the B&W plant category are presented and discussed. The range of conditions and case matrix are provided in Section 11.1. Results from the analysis are presented in Section 11.2. This section is broken into several subsections and the material contained in each subsection is summarized as follows:

- In Section 11.2.1, results from the beginning of the case used to determine t_{block} and K_{max} are used to describe the RCS state at the time of transfer to sump recirculation and the arrival of debris. Since all simulations are identical prior to reaching sump recirculation, the discussion in this section is applicable to all cases. In the simulations, transfer to sump recirculation occurs 20 minutes after the postulated LOCA.

- In Section 11.2.2, results from the case used to determine t_{block} and K_{max} are presented. Since the B&W plant category can meet the acceptance criteria with complete core inlet blockage applied at sump switchover, only one case is needed for both parameters. For this case, complete core inlet blockage was applied instantaneously and was applied uniformly across all core channels.

- In Section 11.2.3, results from additional cases used to determine K_{split} and m_{split} are presented. For these cases, a linear ramp in resistance was applied uniformly across the core inlet and complete core inlet blockage was not simulated. Since these cases were used to assess the timing of the activation of the BB channel, the build-up of core inlet resistance was applied more slowly compared to the cases used to determine K_{max}. As a result, the RCS response to core inlet blockage was much slower in that the downcomer fill rate and the activation of the BB channel occurred over a longer period of time. It is noted that these simulations are more realistic with regard to the timing at which debris is expected to arrive at the core inlet.

Section 11.3 summarizes and discusses the key analysis results.

11.1   RANGE OF CONDITIONS AND CASE MATRIX

The simulation matrix used to determine t_{block} and K_{max} is shown in Table 11-1. Since all BB designs for the B&W plants are the same, the BB flow resistance was not changed. In the table, the loss coefficient column identifies the core inlet losses applied at the designated initiation times to simulate the collection of debris. All cases applied a step change to the loss coefficient applied at the core inlet. The core inlet resistances applied for these cases are presented graphically in Figure 11-1. The sump recirculation flow rate is applied 1200 seconds after the initiation of the event for all simulations.

The simulation matrix used to determine K_{split} and m_{split} is shown in Table 11-2. Since all of the BB designs for the B&W plants are the same, the BB flow resistance was not changed. In the table, the loss coefficient column identifies the core inlet losses applied starting at the designated initiation time and ending at the designated end time. For example, in Case 2a, a timewise-linear ramp of the loss coefficient at a rate of 6000 /hr is applied starting at 1200 seconds and ending at 12,000 seconds. The ending value of the loss coefficient is 18,000. Complete core inlet blockage is not applied to these cases. The core inlet resistances applied for these cases are presented graphically in Figure 11-2. The sump recirculation flow rate is applied at 1200 seconds after the initiation of the event for all simulations.

Table 11-1   Simulation Matrix for t_{block} and K_{max} – B&W Plant Design

Case	Sump Recirculation Flow Rate (gpm/FA)	Debris Bed Model	
		Loss Coefficient	Initiation Time (sec)
1	7.4	1×10^8	1200

Table 11-2   Simulation Matrix for K_{split} and m_{split} – B&W Plant Design

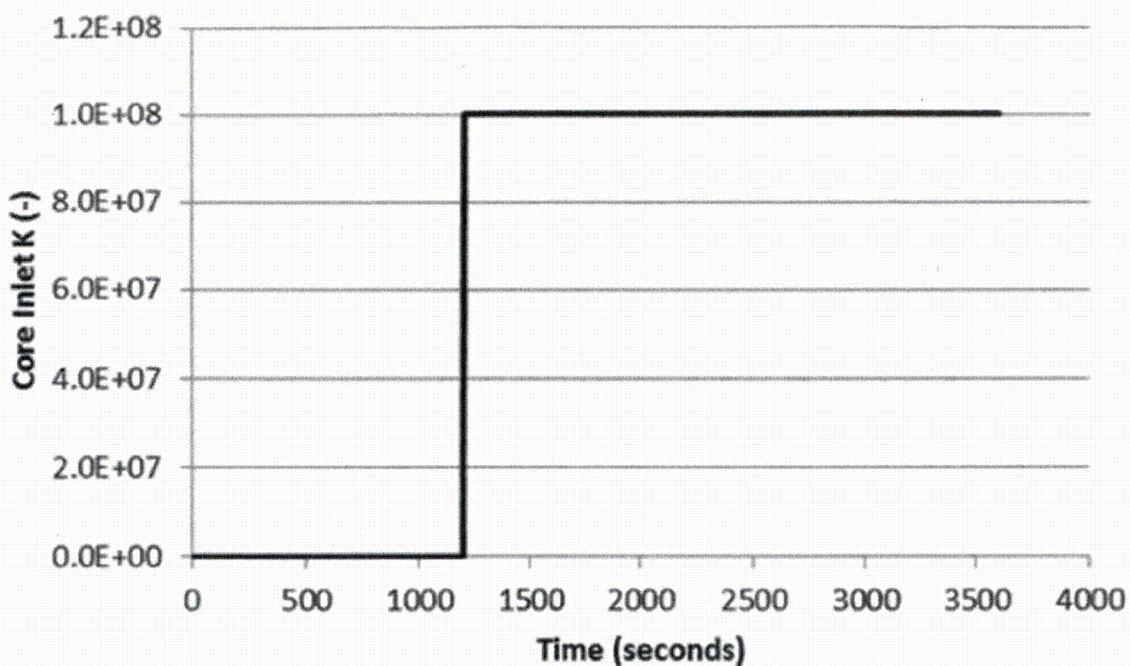| Case	Sump Recirculation Flow Rate (gpm/FA)	Debris Bed Model (Linear Ramp)		
		Loss Coefficient	Initiation Time (sec)	End Time (sec)
2a	43.5	6000/hr	1200	12,000
2b	27.5	6000/hr	1200	12,000
2c	22.5	6000/hr	1200	12,000
2d	17.5	6000/hr	1200	12,000
2e	12.5	6000/hr	1200	12,000
2f	7.5	6000/hr	1200	12,000

Figure 11-1 Core Inlet Resistance Transient Applied to Case 1 Simulations from B&W Analysis
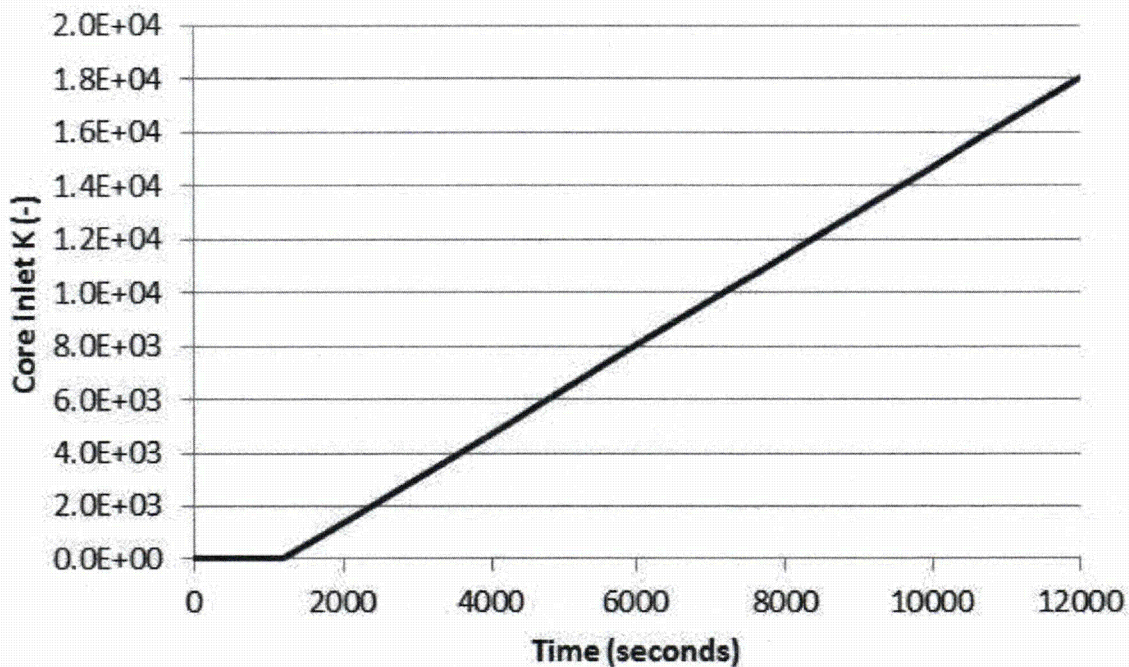

Figure 11-2 Core Inlet Resistance Transient Applied to Case 2 Simulations from B&W Analysis

11.2 RESULTS OF ANALYSIS

Key results from the t_{block} and K_{max} simulations are summarized in Table 11-3. Case 1 applies complete core inlet blockage and determines the minimum time that complete blockage can be tolerated. This case is also used to determine the maximum resistance that can be tolerated prior to reaching complete blockage.

Based on the results presented in Table 11-3, it is concluded that LTCC can be maintained if complete core inlet blockage occurs 20 minutes (1200 sec), or later, after the initiation of the LOCA event. This case also indicates that complete core inlet blockage can be tolerated at the same time, resulting in a K_{max} value of 1×10^8 across the core inlet when a uniform resistance is applied instantaneously upon entering sump recirculation. These results are based on the minimum ECCS recirculation flow case. As shown in Section 8 for the Westinghouse plant design, higher ECCS flow rates will fill the downcomer more quickly, leading to more favorable results and the use of the minimum ECCS flow rate bounds the range of recirculation flows expected.

With regard to BAPC, Case 1 demonstrates that, after core inlet blockage, the break exit quality remains sufficiently low such that boron is flushed from the core and concentrations are expected to remain well below the solubility limit. The core can be considered well mixed and no localized regions containing higher boron concentration are expected to form for the reasons discussed in Section 11.2.2.

Key results from the K_{split} and m_{split} simulations are summarized in Table 11-4. The K_{split} values shown in the table are used in conjunction with the ECCS sump recirculation flow rates to generate the curve shown in Figure 11-4. The time that K_{split} occurs is determined by examination of the BB inlet flow rate. The first timestep in which the BB inlet flow rate becomes positive is defined as the K_{split} time. If flow oscillations (positive BB inlet flow followed by a reversal to negative flow) occur, the time of K_{split} is selected after the flow oscillations stop and the BB inlet flow remains positive. The transient flow split between the core inlet and BB is shown in Figure 11-5 for the six ECCS recirculation flow rates investigated. The flow split is represented as the fraction of total ECCS recirculation flow through the BB inlet and is plotted as a function of the core inlet resistance following K_{split}.

Table 11-3   Summary of Results for t_{block} and K_{max} – B&W Plant Design

Case	Time Core Inlet Resistance Applied	Core Inlet Loss Coefficient (K)	Core Inlet Average Mass Flow Rate per FA	Core Inlet Average Velocity	Pressure Drop across Debris Bed	Break Exit Quality	PCT
---	sec	---	lbm/sec	ft/s	psid	---	°F
1	1200	1×10^8	0	0	NA	<0.4	<310

Table 11-4	Summary of Results for K_{split} and m_{split} – B&W Plant Design	
Case	Time of K_{split}	K_{split}
---	sec	---
2a	1300	167
2b	1460	433
2c	2000	1333
2d	2720	2533
2e	3780	4300
2f	7080	9800

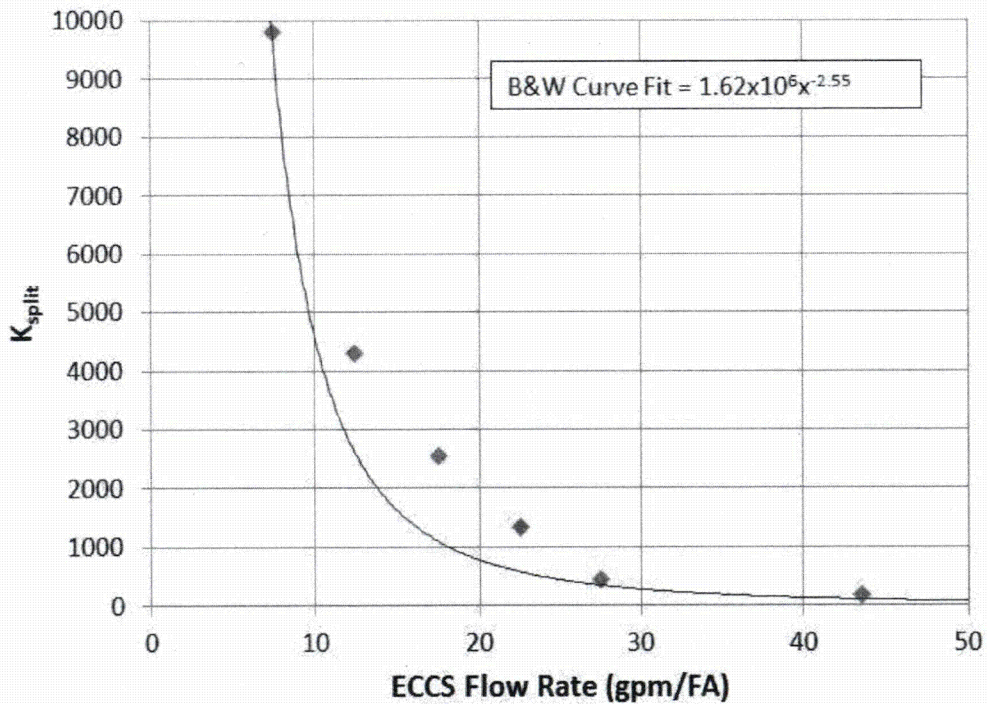B&W Curve Fit = $1.62 \times 10^6 x^{-2.55}$

Figure 11-3 K_{split} **as a Function of ECCS Recirculation Flow Rate from B&W Analysis**
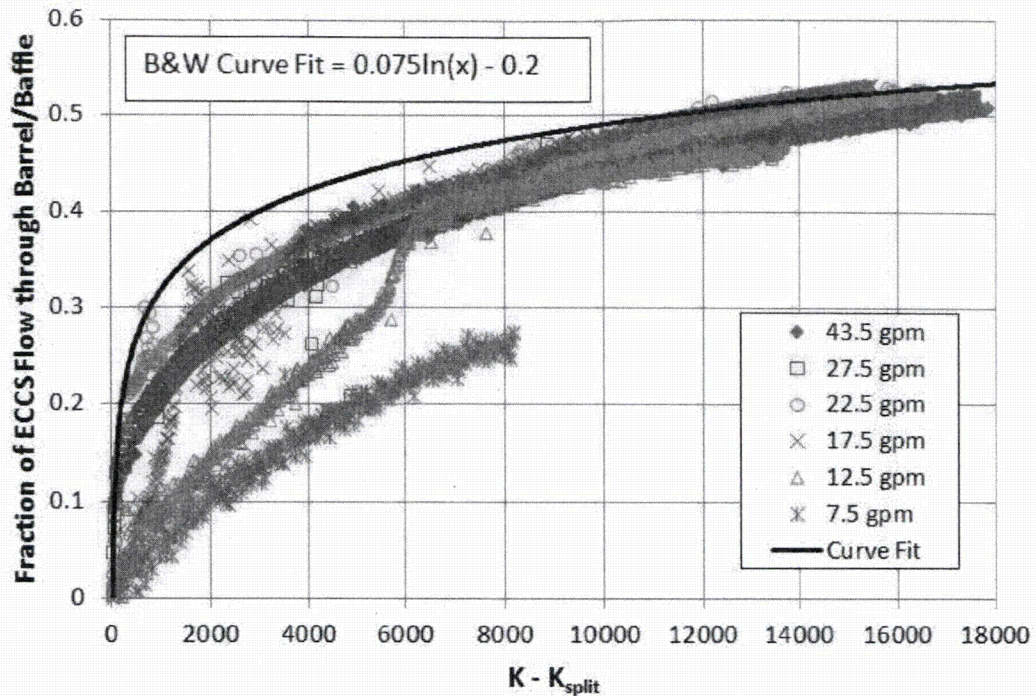
Figure 11-4 Fraction of ECCS Recirculation Flow through the Barrel/Baffle Inlet following K_{split} from B&W Analysis

11.2.1 All Cases – Before Debris Introduction

The results from Case 1 (up to 1200 seconds) are used to describe the RCS state at the point of transfer to sump recirculation and the arrival of debris. Since all simulations are identical prior to that point in the transient, the discussion in this section is applicable to all cases. In the simulations, transfer to sump recirculation occurs 20 minutes after the postulated LOCA. In general, the trends of the B&W analysis mimic those seen for the Westinghouse and CE analyses discussed previously. One difference to note is that the B&W analysis uses two core channels, which leads to differences in the predicted core flow patterns. The limitations of using this type of a model are discussed below.

Figure 11-5 shows the flow patterns at the core inlet. Junctions 315-00 and 415-00 represent flow from the LP to the hot and average channels, respectively. Prior to 1200 seconds, the flow is positive, indicating flow from the LP into the core (i.e., upflow). Junction 314-03 represents flow from the LP to the BB channel (baffle region). Prior to 1200 seconds, the flow is negative, indicating flow from the BB channel to the LP.

Figure 11-6 shows the flow patterns at the core outlet. Junctions 347-00 and 447-00 represent flow from the hot and average channels, respectively, to the UP. Prior to 1200 seconds, the flow is positive from the hot channel to the UP, indicating flow out of the core (i.e., upflow). Flow from the average core to the UP is generally positive, but a bit more oscillatory, indicating that flow is generally upward. This trend gives some indication of the limitation of the two-channel model, which is discussed further below. Junction

456-01 represents flow from the BB channel to the UP. Prior to 1200 seconds, the flow is negative, indicating flow from the UP to the BB (i.e., downflow).

Figure 11-7 shows the axial flow patterns in the BB channel. Up to 1200 seconds, the flow is negative indicating downflow in all junctions in the BB. Figure 11-7 also shows that the mass flow rate in the BB channel increases as elevation decreases which indicates that liquid is entering the BB channel from the core periphery through the LOCA holes. This is further illustrated in Figure 11-8, which shows the cross flow between the BB channel and the average core channel. Junction 452-02 is at the lowermost set of LOCA holes. From approximately 500 seconds to 1200 seconds, the flow direction is positive indicated flow from the BB channel to the average core. At the other junctions, the flow direction is negative during this same time period, indicating flow from the average core to the BB channel.

Due to the large amount of liquid carryover prior to sump recirculation, BAP is controlled and boron concentration levels in the RV upon entry to sump recirculation are expected to be comparable to the ECCS source concentration.
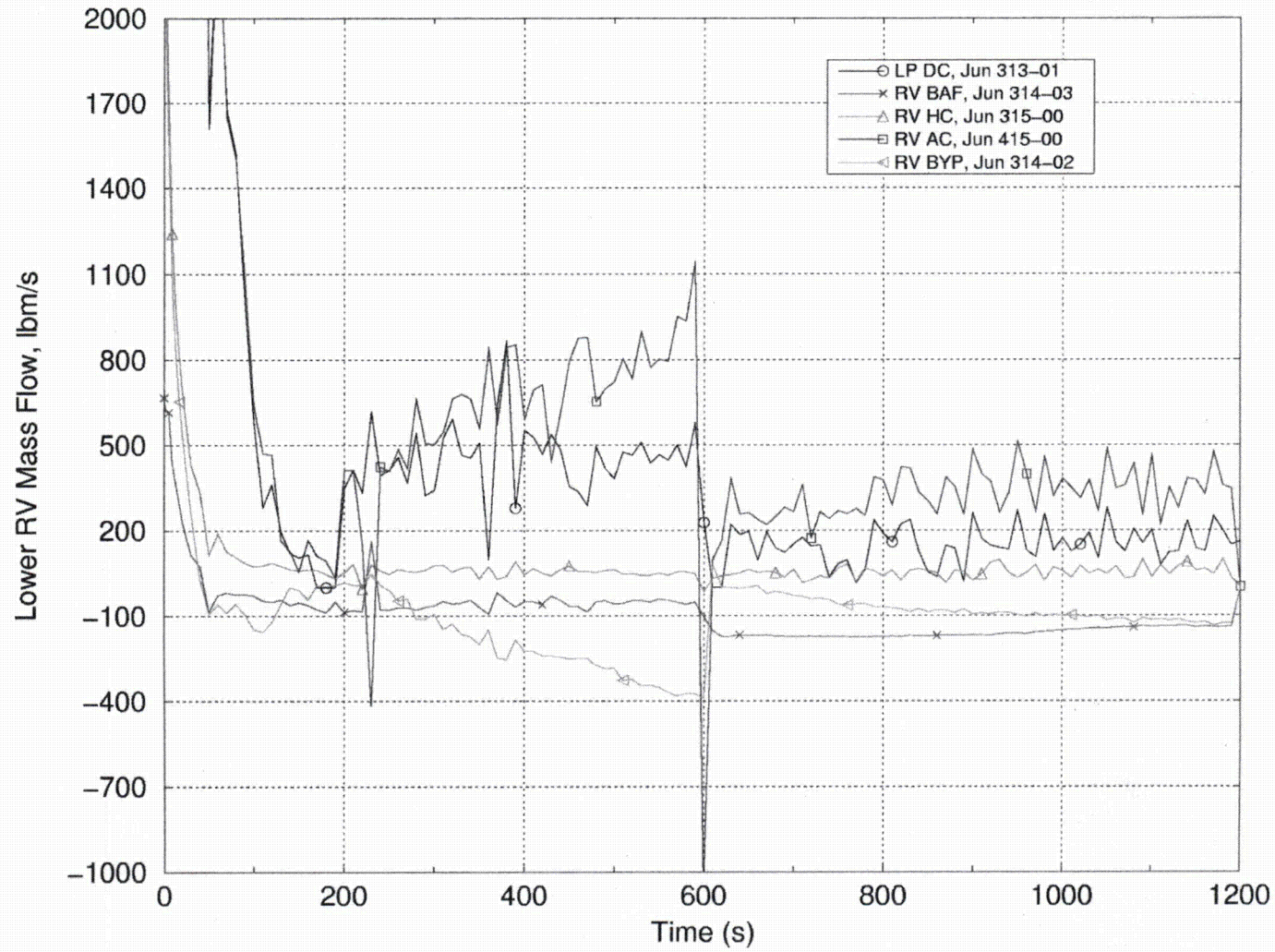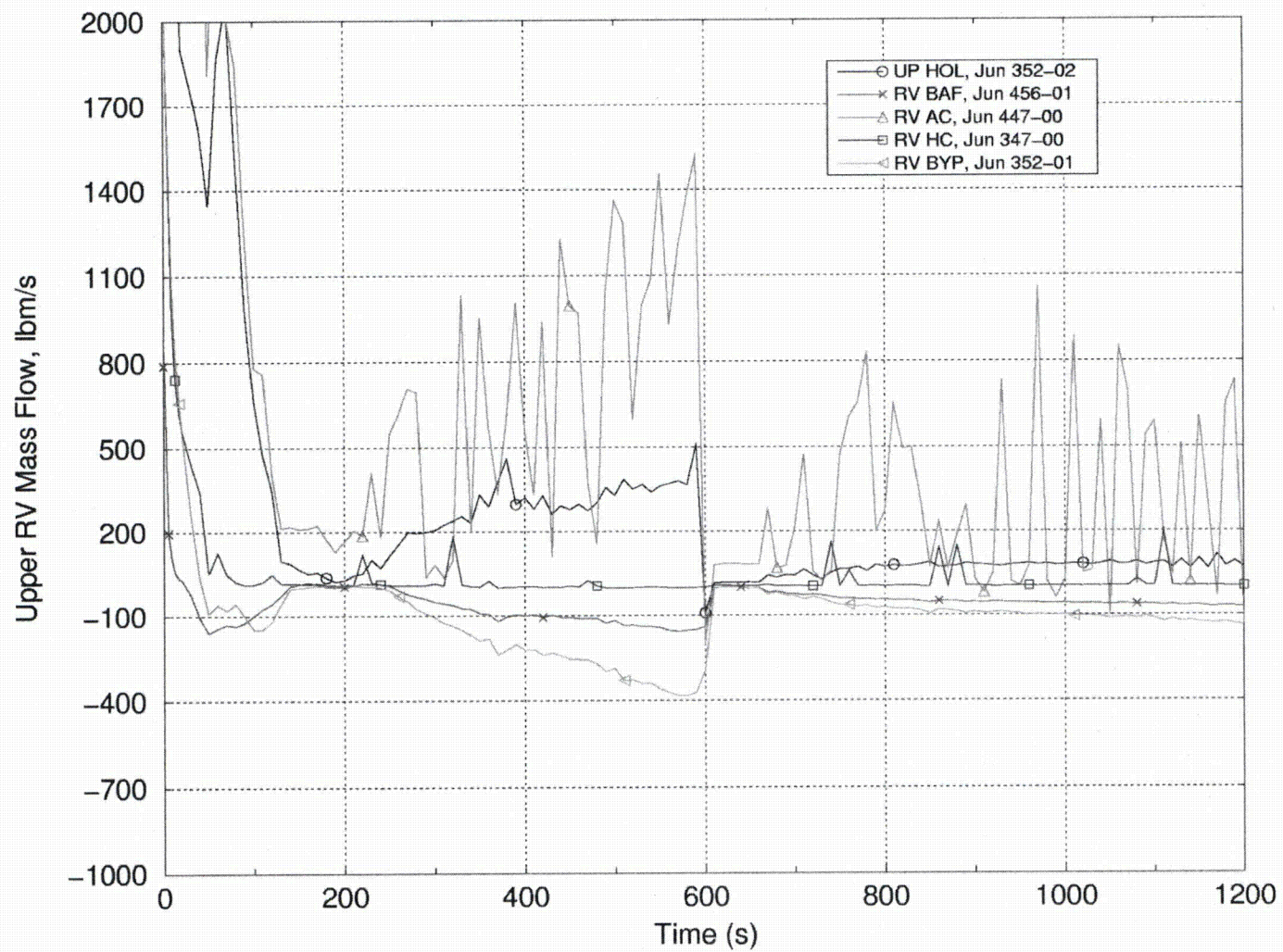
Figure 11-5 Flow from Lower Plenum to Core Region
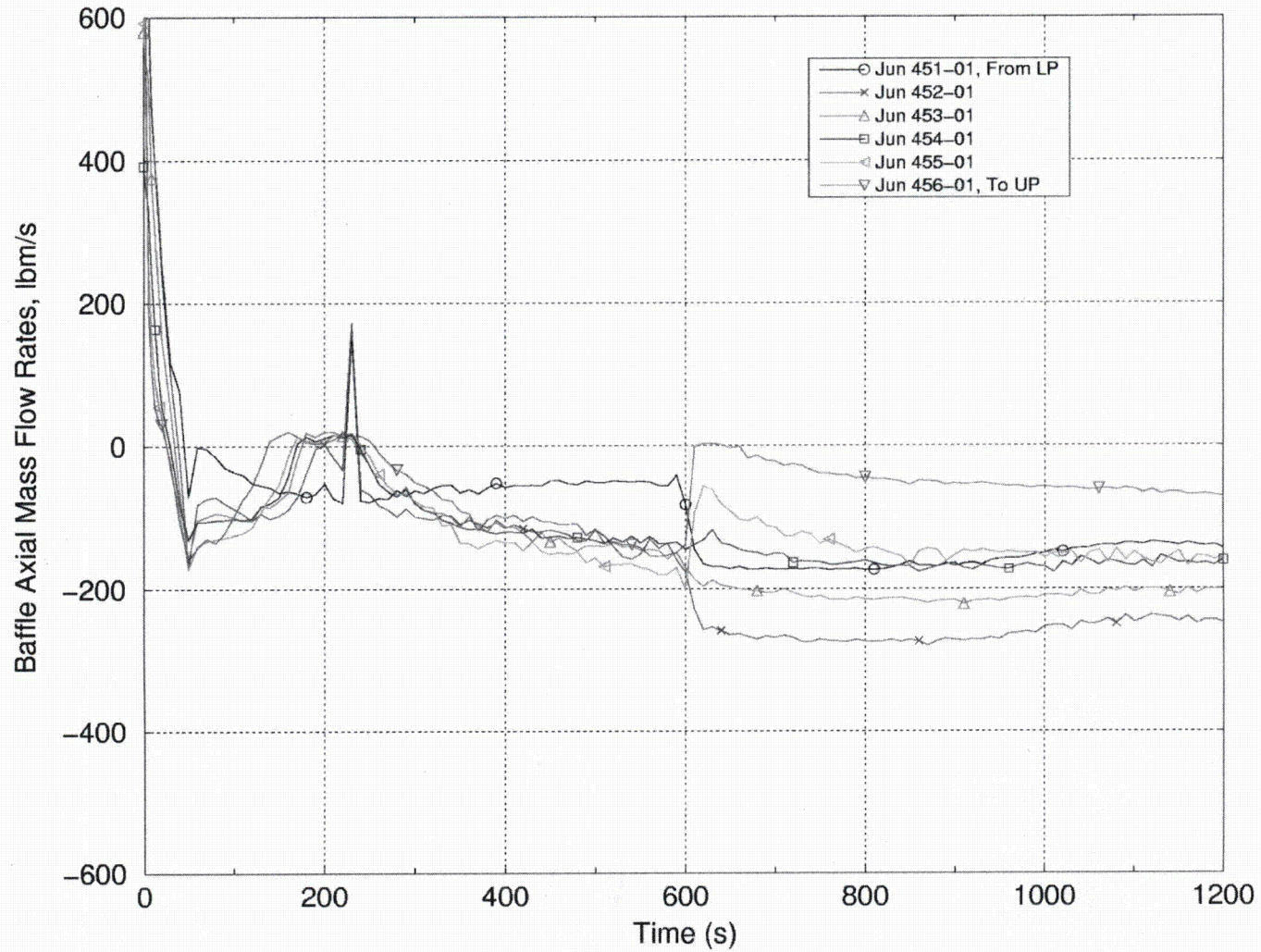
Figure 11-6 Flow from Core Region to the Upper Plenum
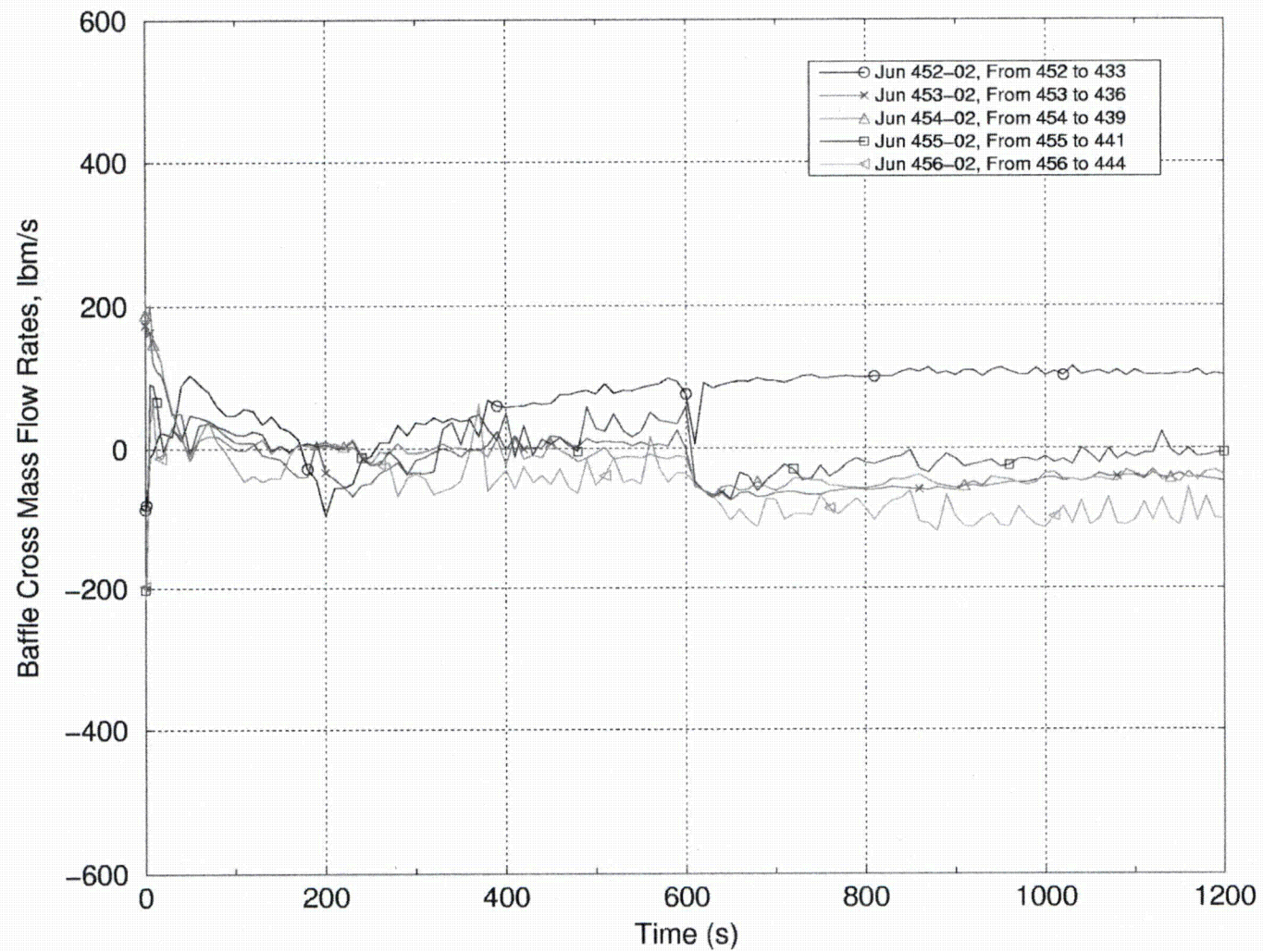
Figure 11-7 Axial Flow in Barrel/Baffle Channel

Figure 11-8 Flow from Barrel/Baffle Channel to Core Average Channel

11.2.2 After Debris Introduction – Calculation of t_{block} and K_{max}

Case 1 is used to determine both t_{block} and K_{max}.

Throughout the duration of the transient, more-than-adequate core cooling flow is provided through the ECCS to the cold legs. Complete core inlet blockage is applied at 20 min (1200 seconds). After this time, coolant from the ECCS backs-up and fills the downcomer until adequate driving head is achieved such that flow can be provided to the core via the BB channel through the first row of LOCA holes. Figure 11-9 shows that the core experiences no temperature excursions after application of complete core inlet blockage. Due to the low resistance of the BB region and the presence of LOCA holes beginning approximately halfway up the core, there is little delay in filling the downcomer to provide adequate driving head such that coolant can flow through the BB channel and into the core region through the LOCA holes.

The RV collapsed liquid levels are shown in Figure 11-10. When complete core inlet blockage is applied, the downcomer level increases quickly, forcing flow through the BB channel to the first row of LOCA holes and into the core. When complete core inlet blockage is applied, there is sufficient liquid inventory in the UP region to replace boil-off during the delay time required to increase the downcomer driving head such that the core never uncovers and no heatups are predicted to occur.

Figure 11-11 shows the flow patterns at the core inlet. Junctions 315-00 and 415-00 represent the flow from the LP to the hot and average channels, respectively. After 1200 seconds, the flow is zero, indicating complete blockage at the core inlet. Junction 314-03 represents the flow from the LP to the BB channel. After 1200 seconds, the flow is positive, indicating flow from the LP into the BB (i.e., upflow) up to the first row of LOCA holes.

Figure 11-12 shows the flow patterns at the core outlet. Junctions 347-00 and 447-00 represent the flow from the hot and average channels, respectively, to the UP. After 1200 seconds, the flow is positive from the hot channel to the UP, indicating flow out of the core (i.e., upflow). The flow from the average core to the UP is generally positive, but a bit more oscillatory, which indicates that flow is generally upward. Junction 456-01 represents the flow from the BB channel to the UP. After 1200 seconds, the flow is negative, indicating flow from the UP into the BB.

Figure 11-13 shows the axial flow patterns in the BB channel. After 1200 seconds, the flow in this region is mixed. In the lower portion (up to the first LOCA hole), the flow is positive, which indicates upflow in this region. Above the first LOCA hole, the flow is negative indicating downflow.

Figure 11-14 shows the flow patterns from the BB channel to the average core. Junction 452-02 and Junction 453-02 are the lowermost connections. After 1200 seconds, the flow direction is positive indicated flow from the BB into the average core. Junction 454-02 is the third junction from the bottom. After approximately 1500 seconds, this flow becomes slightly positive, indicating flow from the BB into the average channel. The other junctions are slightly negative during this same time period, indicating flow from the average core into the BB channel.

These results help to confirm the flow patterns shown in Figure 7-2. However, there is one limitation of the RELAP5/MOD2-B&W model in that there are only two channels in the core region. This lack of

spatial resolution makes it difficult to predict the core flow patterns with any detail. In a typical PWR, higher-power assemblies are placed near the center of the core and along diagonals. Slightly lower-power assemblies are placed around them. The lowest-power assemblies are placed near the periphery, adjacent to the baffle plates with the LOCA holes. This core loading pattern leads to a radial power distribution that can create a temperature or void gradient between the center (higher-power region) and the periphery (lower-power region) of the core. Flow through higher-power assemblies is then likely to be upwards, with flow in the peripheral assemblies being downward. This convection roll, or "chimney effect", is expected to drive the global core flow patterns during the post-LOCA transient.

There are a number of contributing factors in the analyses that also support the description given above. First, the model shows a definitive downflow in the BB channel. Given that there is no decay heat in the BB and the proximity of the BB channel to the low-power core peripheral assemblies, it stands to reason that downflow is occurring in the peripheral assemblies. Second, the oscillatory behavior of the average core channel implies that if a third, lower-power channel was included in the model; downflow is likely in that lower-power region (core periphery). This assertion can be confirmed by examining the results of the Westinghouse and CE plant simulations that include four core channels (see Sections 8, 9, & 10). The differences in the physical core region between a B&W-designed plant and a Westinghouse or CE plant are not significant with regard to the boiling mechanisms present. It stands to reason that the core flow patterns observed in the Westinghouse and CE models, with more core channels, are representative of the flow patterns expected in the B&W core. Indeed, these models show upflow in the high-power channel (core center) and downflow in the lower-power channel (core periphery).

The break exit quality is shown in Figure 11-15. This figure shows that the quality prior to the application of complete core inlet blockage is between 40 and 60%. After the application of blockage, the case shows a spike in the break quality which quickly recovers and stabilizes below 40%. Due to the large amount of liquid carryover out the break before and after complete core inlet blockage, BAP is controlled and boron concentrations in the RV will remain well below the solubility limit for the duration of the transient.
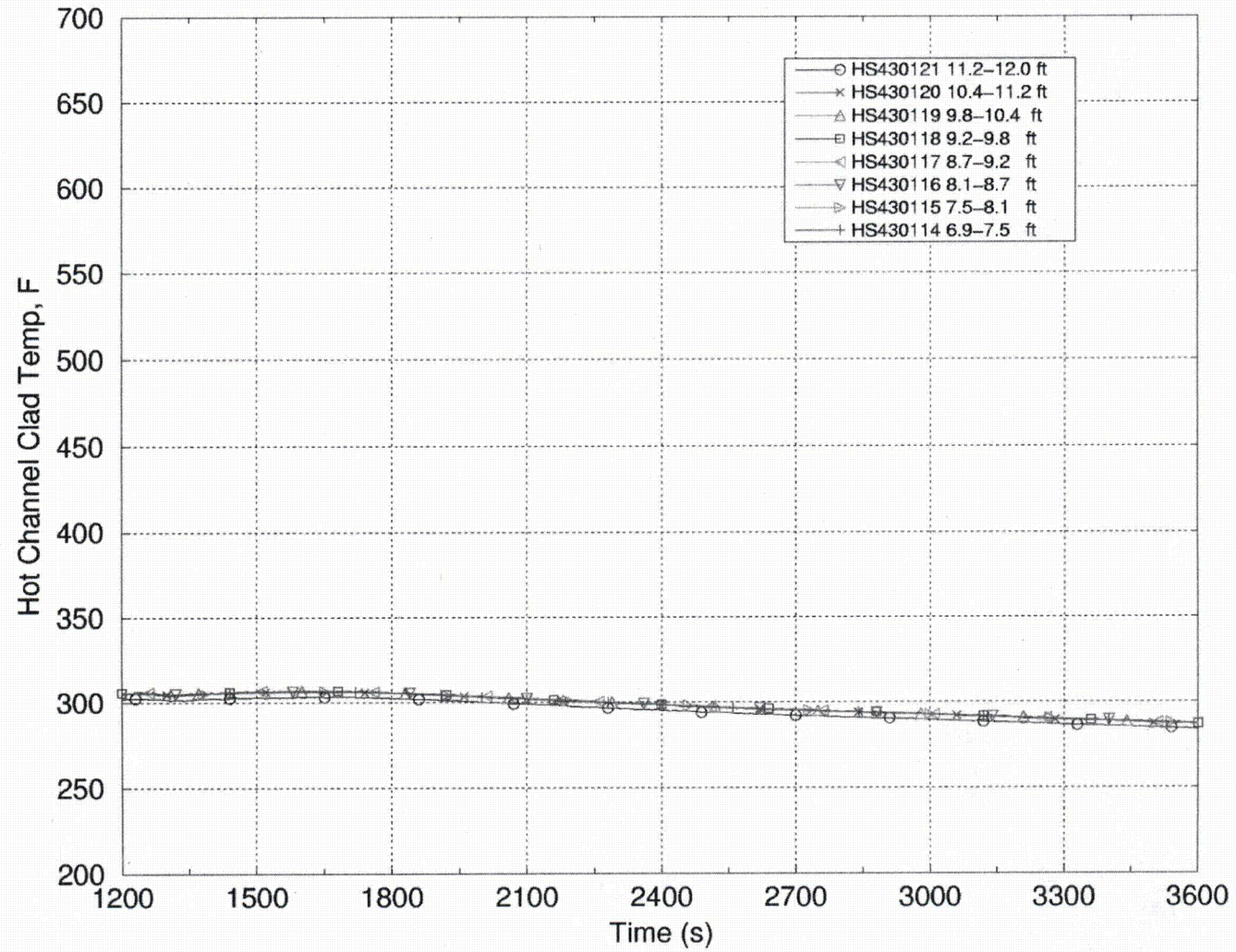
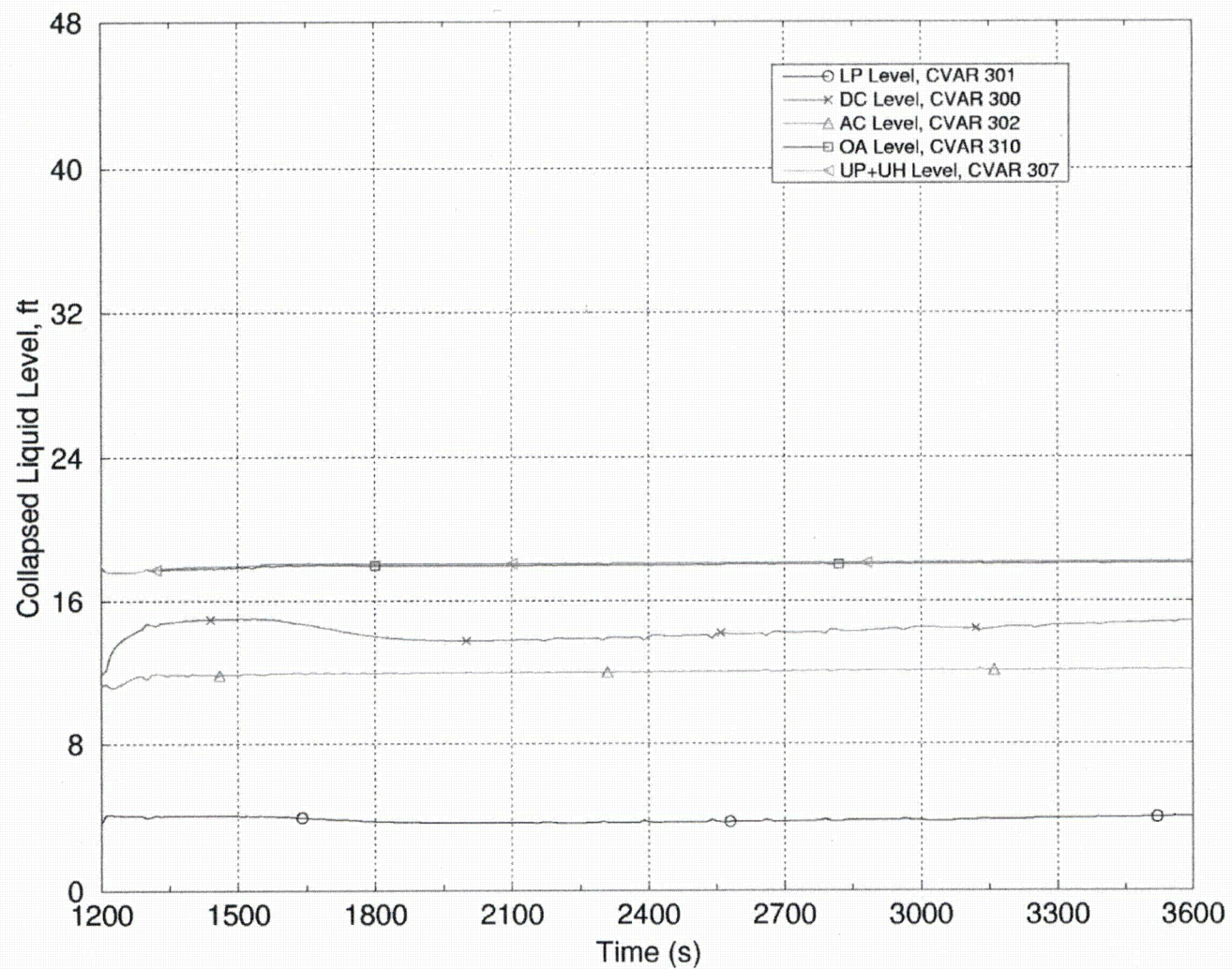**Figure 11-9 Hot Channel Peak Cladding Temperatures**
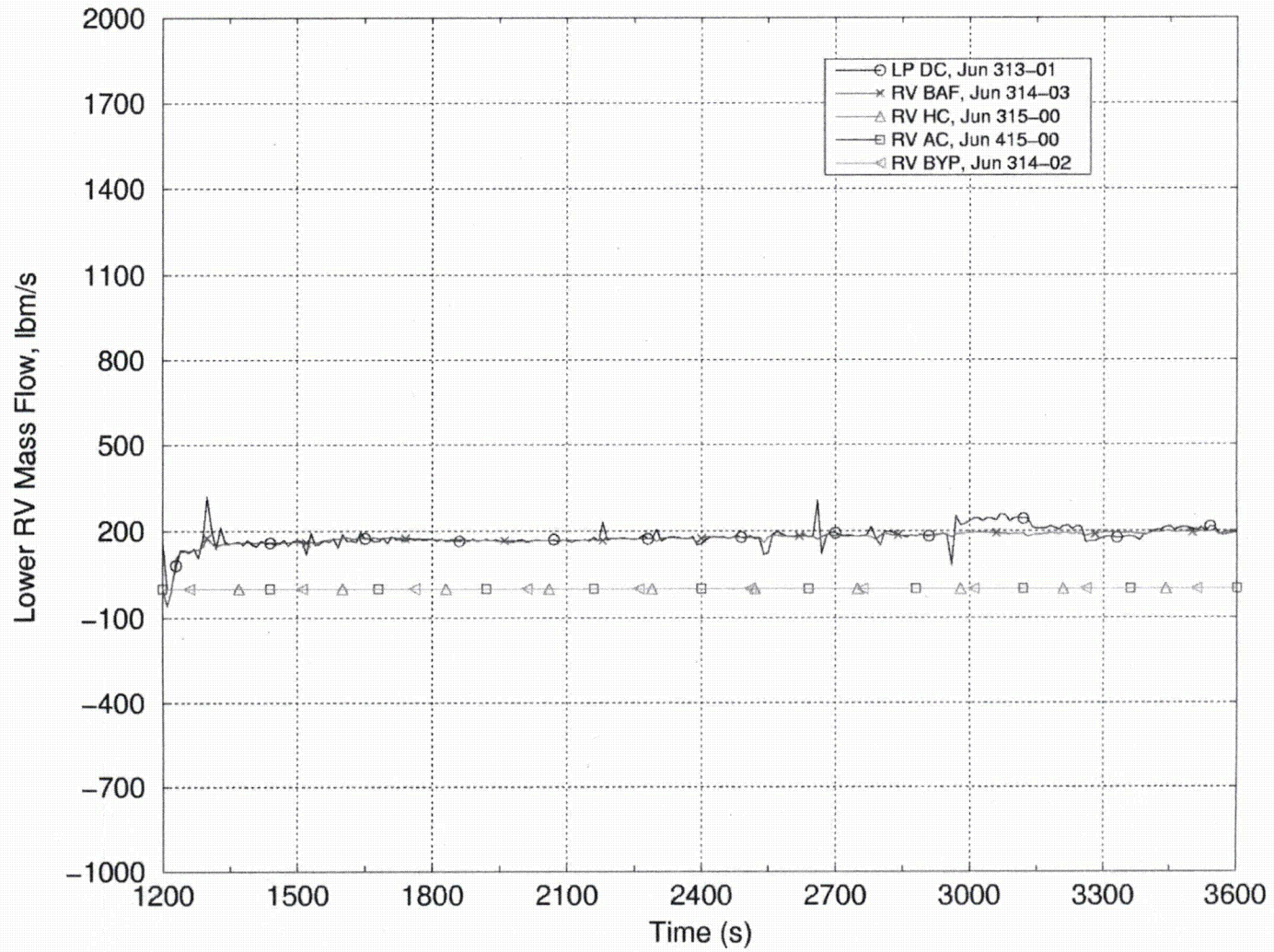
Figure 11-10 Reactor Vessel Collapsed Liquid Levels

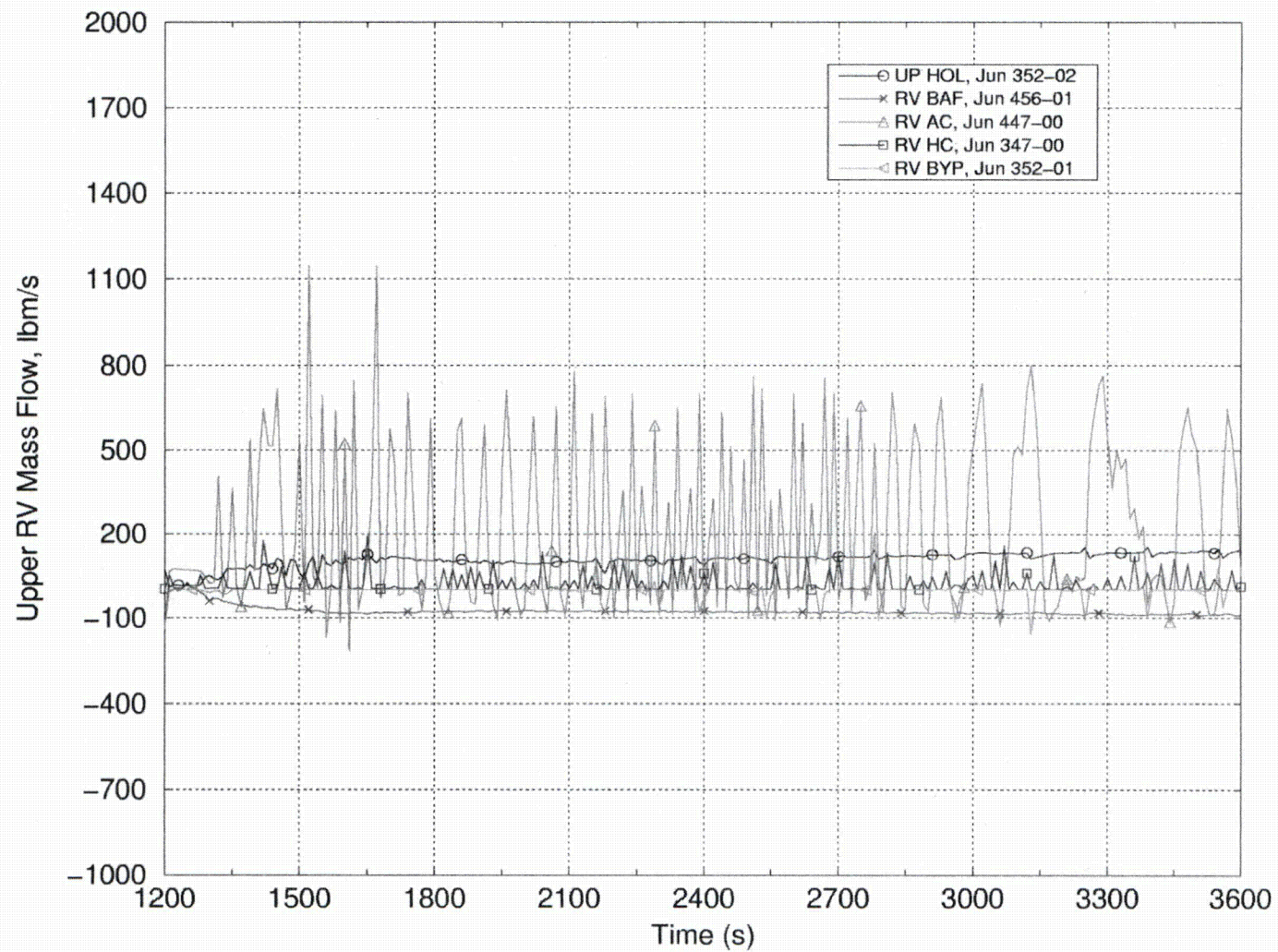**Figure 11-11 Flow from Lower Plenum to Core Region**

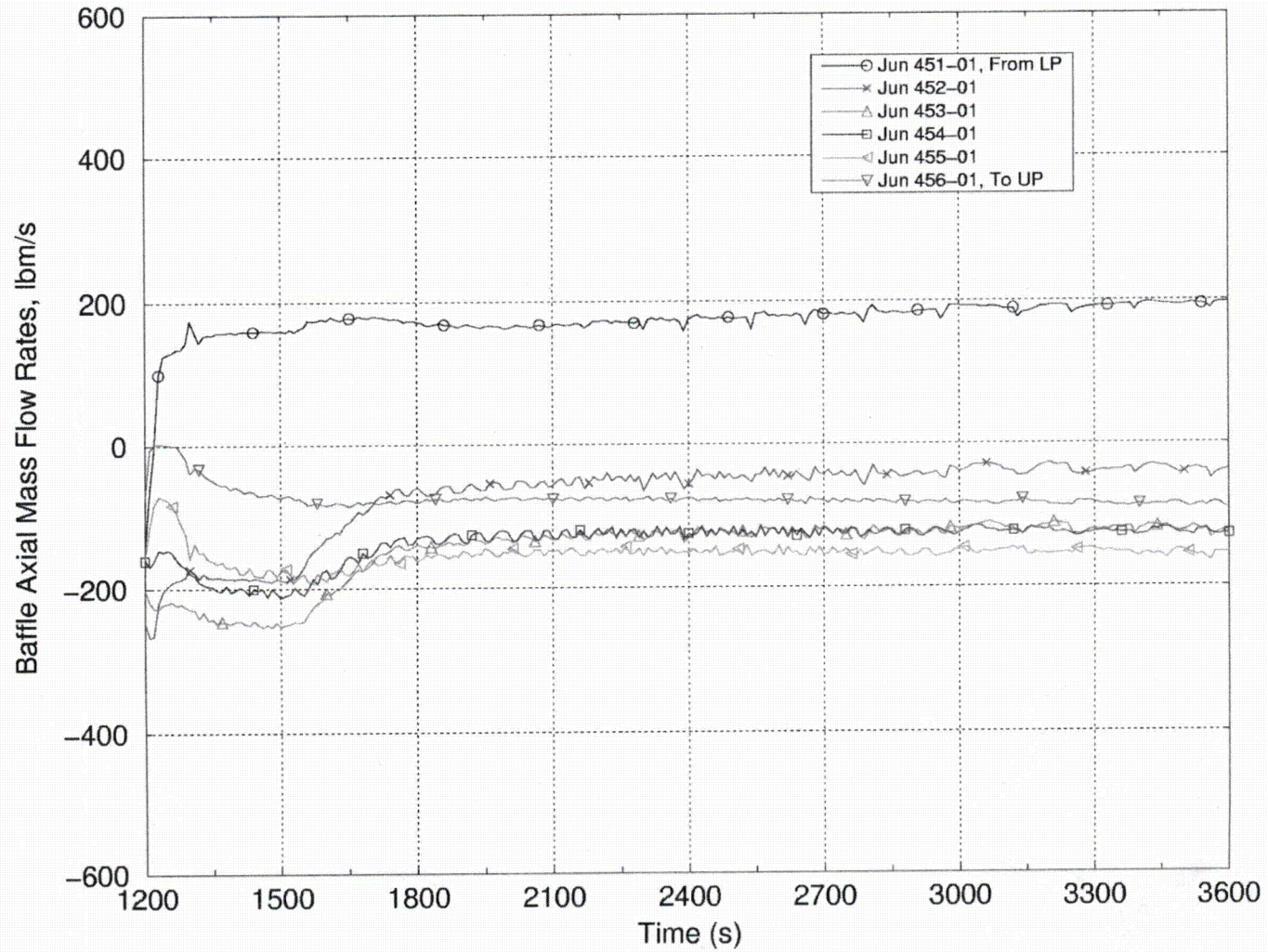**Figure 11-12 Flow from Core Region to Upper Plenum**

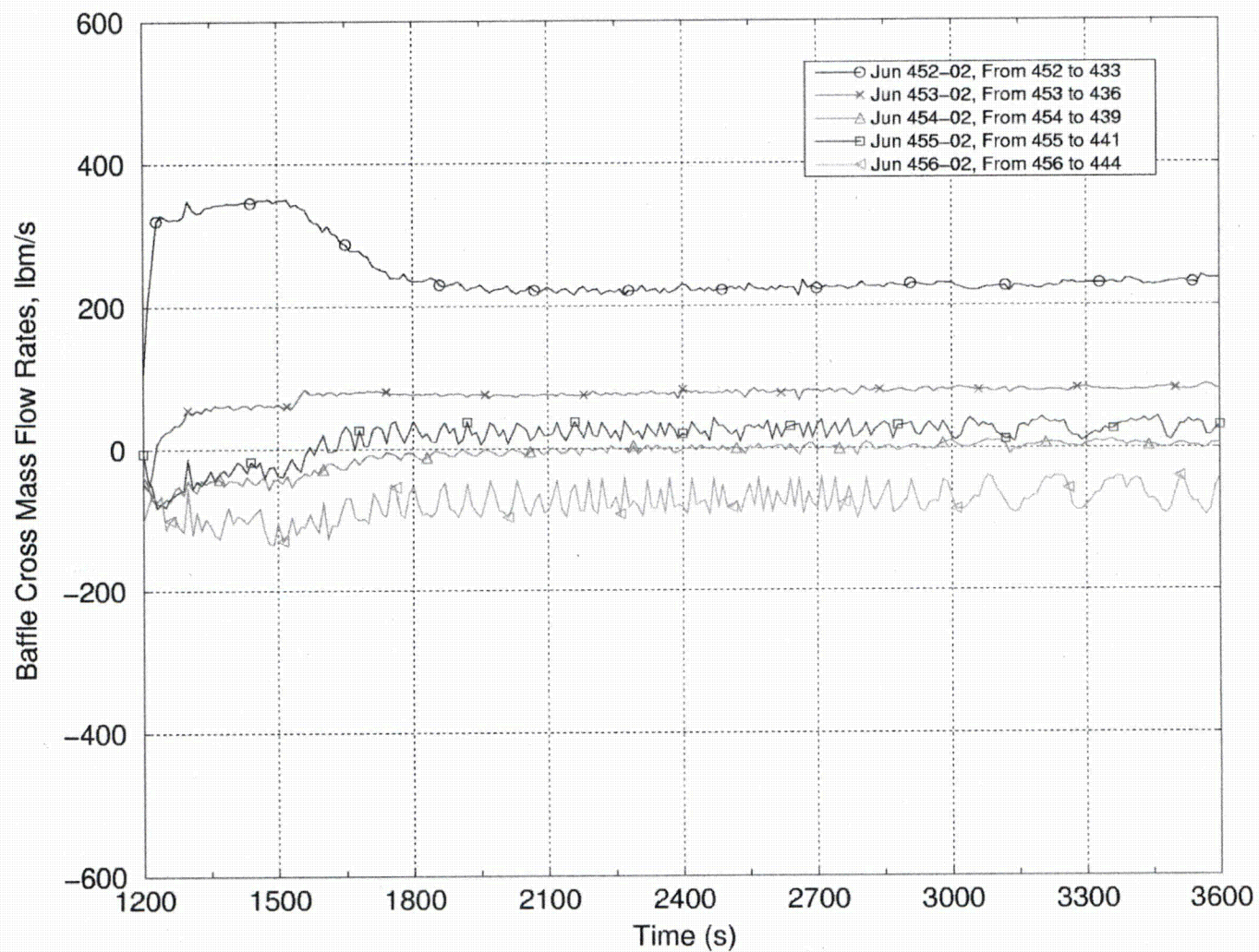**Figure 11-13 Axial Flow in Barrel/Baffle Channel**

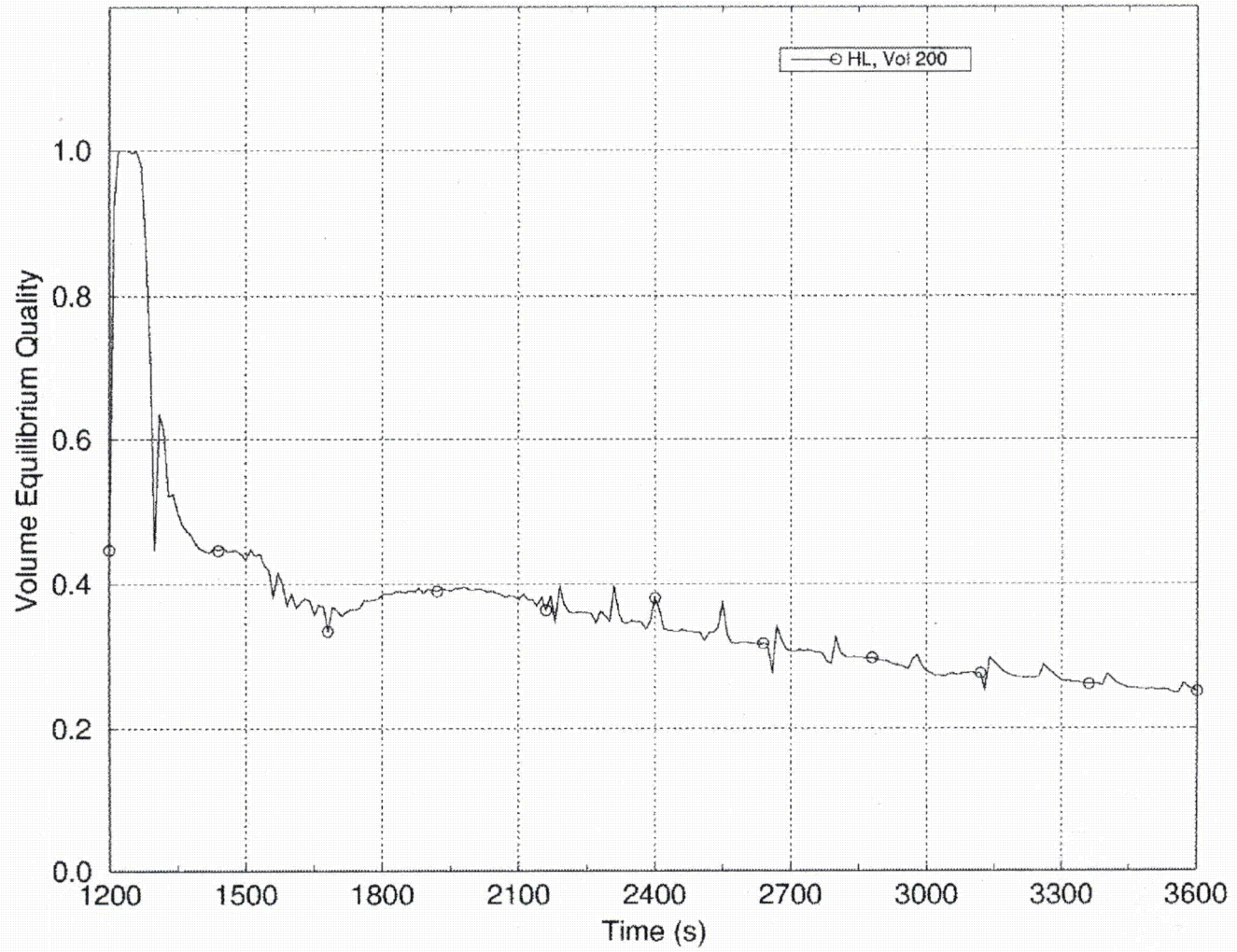**Figure 11-14 Flow from Barrel/Baffle Channel to Core Average Channel**

Figure 11-15 Break Exit Quality

11.2.3 After Debris Introduction – Calculation of K_{split} and m_{split}

Six additional cases were run to determine K_{split} and m_{split}. For these cases, a linear ramp in resistance was applied at the core inlet and complete core inlet blockage was not simulated. Since these cases were used to assess the timing of the activation of the BB channel, the build-up of core inlet resistance was applied more slowly compared to the cases used to determine K_{max}. As a result, the RCS response to core inlet blockage was much slower in that the downcomer fill rate and the activation of the BB channel occurred over a longer period of time. It is noted that these simulations are more realistic with regard to the timing at which debris is expected to arrive at the core inlet.

Even though six simulations were completed to cover the full range of ECCS flows expected during sump recirculation, only Case 2d was selected for discussion in this section. Similar trends were observed in the cases not discussed.

Select transient plots from Case 2d are shown in Figures 11-16 through 11-20. The RCS response to core inlet blockage was expected and is generally consistent with the transient response discussed in Section 11.2.2. Figure 11-16 shows the flow patterns at the core inlet. As the blockage is applied, the flow begins to decrease as the core inlet resistance increases. Concurrently, the downward flow from the BB channel to the LP begins to slow and eventually reverses as the core inlet resistance increases, leading to flow from the LP into the BB channel (i.e., upflow). Figure 11-17 shows the flow patterns at the core outlet. As the blockage is applied at the core inlet, flow at the core outlet is positive from the hot channel to the UP, indicating flow out of the core (i.e., upflow). The flow from the average core to the UP is generally positive, but a bit more oscillatory, indicating that flow is generally upward. This flow gives some indication of the limitation of the two-channel model, which was discussed in Section 11.2.2. After the blockage is applied to the core inlet, the BB flow is negative, indicating flow from the UP to the BB. Figure 11-18 shows the axial flow patterns in the BB channel. After 1200 seconds, the flow in this region is mixed. Flow in the lower portion is positive, which indicates upflow. Flow in the upper portion is negative indicating downflow. Figure 11-19 shows the flow patterns from the BB to the average core. After 1200 seconds, the flow is mixed in that some of the junctions are flowing from the core to the BB channel whereas the other junctions are flowing from the BB to the core.

The PCT response is shown in Figure 11-20. The figure indicates that the PCT remains well below 800°F and the lack of any significant heatups indicates that the core never uncovers after the application of core inlet resistance.
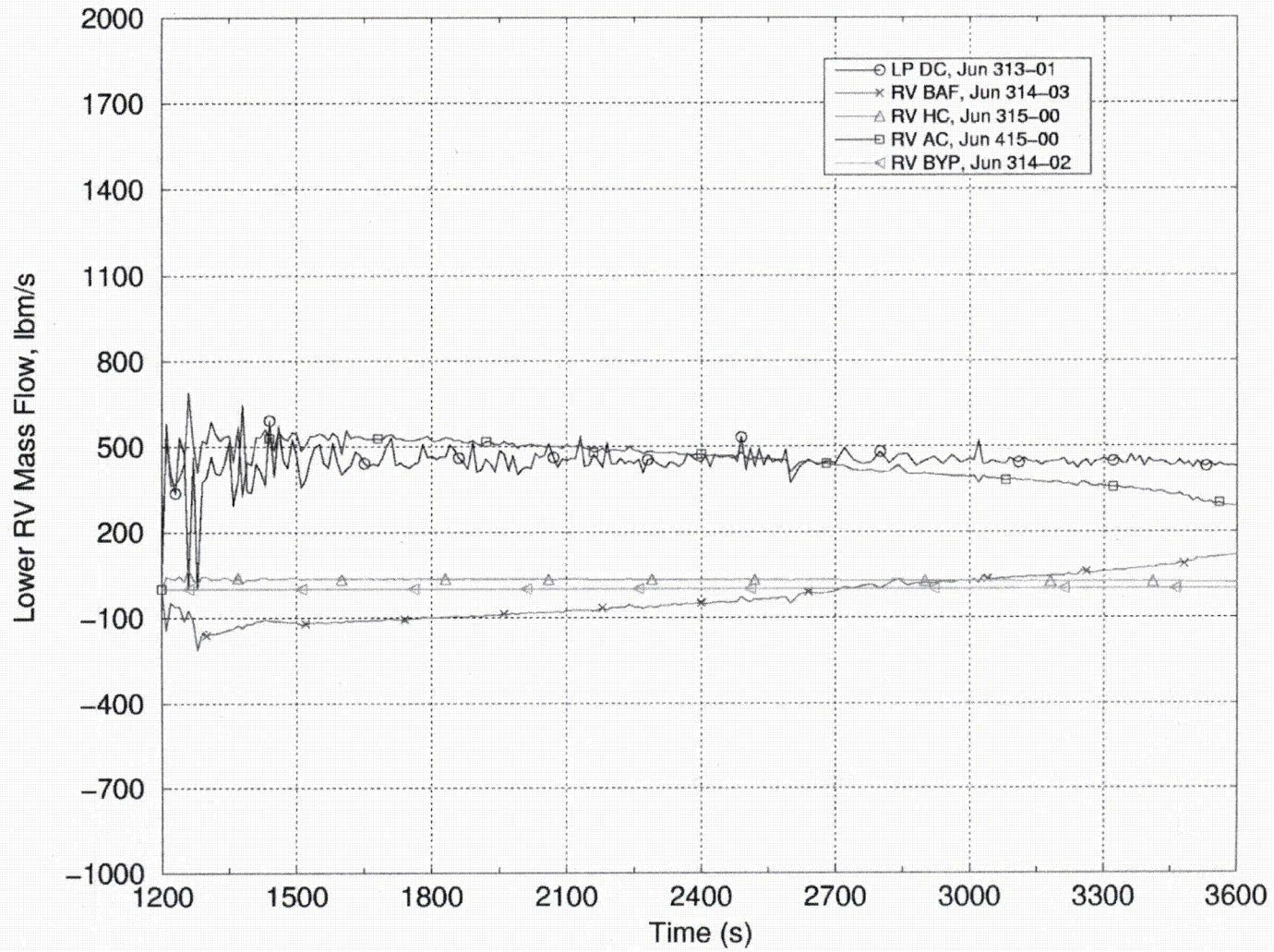
Figure 11-16 K_{split} Case 2d – Flow from Lower Plenum to Core Region
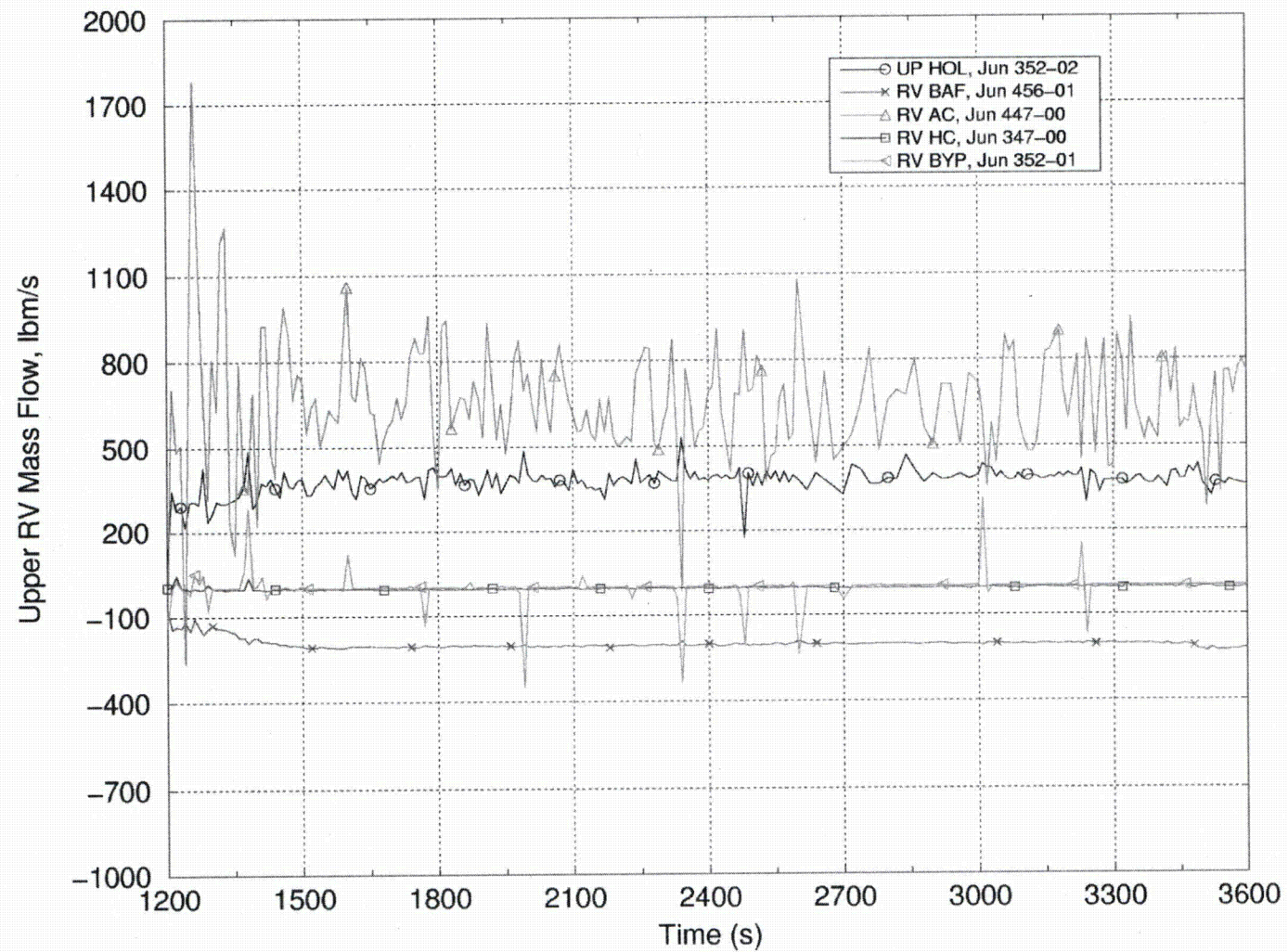
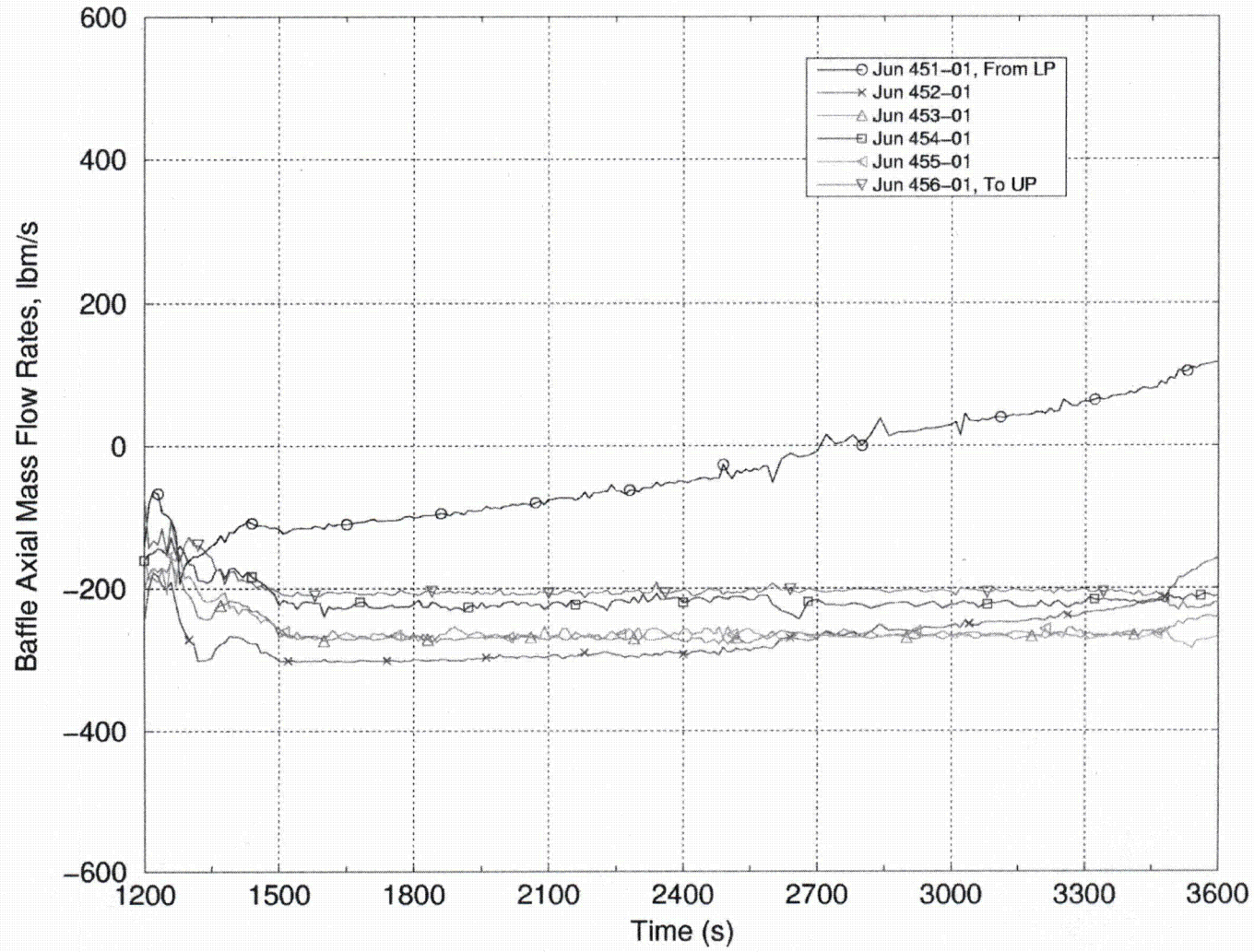**Figure 11-17 K$_{split}$ Case 2d – Flow from Core Region to the Upper Plenum**

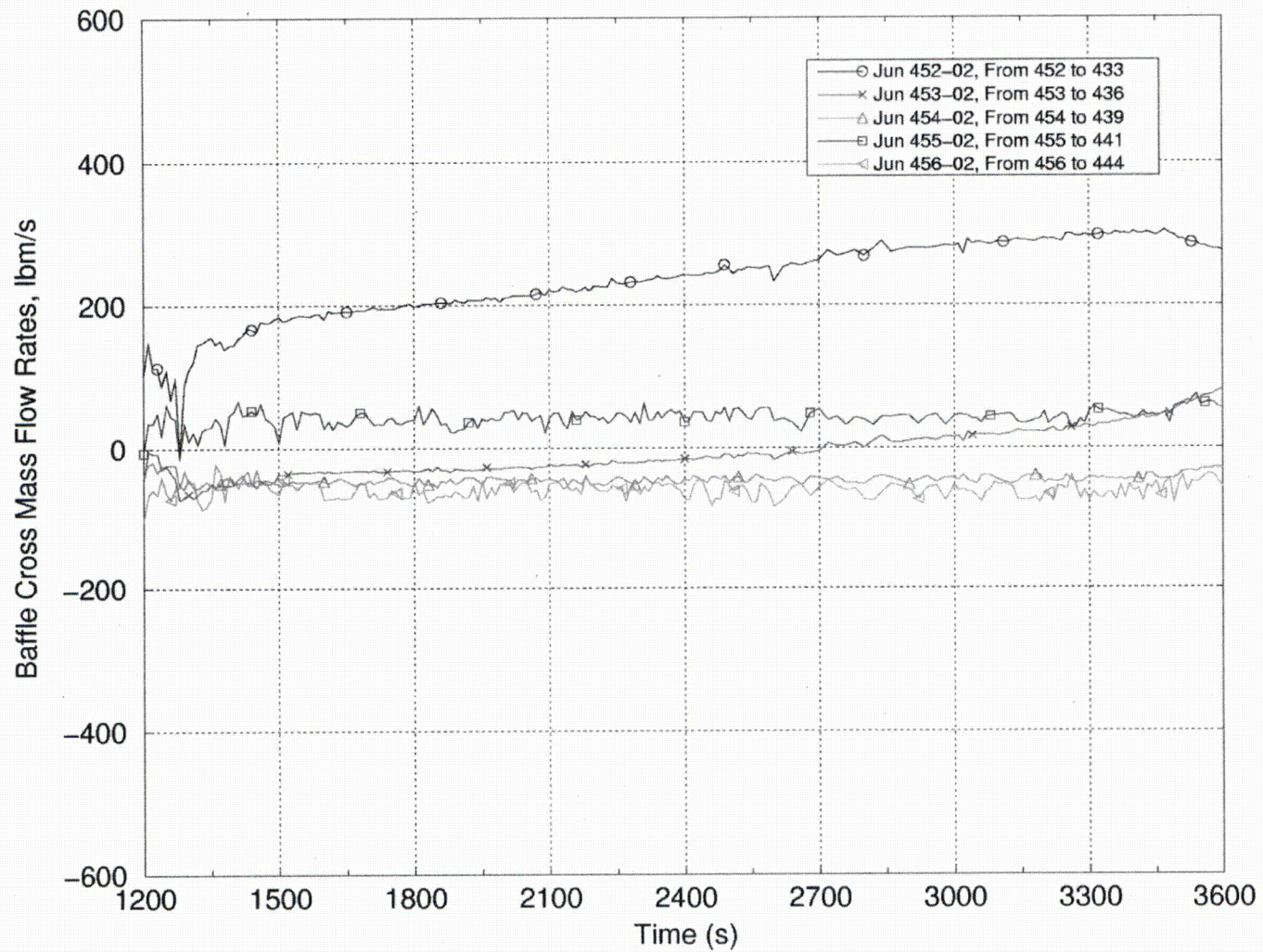**Figure 11-18 K$_{split}$ Case 2d – Axial Flow in Barrel/Baffle Channel**

Figure 11-19 K$_{split}$ Case 2d – Flow from Barrel/Baffle Channel to the Average Core Channel
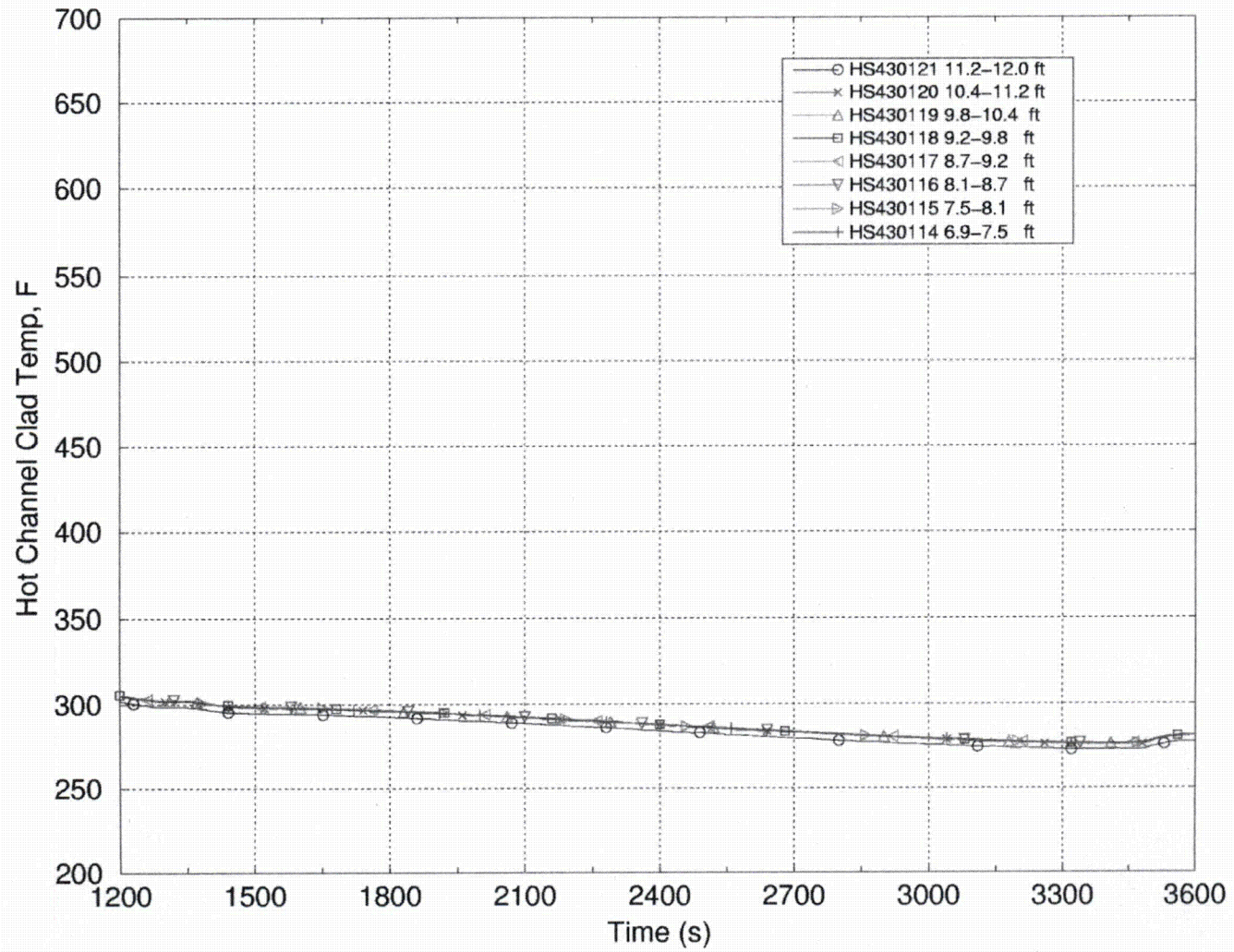
Figure 11-20 K$_{split}$ Case 2d – Hot Channel Peak Cladding Temperatures

11.3 DISCUSSION OF RESULTS

During the first 20 minutes of the transient (before debris arrives), the core region has completely reflooded and the cladding temperatures are just above the saturation temperature. The core is boiling vigorously and the core average void fraction is approximately 50%. The downcomer is filling with coolant supplied to the cold legs via the ECCS. At 20 minutes, the downcomer collapsed liquid level is well below the cold leg elevation. There is a strong recirculation pattern within the core region in which the hot and average assemblies have predominately upflow while the peripheral assemblies have downflow. Vapor generated in the core flows toward the break and liquid carryover to the break is significant.

The first set of core inlet blockage simulations (Section 11.2.2) examined a scenario in which the core inlet was instantaneously completely blocked coincident with the transfer to sump recirculation by applying a large form-loss coefficient at the core inlet. No cladding heatup was predicted for this scenario. When the blockage was applied, flow through the core inlet ceased and flow through the BB channel reversed up to the first row of LOCA holes. Flow through the BB channel was sufficient to replace boil-off and DHR was maintained.

In the prototypic system, it is unrealistic to expect all the fibrous and particulate debris to arrive at the core inlet instantaneously. It is expected that the arrival of debris will occur over some finite period of time that is on the order of hours. Since the exact timing of debris arrival is complex and will vary from plant-to-plant, the approach for determining t_{block} and K_{max} via application of an instantaneous blockage simplifies the approach by taking the timing of debris arrival out of the solution.

The second set of core inlet blockage simulations (Section 11.2.3) examined a scenario in which a gradual build-up of debris was applied at the core inlet. These are considered the most realistic cases relative to how fibrous and particulate debris is expected to arrive at the core inlet; however, these cases do not simulate complete core inlet blockage. The gradual addition of resistance at the core inlet slowly increases the downcomer level and delays the activation of the BB channel. Eventually, the downcomer driving head becomes sufficiently large to change the flow direction in the BB channel. After this point, flow from the LP is split between the core inlet and the BB and, as the core inlet resistance continues to build, the flow fraction to the BB continues to increase while the flow fraction to the core inlet decreases. From these simulations, the core inlet resistance necessary to activate the BB channel (K_{split}) was determined to be a strong function of the ECCS flow. K_{split} plotted as a function of ECCS flow rate is provided in Figure 11-3 and the corresponding flow split between the core inlet and the BB channel (m_{split}) following K_{split} is shown in Figure 11-4.

12   CONCLUSIONS

As part of the PWROG program to increase the in-vessel fibrous debris limit, a rigorous TH analysis of the RCS response to core inlet blockage following a large HLB LOCA was undertaken.

The outcome of the simulations confirms that LTCC can be maintained for all plant types considered when post-LOCA debris is modeled. When a debris bed of uniform resistance is modeled at the core inlet, the simulations predict that, while flow through the core inlet decreases, removal of decay heat continues since sufficient flow is able to bypass the core inlet and reach the core region through AFPs. Even if the collection of debris at the core inlet results in complete core inlet blockage, this bypass flow is sufficient to remove decay heat and keep PCT at acceptably low levels, provided complete core inlet blockage occurs after the times predicted by the TH simulations presented in this report. Due to the large amount of liquid carryover out the break before and after complete core inlet blockage, boric acid precipitation (BAP) is controlled and boron concentrations in the reactor vessel (RV) will remain well below the solubility limit for the duration of the transient.

The results of the simulations were evaluated against the acceptance criteria defined in Section 2.5, which ensures adequate LTCC for the conditions analyzed. The results from this TH analysis are used as acceptance criteria in subsequent debris testing performed as part of the PWROG program as described in Volumes 5 and 6. Debris testing provides the link between what was modeled in the analysis and a physical debris limit. In addition, simulation results are used as inputs to the overall methodology that allows PWR licensees to calculate a plant specific in-vessel fibrous debris limit.

The parameters used in subsequent work are summarized below for the four plant categories.

12.1   WESTINGHOUSE UPFLOW PLANT CATEGORY CONCLUSIONS

1.   The minimum time that complete core inlet blockage can be tolerated (defined as t_{block}) was found to be 143 minutes.

2.   The maximum resistance at the core inlet that can be tolerated prior to reaching complete core inlet blockage (defined as K_{max}) was found to be 5×10^5.

3.   The resistance at the core inlet that begins to divert flow into the AFP (defined as K_{split}) was found for a range of ECCS flow rates. These results are shown in Figure 8-4.

4.   The flow split between the core inlet and the AFP after K_{split} (defined as m_{split}) was found for a range of ECCS flow rates. A curve that bounds the results was also developed. These results are shown in Figure 8-5.

12.2   WESTINGHOUSE DOWNFLOW PLANT CATEGORY CONCLUSIONS

1.   The minimum time that complete core inlet blockage can be tolerated (defined as t_{block}) was found to be 260 minutes.

2. The maximum resistance at the core inlet that can be tolerated prior to reaching complete core inlet blockage (defined as K_{max}) was found to be 6×10^5.

3. The resistance at the core inlet that begins to divert flow into the AFP (defined as K_{split}) was found for a range of ECCS flow rates. These results are shown in Figure 9-3.

4. The flow split between the core inlet and the AFP after K_{split} (defined as m_{split}) was found for a range of ECCS flow rates. A curve that bounds the results was also developed. These results are shown in Figure 9-4.

12.3 COMBUSTION ENGINEERING PLANT CATEGORY CONCLUSIONS

1. The minimum time that complete core inlet blockage can be tolerated (defined as t_{block}) was found to be 250 minutes.

2. The maximum resistance at the core inlet that can be tolerated prior to reaching complete core inlet blockage (defined as K_{max}) was found to be 6.5×10^6.

3. The resistance at the core inlet that begins to divert flow into the AFP (defined as K_{split}) was found for a range of ECCS flow rates. These results are shown in Figure 10-4.

4. The flow split between the core inlet and the AFP after K_{split} (defined as m_{split}) was found for a range of ECCS flow rates. A curve that bounds the results was also developed. These results are shown in Figure 10-5.

12.4 BABCOCK & WILCOX PLANT CATEGORY CONCLUSIONS

1. The minimum time that complete core inlet blockage can be tolerated (defined as t_{block}) was found to be 20 minutes.

2. The maximum resistance at the core inlet that can be tolerated prior to reaching complete core inlet blockage (defined as K_{max}) was fund to be 1×10^8.

3. The resistance at the core inlet that begins to divert flow into the AFP (defined as K_{split}) was found for a range of ECCS flow rates. These results are shown in Figure 11-3.

4. The flow split between the core inlet and the AFP after K_{split} (defined as m_{split}) was found for a range of ECCS flow rates. A curve that bounds the results was also developed. These results are shown in Figure 11-4.